DEVELOPMENT AND APPLICATION OF NOVEL SOLVENTS FOR SUSTAINABLE REACTIONS AND SEPARATIONS

A Thesis
Presented to
The Academic Faculty

by

Megan Elizabeth Donaldson

In Partial Fulfillment
of the Requirements for the Degree
Doctor of Philosophy in Chemical and Biomolecular Engineering

Georgia Institute of Technology
August 2008

DEVELOPMENT AND APPLICATION OF NOVEL SOLVENTS FOR SUSTAINABLE REACTIONS AND SEPARATIONS

Approved by:

Dr. Charles A. Eckert, Advisor
School of Chemical & Biomolecular Engineering
Georgia Institute of Technology

Dr. Thomas F. Fuller
School of Chemical & Biomolecular Engineering
Georgia Institute of Technology

Dr. Charles L. Liotta, Co-Advisor
School of Chemistry & Biochemistry
Georgia Institute of Technology

Dr. Christopher W. Jones
School of Chemical & Biomolecular Engineering
Georgia Institute of Technology

Dr. Facundo M. Fernandez
School of Chemistry & Biochemistry
Georgia Institute of Technology

Date Approved: June 20, 2008

For my Mom and Dad –
who taught me that life is limitless

Acknowledgements

I would first like to acknowledge my advisors, Dr. Eckert and Dr. Liotta. Both have taught me so much about research and have helped to truly guide my development. I especially want to thank Dr. Eckert for his combination of support and independence that has allowed me to pursue the many new and unexpected directions of my research. I thank Dr. Liotta for his constant excitement for research, which has taught me to always look at the positive side of any strange result.

I also would like to recognize my committee, Dr. Jones, Dr. Fernandez, and Dr. Fuller, for their advice and support on my research and their continuing ideas for possibilities beyond the initial scope of this work.

I thank Deborah Babykin, whose expertise in everything from Georgia Tech guidelines and purchasing to photography and powerpoint has made all my work easier.

I would also like to thank all the members of the Eckert-Liotta group, especially Michelle Kassner, Tori Blasucci, Ejae John, Reagan Charney, Hillary Huttenhower, Liz Hill, and Laura Draucker. Whether its advice on research or life in general, each has contributed a great deal to this work and I am grateful for their friendships.

I also owe a lot to the post-docs in the group. I would especially like to thank Veronica Llopis Mestre for all her help on the switchable solvents, Jason Hallett who guided a lot of my projects in the first few years and really helped me learn how to be a researcher, and Cerag Dilek for her constant support in both research and the general craziness of life. I also want to acknowledge all the undergrads who helped me work on almost every aspect of my research, including Craig, Hye Jin, Laura, and Nicole.

Mostly, I want to thank my family who has always been there for me through all of life's ups and downs. They always told me I could do anything I wanted and I find I have done exactly that. I want to especially thank my parents who helped me figure out where I truly wanted to go with my life and my sisters, Courtney and Ashleigh, who can keep me going even when I sometimes feel like I'm in over my head. Finally, I have to thank my best friend and boyfriend, Jesse, who has stuck by me no matter what. His love and support has kept me going many a time and his craziness has kept me sane. And last but not least, I can't forget about my dog, Peaches, whose big puppy grin always brightens my day.

Table of Contents

List of Tables

List of Figures

List of Symbols & Abbreviations

AARD	Absolute average relative deviation
ATH	Asymmetric transfer hydrogenation
CO_2	Carbon dioxide
DBU	1,8-Diazabicyclo-[5.4.0]-undec-7-ene
DIMCARB	Dimethylammonium dimethylcarbamate
DMF	Dimethylformamide
DMSO	Dimethylsulfoxide
EA	Elemental analysis
EOS	Equation of state
FID	Flame ionization detector
GAS	Gas antisolvent
GC	Gas chromatagraph
GXL	Gas-expanded liquid
HMF	5-Hydroxymethylfurfural
HPLC	High performance liquid chromatography
IL	Ionic liquid
IR	Infrared
K	Partition coefficient
KCN	Potassium cyanide
KOAc	Potassium acetate
KSCN	Potassium thiocyanate
LCST	Lower critical solution temperature
LF	Lattice fluid
L-L	Liquid-liquid
LLE	Liquid-liquid equilibria
MIBK	Methylisobutylketone
MS	Mass spectrometer
MW	Molecular weight
NCW	Nearcritical water
NMR	Nuclear magenetic resonance

NRTL	Non-random two liquid
OATS	Organic aqueous tunable solvent
P	Pressure
PDMS	Polydimethylsiloxane
PEG	Polyethylene glycol
PEG-DME	Polyethylene glycol-dimethylether
PNIPAM	Poly(N-isopropylacrylamide)
PRSV	Peng-Robinson with Stryjeck and Vera modification
PTAD	4-Phenyl-1,2,4-triazoline-3,5-dione
PTC	Phase transfer catalysis
PTFE	Polytetrafluoroethylene
PVT	Pressure, volume, temperature
RTD	Resistance temperature detector
$scCO_2$	Supercritical carbon dioxide
SFC	Supercritical fluid chromatagraph
SL	Sanchez-Lacombe
S-L	Solid-liquid
SO_2	Sulfur dioxide
S-SCF	Solid-supercritical fluid
T	Temperature
TBACl	Tetrabutylammonium chloride
TGA	Thermal gravimetric analyzer
THF	Tetrahydrofuran
UNIFAC	Universal functional activity coefficient
UNIQUAC	Universal quasi-chemical
UV-vis	Ultra violet - visible
VLE	Vapor-liquid equilibria
VOC	Volatile organic compound
x	Conversion

Summary

Environmentally benign alternatives for solvents and catalysts are essential for the development of sustainable chemical processes. Toward this end, we focused our research on the design of novel solvents and catalysts that reduce the environmental impact of these important materials. In this research, we develop switchable and tunable systems that couple reaction and separation to ease the processing requirements for product isolation and catalyst recovery.

The switchable solvents use a "switch" to transition from non-volatile, polar, aprotic solvents to volatile gases that can be easily separated. This allows us to facilitate reactions within the solvent and then enable easy separation through activation of the switch. We have used these materials for numerous reaction applications, including difficult reactions involving highly immiscible compounds. We also extended the work to acid-catalyzed reactions, in which we can avoid wasteful neutralization processes that are often associated with homogeneous acid catalysis.

The tunable solvents use carbon dioxide pressure to "tune" into desired solvent properties. We enable this through the dissolution of carbon dioxide into organic solvents, which generates gas-expanded liquids with solvent properties highly dependent on the carbon dioxide pressure. We can use this effect to couple homogeneous reaction with heterogeneous separation, allowing for recovery of expensive catalysts and ligands. In this work, we assess the possibilities of using liquid polyethylene glycol in the tunable systems, studying the phase behavior and industrial applications.

Chapter I: Introduction

Due to increasing environmental awareness, there has been a push toward research related to sustainable technology and green chemistry. This approach emphasizes the design of new systems that incorporate environmental considerations within the chemistry of both reactions and separations. As illustrated by the vast amount of literature on novel, sustainable systems, these ideas have been readily adopted and developed within academia. They have also seen industrial implementation due to legislative pressure, public perception, as well as financial advantages. From an economic perspective, these developments can have profound implications, reducing the energy burden related to separations and the capital costs related to pollution remediation. From the environmental perspective, they can make an impact upon worldwide problems associated with pollution, global warming, energy, and more of the key issues that drive our research.

In order to achieve the goals of green chemistry, researchers have developed environmentally benign alternatives to conventional solvents and catalysts. Solvents are an important aspect of the chemical process, because they are often needed to maintain efficient reaction rates. Every year 15 billion kilograms of organic solvents are produced to enable the reactions and separations of worldwide chemical processes.[1] More importantly, solvents can account for a significant portion of the materials involved in chemical production, with an estimated 85% of the total mass in certain pharmaceutical processes.[2] All of these materials must be separated and processed, resulting in substantial separation costs and hazardous waste. Therefore, numerous sustainable alternatives have come about in recent years to improve reaction and separation,

including ionic liquids[3], supercritical carbon dioxide[4], gas-expanded liquids[5], near critical water[6], liquid polymers[7], and fluorous compounds[8]. There has also been a great deal of research into solventless systems and reactions in water.[2]

Catalysts are also important for the sustainability of processes. In organometallic catalysis, this is due to the need to recycle expensive metals and ligands. In other types, such as acid catalysis, the sustainability relates to reduction in processing waste that can result from neutralization or regeneration of the catalysts. Hence, researchers have developed a variety of benign alternatives, such as heterogeneous catalysts, biphasic systems, and gas-expanded liquids.[2]

In order to develop sustainable alternatives, we focused our research on two primary areas, switchable and tunable solvents. Both novel systems utilize mechanisms by which a property change can be induced, allowing for transition from a reaction to a separation environment. The two can be distinguished by the type of mechanism that we use to induce the change. In the switchable solvents, we build a "switch" into the compound, which enables properties to be turned off or on by activation of a stimulus. The solvents we will look at use a thermal switch to change the material from a non-volatile state to a volatile one. For the tunable solvents, we use a mechanism that can impart a range of properties. In this work, we use CO_2 pressure to manipulate the properties of solvents, giving us the ability to "tune" into the desired characteristics that can ease reactions and separations. These solvents are designed from a sustainable perspective, considering both the reaction and the separation to minimize the environmental impact of the materials.

In Chapters 2 and 3, we explore switchable solvents and their applications to numerous reaction and separation systems. We use sulfolenes to create polar, aprotic solvents with properties similar to dimethylsulfoxide (DMSO). This allows us to dissolve both hydrophobic and hydrophilic compounds, enabling monophasic reaction for highly immiscible materials. Contrary to conventional polar, aprotic solvents, the sulfolenes can be separated easily through decomposition of the solvent to volatile components. Additionally, the system is completely reversible, allowing us to collect the volatile materials and recombine them to reform the solvent. This process has enabled both product and catalyst recovery, providing a viable alternative to conventional solvents.

Chapter 2 discusses the properties of our prime switchable molecule, piperylene sulfone. We compare several key solvent parameters with DMSO and show comparable solvent properties. We then apply the reaction and separation system to a number of reactions, including nucleophilic substitutions, Diels-Alder, telomerization, and asymmetric transfer hydrogenations. With this research, we show that we can successfully react benzyl chloride with a variety of nucleophiles without the aid of phase transfer catalysts and then isolate the products through decomposition of the solvent. For these reactions, we illustrate excellent reactivity and recovery of both products and solvent. The Diels-Alder and telomerization reactions were unsuccessful due to interactions between the reactants or the catalysts and the solvent. However, we were successful in the asymmetric transfer hydrogenation of actophenone.

In Chapter 3, we expand the scope of the applications by using the switchable materials as both solvents and catalysts. We can accomplish this by using the

thermodynamics of the solvent equilibrium. We "switch" the solvent by increasing the temperature, which alters the equilibrium from the solvent to the decomposition products. At low temperatures, the equilibrium favors the solvent, but small amounts of the decomposition products must be present to satisfy the equilibrium. Since one of the products is sulfur dioxide, we can form an in-situ catalyst by simply adding water to the system, generating sulfurous acid. This application not only benefits from the recyclable solvent, but also from the reversibility of the acid, which eliminates the need for wasteful neutralization processes. In this work, we use the acid catalyst to complete the hydrolysis of β-pinene and several rearrangement reactions. We show a full study of the hydrolysis reaction, illustrating high activity and selectivity with recycle of the solvent at least five times without loss in activity. The initial rearrangement work shows limited success for the benzopinacol reaction, but has the potential to extend the application opportunities to new areas through further optimization.

In Chapter 4, we shift our focus to tunable solvents. For this research, we have developed a novel system for homogeneous catalyst recovery by using mixed solvents that can be separated with CO_2. Homogenous catalysis enables high activity and selectivity for many reactions, but is limited by the difficulty in separating the catalysts, which often must be recycled due to their cost and/or toxicity. It is necessary to develop methods that allow for efficient catalyst recycle yet retain high catalytic activity in the homogeneous medium. Therefore, we have worked on the development of solvent systems that couple homogeneous reaction with heterogeneous separation. In this research, we use benign polyethylene glycol (PEG) in combination with conventional solvents. These are miscible solvents that can be used to run homogeneous reactions.

However, we can phase separate the solvents by addition of CO_2 pressure, which causes the organic to become a gas-expanded liquid (GXL) that is immiscible with PEG. This separation creates the possibility for us to immobilize the homogeneous catalyst in the PEG phase and to extract the products into the organic phase, enabling easy recovery and recycle of the materials. We investigate the phase behavior of PEG-400 with CO_2 and both 1,4-dioxane and acetonitrile to assess their potential for reaction and separation systems. The results show good separation for most systems and conditions, but work only over limited pressure ranges due to the elevated pressures required to induce the phase split. However, the data show comparable behavior to our previous work on organic-aqueous tunable solvents (OATS), indicating high potential for use in homogeneous catalysis. Based on this information, we applied the systems to the production and recovery of phenols. Our work shows good reactivity in the PEG medium and positive initial results for the product recovery.

In Chapter 5, we look to more conventional processes to enable the coupling of materials with widely varying properties. In this work, we use phase transfer catalysis (PTC) to overcome the mass transfer limitations of siloxylated materials and biomolecules, which are highly immiscible and have little to no reaction in typical organic solvents or the neat medium. In order to illustrate the technique on biomolecules, we reacted a siloxylated benzyl chloride with the amino acid, L-lysine. We also showed the reaction with a number of salts in order to facilitate the analysis and assess the variability in rate between the salts and the amino acid. We also synthesized and tested novel, siloxylated PTCs that should have improved interaction with the siloxane electrophile. The technique functioned efficiently for the coupling of the hydrophilic

agents with the siloxylated moiety. However, the traditional PTCs outperformed the siloxylated materials for most of the tested conditions. PTC shows potential for coupling larger molecules, such as peptides or proteins, with siloxylated materials, allowing for efficient generation of novel compounds.

Finally, in Chapter 6, we look at the conclusions and recommendations related to this research. We show that there are many opportunities for extension of this work into additional applications.

1.1 References

1. DeSimone, J.M., *Practical Approaches to Green Solvents.* Science, 2002. **297**: p. 799-802.

2. Sheldon, R.A., *Green Solvents for sustainable organic synthesis: state of the art.* Green Chemistry, 2005. **7**: p. 267-278.

3. Welton, T., *Room-Temperature Ionic Liquids. Solvents for Synthesis and Catalysis.* Chemical Reviews, 1999. **99**: p. 2071-2083.

4. Beckman, E.J., *Supercritical and near-critical CO2 in green chemical synthesis and processing.* Journal of Supercritical Fluids, 2004. **28**: p. 121-191.

5. Jessop, P.G.S., Bala, *Gas-Expanded Liquids.* Chemical Reviews, 2007. **107**: p. 2666-2694.

6. Kruse, A.D., E., *Hot compressed water as reaction medium and reactant: Properties and synthesis reactions.* Journal of Supercritical Fluids, 2007. **39**: p. 362-380.

7. Heldebrant, D.J.W., Heather N.; Walsh, Sarah M.; Ellis, Taryn; Rauscher Japheth; Jessop, Philip G., *Liquid polymers as solvents for catalytic reductions.* Green Chemistry, 2006. **8**: p. 807-815.

8. West, K.N.H., Jason P.; Jones, Rebecca S.; Bush, David; Liotta, Charles L.; Eckert, Charles A., *CO2-Induced Miscibility of Fluorous and Organic Solvents for Recycling Homogeneous Catalysts.* Industrial and Engineering Chemistry Research, 2004. **43**(4827-4832).

Chapter II: Piperylene Sulfone: Characterization and Reaction Media

2.1 Introduction

Solvents are important for a multitude of industrial reactions but must be separated in order to remove and purify the products. This usually involves any number of separation techniques, from distillation to chromatography. Such methods not only produce environmental pollution in the form of volatile organic compounds (VOCs) but also create huge process expenses. Therefore, researchers have developed numerous types of novel solvents to reduce their environmental impact and ease separations, including supercritical fluids[1], gas-expanded liquids[2], ionic liquids[3], and fluorinated compounds[4].

One important application of solvents involves the dissolution of both hydrophobic and hydrophilic compounds. Due to the property differences, these materials are extremely difficult to dissolve in a single solvent, often times creating biphasic systems. In order to achieve reasonable reaction rates, it becomes necessary to use powerful solvents that can facilitate monophasic conditions. These solvents are usually polar, aprotic materials, such as dimethylsulfoxide (DMSO) or dimethylformamide (DMF). However, these solvents are usually extremely difficult and expensive to remove due to their low volatilities with boiling points of 189 and 153ºC,

respectively. Also, in a recent pharmaceutical industry evaluation, the replacement of DMSO was cited as a key research need.[5] In order to avoid these difficult solvents, phase transfer catalysis (PTCs) is often used to enable reactions in a biphasic environment. There are many types of PTCs, but they are generally onium salts or complexing agents that allow the catalyst to shuttle ions between phases.[6] This allows for improvement in reaction rates of biphasic systems and has been readily adopted in industry with approximately 500 commercial processes using the technique as of the early 1990's.[7] However, PTCs can be toxic and must be removed through aqueous extractions, creating additional waste from the reaction process.

Therefore, we have worked on the development of novel solvents that can facilitate difficult reactions and ease separation. The primary focus for this research involves smart or switchable systems. Smart molecules are compounds that can be irreversibly or reversibly altered to a distinctly different state by activation of a stimulus. The general idea behind these smart molecules is that by changing the properties, we can integrate both reaction and separation into the system. The mechanism for this "switch" can be such stimuli as heat, light, pH, or pressure, forcing the material to undergo a chemical or physical change.

For the design of these molecules, we focus on a number of desirable characteristics for both reaction and separation. For reaction, the solvent should exist as a liquid at reasonable reaction conditions, simultaneously dissolve organics and salts, and have high chemical stability to avoid reaction with substrates. For separation, we want the solvent to "switch" quickly at moderate conditions, "switch" to separable components, and reverse easily.

There have been a number of developments in smart materials primarily related to ionic liquids, surfactants, and responsive systems. Much this work has focused on ionic liquids, which are generally defined as salts that are in the liquid phase below 100ºC. There has been great interest in these systems as solvents due to their incredibly low volatilities, making them a possible "green" option for reaction media. However, due to their low vapor pressures, separation of the solvent can be extremely difficult, providing a key motivation for development of novel solvents that allow for easy separation.

Dialkylammonium dialkylcarbamates represent one of the first classes of switchable ionic liquids. The most common form is dimethylammonium dimethylcarbamate (DIMCARB), which has been active since the 1950's. It was utilized in the petroleum industry to extract aromatics and sulfur products from hydrocarbon streams.[8] It is reversible through thermal decomposition at modest temperatures (60ºC), breaking down into two gaseous products, carbon dioxide and dimethylamine. The solvent can be reformed by combining the decomposition products at a low temperature.[9] The general form is illustrated in Figure 2-1 and the key properties, including melting point and decomposition temperature, can be tuned by altering the R groups attached to the amine. Jessop *et al.* recently extended this work, by completing the characterization of a number of structural variations and application to homogeneous catalyst recovery.[10]

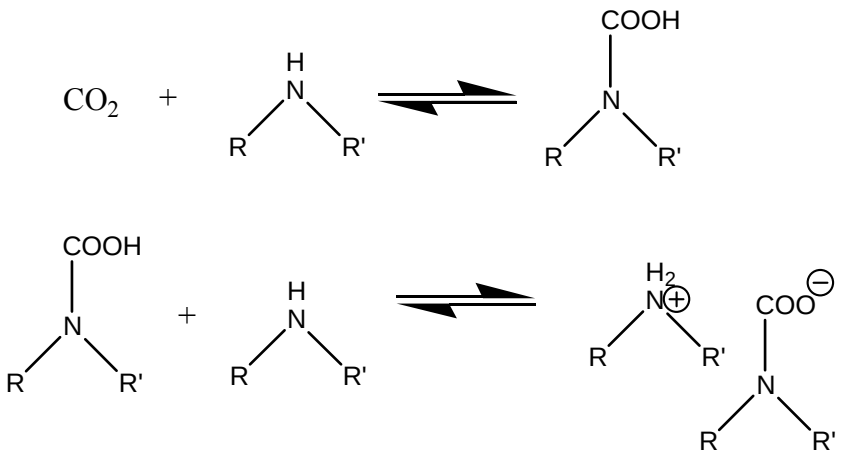

Figure 2-1 Reversible Ionic Liquid: DIMCARB

More recently, we have developed switchable ionic liquids that use amidines or guanidines in combination with alcohols and carbon dioxide.[11, 12] These materials are formed by bubbling carbon dioxide through a mixture of amidine/alcohol or guanidine/alcohol. They can be reversed by bubbling nitrogen through or heating the liquid to revert back to the non-ionic form. Figure 2-2 illustrates the guanidine based systems with 2-butyl-1,1,3,3-tetramethylguanidine, while Figure 2-3 shows the amidine-based systems with 1,8-diazabicyclo-[5.4.0]-undec-7-ene (DBU). The reversibility from a molecular to ionic state allows for a distinct change in polarity, enabling separations to take place. The non-ionic forms are miscible with alkanes, such as heptane and decane, while the ionic form separates from such solvents. We have utilized this system to enable homogenous reaction and heterogeneous separation.[13]

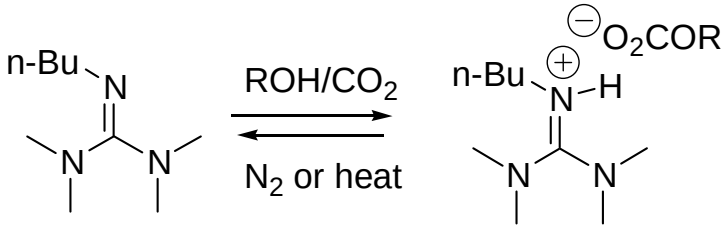

Figure 2-2 Guanidine Reversible Ionic Liquids

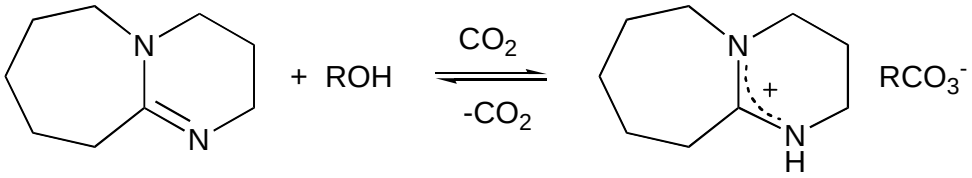

Figure 2-3 Amidine Reversible Ionic Liquid

We have focused this research on the development of polar, aprotic solvents that can exhibit excellent solvent properties along with easy separation. Therefore, we investigated the potential of sulfolenes, which are generated through the reversible cheletropic reaction of sulfur dioxide and a diene. These are reversible and recyclable dipolar, aprotic solvents that have similar solvent properties to DMSO, but can be easily separated through thermal decomposition to volatile components. Figure 2-4 illustrates the structural variety of these molecules by simply altering the choice of diene, allowing for variable melting points and decomposition rates.

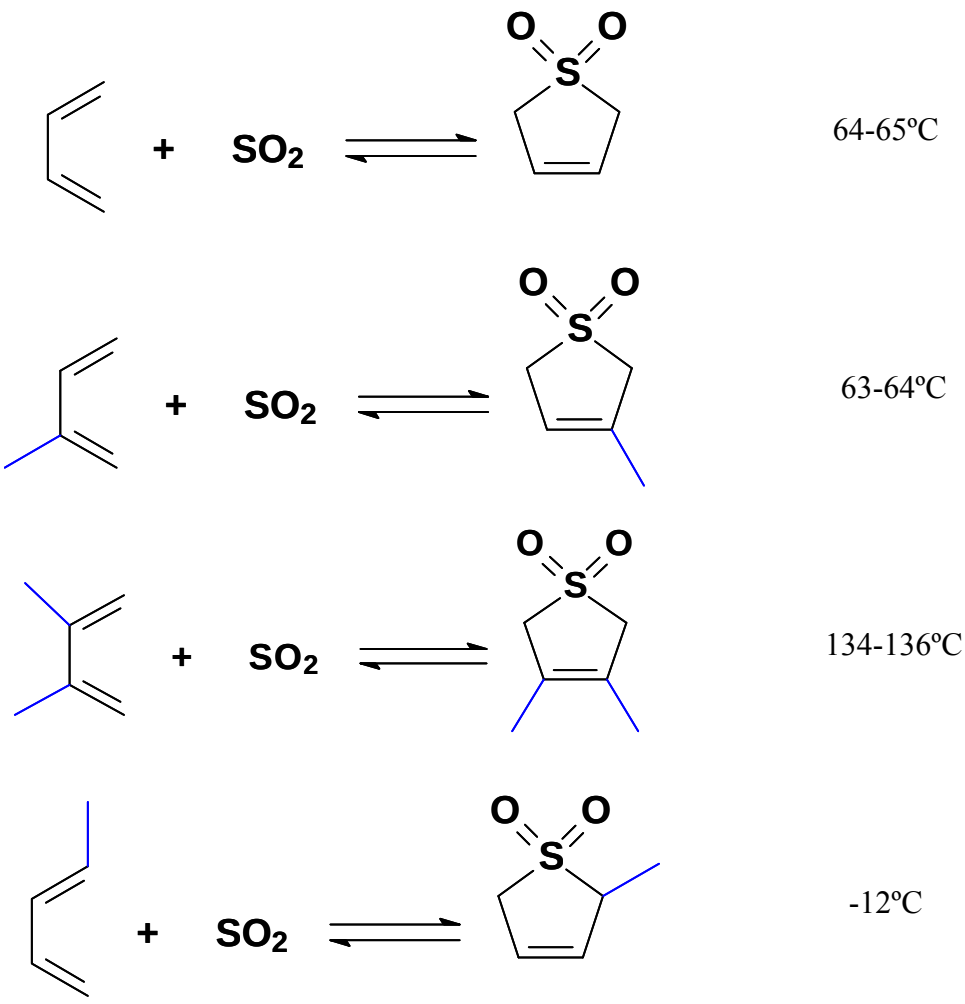

Figure 2-4 Cheletropic Reactions of Sulfur Dioxide with Various Dienes

These switchable solvents use heat to switch from molecules with low volatility to those with high. At low temperatures, we can use the sulfolenes as reaction media, providing a low-volatility solvent with excellent properties for the dissolution of a wide variety of substrates. After reaction completion, the solvent can be thermally decomposed, undergoing the retro-cheletropic reaction to the highly volatile products of diene and sulfur dioxide. The reaction is illustrated in Figure 2-5. The decomposition

allows for easy product isolation and solvent recycle through recombination of the volatile components at low temperatures.

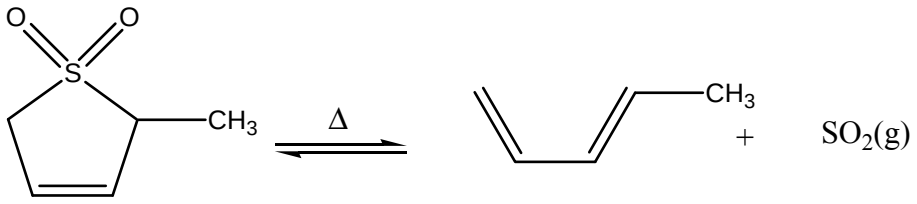

Figure 2-5 Retro-Cheletropic Reaction of Piperylene Sulfone to Piperylene and Sulfur Dioxide with Heat

Figure 2-6 illustrates the decomposition half lives of these sulfolenes calculated from kinetic data in the literature.[14] As the plot indicates, the structural variation on the sulfolenes influences the stability of the molecule. Based on this information and the melting points, we chose to focus our research on piperylene sulfone. It has a low melting point at -12ºC and reduced decomposition temperature, allowing it to exist as a liquid at room temperature and decompose at around 100ºC. In order to assess the potential of this novel switchable solvent, we characterized it for a number of solvent parameters and applied it to several reaction systems, including nucleophilic substitutions, Diels-Alder, and organometallic-catalyzed reactions.

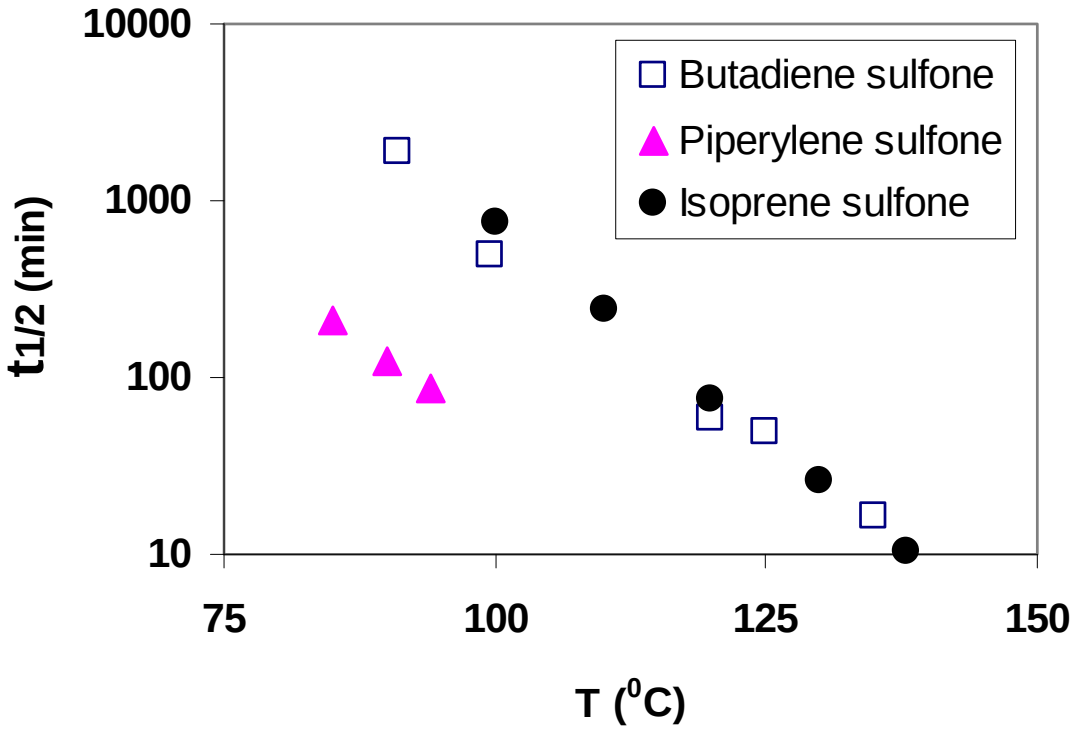

Figure 2-6 Decomposition Half Life of Several Sulfones

2.2 Experimental

2.2.1 Materials

The following materials were used as received from the suppliers: piperylene (Aldrich, 90% mixture of isomers), sulfur dioxide (Air Gas, 99.98%), n-phenyl-β-napthylamine (Aldrich, 97%), dichloromethane (EMD, 99.97%), N,N-dimethyl-4-nitroaniline (Alfa-Aesar, 98+%), N,N-dimethyl-4-nitrosoaniline (Sigma-Aldrich, 97%), 2,6-diphenyl-4 (2,4,6-triphenylpyridinium-1-yl) phenolate dehydrate, dimethylsulfoxide (Baker, 99.9%), benzyl chloride (Aldrich, 99%), potassium thiocyanate (Fisher, 99.0%), potassium cyanide (Aldrich, 97%, ACS reagent grade), potassium acetate (Sigma-Aldrich, ACS, 99+%), potassium thioacetate (Fluka, >98%), cesium azide (Aldrich, 99.99%),

cesium acetate (Aldrich, 99.99%), sodium pyrrolidindithiocarbamate, 4-Phenyl-1,2,4-triazoline-3,5-dione, anthracene (Aldrich, 99%), 9-methylanthracene (Aldrich, 98%), butadiene (Sigma-Aldrich, >99%), acetophenone (Aldrich, 99%), and dichloro(*p*-cymene)ruthenium(II) dimer (Aldrich, 97%). The carbon dioxide was SFC grade (Air Gas, 99.999%) and further purified to remove trace water and other impurities with a Matheson gas purifier and filter cartridge (Model 450B, Type 451 filter).

2.2.2 Piperylene Sulfone Synthesis

The synthesis of piperylene sulfone is an adaptation of the method developed by Krug and Rigney.[15] In a 1 L Parr hydrogenator bottle, we combine 1,3-pentadiene (mixture of isomers) with sulfur dioxide and phenyl-β-naphthylamine, an inhibitor that prevents the polymerization of the diene. The mixture is then shaken in the hydrogenator bottle and reacted at room temperature for two days. The reaction primarily takes place with the trans-piperylene, resulting in approximately 50% product yield. We then extract the product with water and filter it, eliminating the inhibitor and removing the product from the mixture. Finally, we complete the purification with a back extraction into dichloromethane, which can then be evaporated, leaving pure piperylene sulfone. Additionally, further purification was completed on the material used for the characterization studies due to the need for high solvent purity. To this end, we used short-path distillation to remove trace contaminants, primarily consisting of inhibitor. The purified material was analyzed by ^{1}H and ^{13}C NMR (^{1}H NMR (ppm): δ = 1.36 (d, 3H), 3.69 (m, 3H), 5.96 (m, 2H), ^{13}C NMR (ppm): δ = 12.9, 54.8, 59.4, 122.5, 131.4) and verified according to literature sources.[16, 17] Most of the early work on the

nucleophilic substitution and Diels-Alder reactions used piperylene sulfone from this early method. However, later reactions used the synthetic method described in Appendix A, which details the scale-up production of the solvent.

2.2.3 Nucleophilic Substitutions Reactions

The nucleophilic substitution of benzyl chloride with various nucleophiles, as shown in Figure 2-11, was carried out in round bottom flasks equipped with Teflon-coated magnetic stir bars. The vessels were filled with 1 mL of piperylene sulfone or DMSO and between 0 and 10% water. The nucleophiles were added to the mixture and then the vessels were covered with rubber septa. The flask was then placed in an oil bath set to the appropriate temperature. We allowed the system to mix at the reaction temperature for 30 minutes and then added 0.15 mmol benzyl chloride with an Eppendorf pipette. In order to ascertain the kinetics, we took between 0.05 and 0.1 mL aliquots from the reaction mixture at regular intervals of 10 minutes over 1 hour and then quenched the samples in toluene. The samples were then analyzed by GC-FID (HP 6890 GC) to follow the reaction progress. The concentrations for the initial reactions with potassium thiocyanate were determined with calibration curves for the reactant and product. The calibration allowed for direct calculation of the concentrations, which led to determination of the conversions over time and the rate constant. For the various nucleophiles, we used direct comparison of the GC peak areas to determine the conversions.

2.2.4 Telomerization Reaction

The telomerization shown in Figure 2-14 was carried out in a 300 mL windowed, Parr reactor. The reactor was loaded with catalyst, ligand, water, and solvent, and then closed to the atmosphere. The cell was evacuated with a vacuum pump to remove all traces of air and 1,3-butadiene was added. The reactor was then pressurized to 200 psi with carbon dioxide via an ISCO syringe pump. Finally, the temperature was increased to 70ºC to allow the reaction to start. The 1,3-butadiene was in excess during these runs in order to use the loss of water to determine the reaction conversion. This was analyzed by Karl-Fisher titration with Mettler-Toledo Model DL31 device. The selectivity toward 2,7-octadienol was determined by GC-MS with an HP 6890 with HP 5973 MS.

2.2.5 Asymmetric Transfer Hydrogenation

The asymmetric transfer hydrogenation of acetophenone shown in Figure 2-15 was carried out with piperylene sulfone in glass tubes equipped with magnetic stir bars. The piperylene sulfone was pretreated with sodium bicarbonate and placed under vacuum for at least one hour to remove any trace sulfur dioxide. The catalyst, ligand, and sodium formate (260 mg) were weighed out and added to the glass tube. Next, we degassed the vessel and added the 1 mL of piperylene sulfone with 0.1 mL water under nitrogen. We then placed the system in an oil bath set to the 40ºC and allowed it to react for one hour to form the in-situ catalyst. The acetophenone was then added to start the reaction, allowing it to proceed from one to twelve hours. After reaction completion, we removed an aliquot to test for conversion and enantioselectivity. The conversion analysis was completed with GC-MS (GC-2010 Shimadzu with GCMS-QP2010S), while the

enantioselectivity was assessed with HPLC-MS (HP Series 1100 MSD). The products were extracted with ether to allow for recycle of the solvent and catalyst

2.2.6 Decomposition/Reformation of Piperylene Sulfone

The decomposition of piperylene sulfone was performed with TA instruments thermal gravimetric analyzer (TGA) Model Q50. The analysis conditions included a heat rate of 5ºC/min up to 120ºC, where it was held for 30 minutes. For the full recycle process, we decomposed the piperylene sulfone at 110ºC with a heating mantle connected to a temperature controller. At this temperature, both decomposition species are gaseous and can be transferred to a vessel containing liquid sulfur dioxide at approximately -30ºC. The reformation vessel contains a substantial excess of the sulfur dioxide to ensure minimal concentrations of piperylene and avoid polymerization of the species. After the solvent is fully decomposed, the reformation vessel with liquid sulfur dioxide and piperylene is transferred to a bomb and mixed for two days at 25ºC to complete the reformation process. The solvent can then be purified and reused for reaction.

2.3 Results

2.3.1 Characterization

In order to characterize piperylene sulfone, we determined its Kamlet-Taft parameters, π^*, α, and β, as well as its $E_T(30)$ solvent parameter and dielectric constant.[18, 19] These parameters have been well studied in numerous solvents, allowing for comparison of properties related to polarity and hydrogen bonding. Besides dielectric constant, all the parameters can be determined spectroscopically based on

solvatochromic effects, which use the UV absorbance of various probe dyes to assess the properties. The spectra will change depending on certain properties of the solvent and can be observed by following the wavelength at the maximum absorbance.

The Kamlet-Taft parameters are solvatochromic indicators that determine relative solvent strength in terms of polarity and hydrogen bonding ability.[20-22] The parameter π^* is indicative of the dipolarity and polarizability of the solvent, characterizing its ability to stabilize charges and dipoles. This factor was observed with the probe dye, N,N-dimethyl-4-nitroaniline, as shown in Figure 2-7.

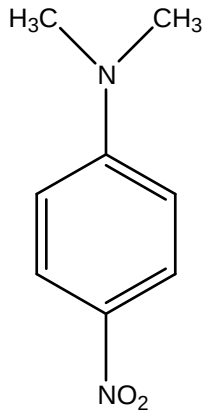

Figure 2-7 Structure of N,N-dimethyl-4-nitroaniline for π* Determination

The parameter α represents the hydrogen bond donating capability of the solvent, indicating the acidity. This value is related to π^* and E_T30 through equations defined in the literature and can thus be determined by measuring these factors. The β parameter represents the solvent's hydrogen bond accepting ability or its basicity. For the β parameter, we used N,N-dimethyl-4-nitrosoaniline and N-methyl-nitrosoaniline as the indicator dyes, which are illustrated in Figure 2-8.

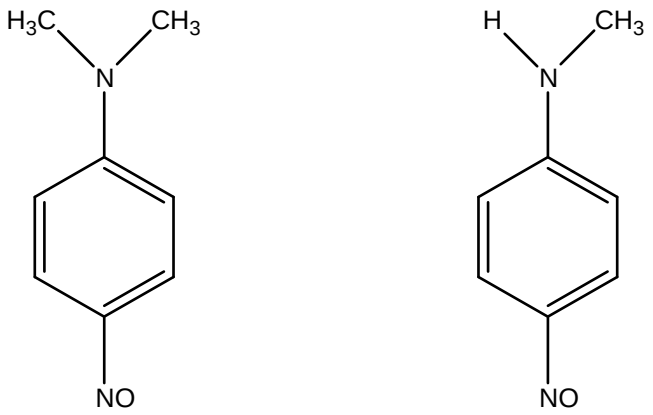

Figure 2-8 Structure of N,N-dimethyl-4-nitrosoaniline (left) and N-methyl-nitrosoaniline (right) for β Determination

The $E_T(30)$ value is defined as the transition energy required to raise one mole of dissolved dye to its excited state. It represents a combination of the dipolarity/polarizability and the hydrogen bond donating ability and can be determined with the UV absorbance of Reichardt's dye (2,6-diphenyl-4 (2,4,6-triphenylpyridinium-1-yl) phenolate dehydrate, $C_{41}H_{29}NO\ 2H_20$), shown in Figure 2-9.

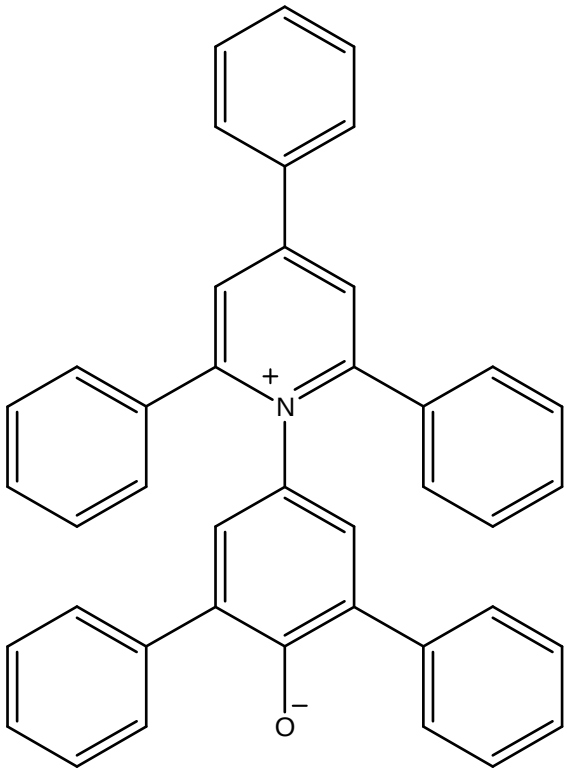

Figure 2-9 Structure of Reichardt's dye (2,6-diphenyl-4 (2,4,6-triphenylpyridinium-1-yl) phenolate dehydrate for $E_t(30)$ Determination

The last value for characterization is the dielectric constant, or the permittivity of a medium relative to a vacuum. This is another parameter often used for assessing the polarity of the solvent, providing an additional indicator for solvent comparison. Table 2-1 illustrates the values we obtained for these parameters, as well as some common solvent properties:

Table 2-1 Solvent Properties of DMSO and Piperylene Sulfone

Property	***DMSO*** 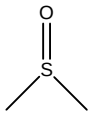	***Piperylene Sulfone*** 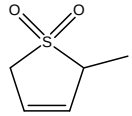
Boiling Point (ºC)	189	decomposes
Melting Point (ºC)	16-19	-12
α	0	0 ± 0.1
β	0.76	0.46 ± 0.08
π^*	1.00	0.87 ± 0.04
$E_t(30)$ (kJ/mol)	189	189 ± 0.3
ε	46.7	42.6

As the above table shows, the solvent properties of piperylene sulfone are comparable to those of DMSO, indicating that they possess approximately the same solvent strength. The primary difference between the solvents is the β parameter, which is much smaller in the piperylene sulfone. This is most likely a result of the differences between sulfoxide and sulfone functionality. However, the overall differences are relatively small, indicating that the solvents should exhibit similar solvation behavior.

2.3.2 Reaction Applications

2.3.2.1 Nucleophilic Substitution Reactions

We used the nucleophilic substitution of benzyl chloride with potassium thiocyanate as a probe reaction to demonstrate the ability of piperylene sulfone to accommodate a reaction involving both an organic and a salt. This reaction characterized the types of systems that involve highly hydrophobic and hydrophilic materials, which usually require phase transfer catalysts to overcome the mass transfer limitations. The model reaction is shown in Figure 2-10.

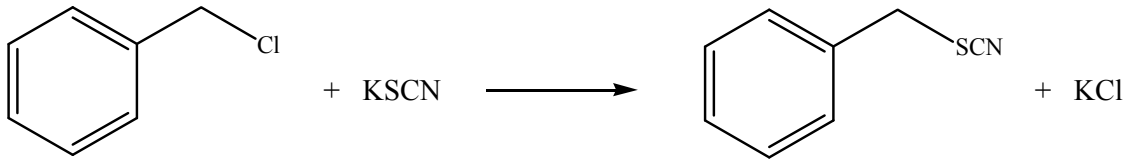

Figure 2-10 Reaction of Benzyl Chloride with Potassium Thiocyanate

The reaction was tested at temperatures ranging from 40 to 60ºC to obtain kinetic data for the rate constants and activation energy. For this initial set of data, we did not monitor nor factor in the solvent water concentration. Though relatively small, we found in our later work that even low levels of water can make a significant impact upon the rate. However, the initial data provide important insights into the temperature effect and, thus, the activation energy, which we did not address in the subsequent work on additional nucleophiles and exact water concentrations. The results for the nucleophilic substitution of benzyl chloride with potassium thiocyanate are shown in the Table 2-2 with a comparison to DMSO:

Table 2-2 Second Order Rate Constants for the Reaction of benzyl chloride with potassium thiocyanate

Temperature (°C)	Second Order Rate Constants (mL/mol/sec)	
	DMSO	Piperylene Sulfone
40	0.97	0.6 ± 0.06
50	1.46	1.08 ± 0.06
60	3.35	2.32 ± 0.01

The rates in piperylene sulfone are slightly slower than those in DMSO but they are within the same order of magnitude, indicating that piperylene sulfone is a competitive replacement for DMSO. From these data, we were able to determine the activation energy of the reaction within each solvent by using the Arrhenius equation and plotting the natural log of the rate constant versus the inverse temperature. The activation energies are very similar at 58.4±2.5 kJ/mol and 66.6 kJ/mol in piperylene sulfone and DMSO, respectively, indicating comparable reactivity in the novel solvent medium.

In order to present a full characterization of the kinetic behavior, we continued the investigation by testing the nucleophilic substitution of benzyl chloride with a variety of nucleophiles within piperylene sulfone. The general scheme for the reaction is shown in Figure 2-11 with the data illustrated in Table 2-3.

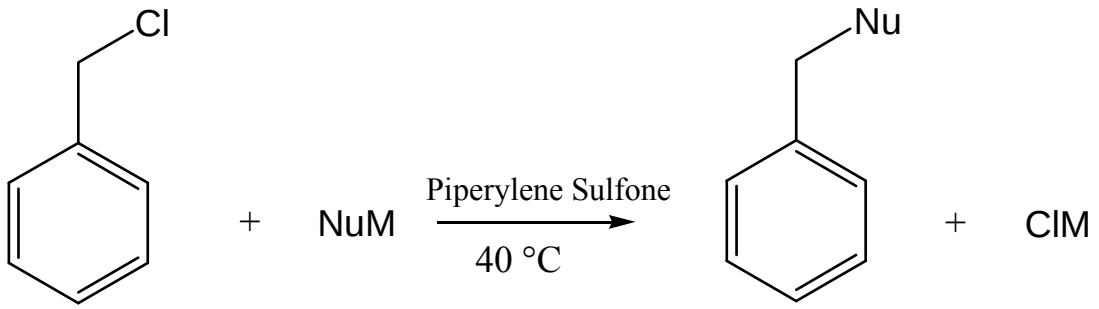

Figure 2-11 Nucleophilic Substitution of Benzyl Chloride with Various Nucleophiles in Piperylene Sulfone at 40°C

Table 2-3 Second Order Rate Constant (mL mol $^{-1}$ sec^{-1}) for Nucleophilic Substitution of Benzyl Chloride with Various Nucleophiles at 40°C (k x 10^{1})

Nucleophile	DMSO	DMSO + 3% H_2O	Piperylene Sulfone	Piperylene Sulfone + 1% H_2O
KTA[a]	>1800	>1800	>1800	>1800
NaPDTC[b]	>1800	>1800	>1800	>1800
CsN_3	69 ± 1	16.7 ± 0.9	2.4 ± 0.9	5.8 ± 0.9
CsOAc	22.7 ± 0.6	16.4 ± 0.2	0.35 ± 0.04	0.35 ± 0.06
KOAc	3.4 ± 0.1	11.0 ± 0.1	0.013 ± 0.004	0.19 ± 0.01
KCN[c]	5.8 ± 0.8	17 ± 5	-	0.15 ± 0.01
KSCN	1.4 ± 0.1	1.7 ± 0.1	2.1 ± 0.1	2.3 ±0.2

[a] Potassium thioacetate, [b] Sodium pyrrolidinedithiocarbamate, [c] No reaction in KCN in piperylene sulfone without water

The nucleophilic substitution data illustrate that we can achieve excellent reactivity within piperylene sulfone. In general, the rate constants for the novel solvent are slightly lower than that of DMSO. We attribute this to the difference in the solvent properties, specifically related to the reduction in the hydrogen bond accepting capability. This could influence the solvation of the cation, which could affect the ion-pair separation and, thus, the nucleophilicity of the anion.[7] DMSO could solvate the cation better due to its solvent properties, thereby increasing the reaction rate beyond that in piperylene sulfone. Also, we found that by adding a mere 0.1% of water to the piperylene sulfone, the rate constants could be significantly affected. In the case of potassium cyanide, we observed no reaction without the presence of water. The other nucleophiles were not as drastically affected, but did show modest rate increases from small additions of water for many of the reactions. We believe this effect could be due to a phenomenon that is frequently observed in solid-liquid PTC, in which small concentrations of water enable enhancement in the dissolution of salts.[7] In our work, most of the nucleophilic salts were only partially soluble in the piperylene sulfone, allowing for a heterogeneous salt phase to remain present during reaction. Hence, the water could have a strong influence on the dissolution of these salts into piperylene sulfone.

2.3.2.2 Diels-Alder Reaction

In order to assess the breadth of reaction applications possible in piperylene sulfone, we attempted to test the Diels-Alder reaction of anthracene with 4-Phenyl-1,2,4-triazoline-3,5-dione (PTAD), as shown in Figure 2-12. This reaction has been used

extensively to characterize solvent properties of organic and supercritical media. [23] We have recently used this system to study solvent effects in gas-expanded liquids [24], making it a natural selection for the further characterization of piperylene sulfone. We studied the kinetics of the reaction with fluorescence spectroscopy by following the disappearance of anthracene under pseudo-first order conditions.

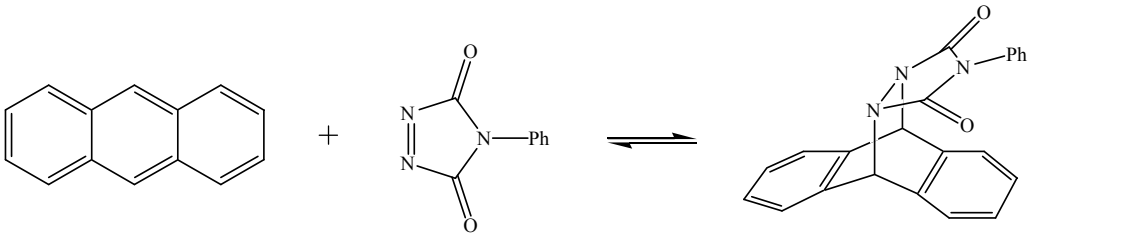

Anthracene

4-Phenyl-1,2,4-triazoline-3,5-dione (PTAD)

8,9,10,11-Dibenzo-4-phenyl-2,4,6-triaza[5,2,5,$0^{2,6}$]tricyclo-undeca-8,10-diene-3,5-dione (Adduct)

Figure 2-12 Diels-Alder Reaction Between Anthracene and PTAD in Piperylene Sulfone

However, we were unable to monitor the reaction due to the extremely low solubility of anthracene in piperylene sulfone. Hence, we switched the diene to 9-methylanthracene, thereby reducing the symmetry and increasing the solubility in the solvent. The modified reaction is shown in Figure 2-13.

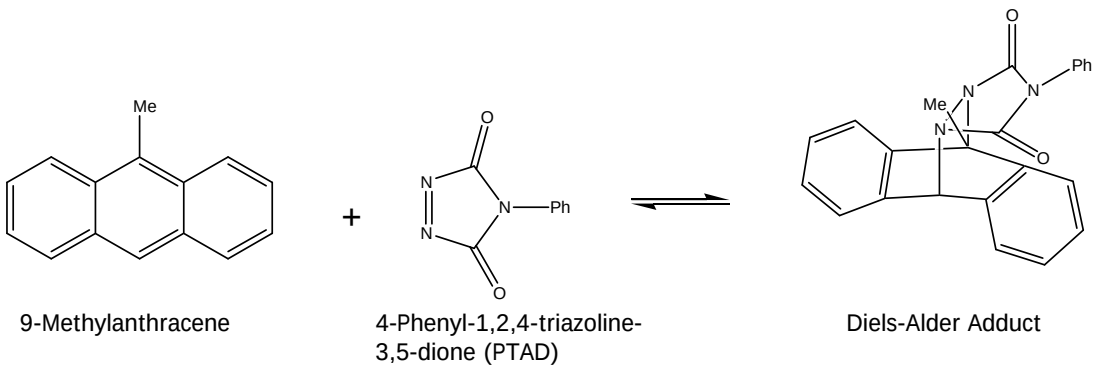

Figure 2-13 Diels-Alder Reaction Between 9-Methylanthracene and PTAD in Piperylene Sulfone

We observed significant improvements in solubility of the diene in piperylene sulfone. However, after making the solution of PTAD and piperylene sulfone, we observed a rapid color change, indicating reaction or decomposition of the reactant. This dienophile is known to be highly reactive, allowing for fast reaction times but also frequent interaction with the solvent. Ford *et al.* observed similar color changes in a number of common solvents, including tetrahydrofuran, ethyl acetate, and chloroform.[24] Therefore, we concluded work on this reaction system and switched our focus to other applications that are described in the following sections.

2.3.2.3 Telomerization of Butadiene with Water

The next reaction for our switchable solvents is the industrial telomerization of butadiene with water. The reaction produces 2,7-octadienol, which is used as a fine chemical intermediate for the production of n-octanol and 1,9-nonanediol.[25] The reaction scheme is shown in Figure 2-14. By completing this work, we wanted to demonstrate the full potential of our switchable solvents for a relevant engineering

process. This is important for the implementation of our solvent system beyond the laboratory, illustrating its applicability to industrial reactions and separations.

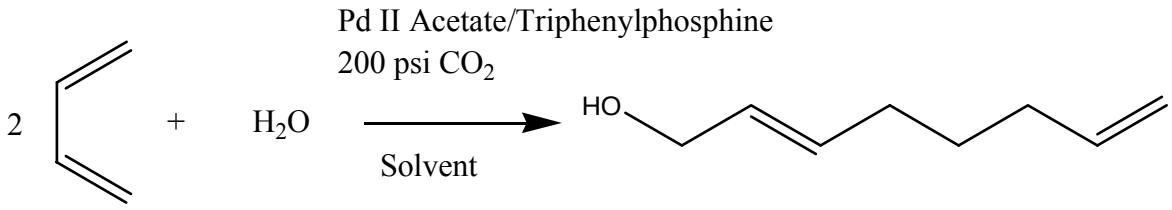

Figure 2-14 Reaction Scheme for Telomerization of Butadiene with Water

The current process in use was patented by Kuraray Company in 1988.[26] It involves a biphasic system containing an aqueous phase and an organic, butadiene phase. The reaction is catalyzed by a water-soluble palladium catalyst and enhanced by the presence of a phosphine ligand. To improve contact between the water and butadiene, the authors added sulfolane as a cosolvent, increasing the solubility of butadiene in the water. This allows for reasonable reaction rates for the production of 2,7-octadienol, but the presence of a cosolvent causes the product to partition into both phases. Normally, one could use distillation to remove the product, but this was deemed unacceptable due to deactivation of the palladium catalyst. Instead, the authors used multiple hexane extractions to remove the product. However, this process removed small amounts of catalyst that could create problems later in the system during purification of the product. Hence, the authors added an additional water extraction step to remove the catalyst. The material can then be safely sent on to the purification steps. In general, product isolation

is the main problem associated with this process. The issue stems directly from the use of sulfolane as a cosolvent. However, its use is absolutely essential in order to maintain reaction efficiency. This represents a key opportunity for our switchable solvents, which can use their built-in switch to simplify the separation of the cosolvent and product.

In order to verify our technique, we replicated the literature reaction that used palladium acetate and triphenylphosphine as the catalyst/ligand combination and dimethylformamide (DMF) as the solvent.[27] The reaction resulted in over 80% conversion with 98% selectivity, illustrating comparable values to those described in the literature. We then replaced the solvent with our switchable solvent, butadiene sulfone. We chose this sulfolene instead of piperylene sulfone due to its enhanced stability under the elevated reaction temperature. However, in this case, we were unable to observe any reaction.

We believe this is due to the way in which our switchable solvents work. Essentially, the switch is an equilibrium that can be controlled by manipulation of the temperature. At low temperatures, the equilibrium constant is very high for the solvent, but we will have a small fraction of the material in the form of the decomposition products. This means that we could possibly have parts per million levels of sulfur dioxide in our system. It is well known that a variety of metal catalysts, including palladium, are easily deactivated by sulfur dioxide at low concentrations.[28, 29] Hence, we believe the equilibrium of the butadiene sulfone generated enough sulfur dioxide to completely deactivate the palladium acetate, causing the reaction to fail.

Despite this loss, we believe other metal catalyzed reactions could be successful in the switchable solvent medium. This is due to the fact that the telomerization reaction

had a number of key issues that could not be readily modified. The primary point is related to catalyst sensitivity. In this reaction, we were focused on using palladium catalysts, which are highly sensitive to poisoning and deactivation. We believe that by focusing on less sensitive catalysts, such as Ruthenium, the sulfones will be able to accommodate organometallic catalysts and allow for homogeneous catalyst recycle.[30]

2.3.2.4 Asymmetric Transfer Hydrogenations

Therefore, we continued our work on organometallic-catalyzed reactions with the asymmetric transfer hydrogenation (ATH) of ketones, which represents an important type of reaction for the generation of chiral alcohols.[31] Such alcohols are important intermediates for a wide array of applications for such areas as pharmaceutical syntheses. In recent years, numerous strategies have been developed to enable recycle of the expensive homogenous catalysts that are typically employed in the process. These types of catalysts are excellent for both activity and selectivity, but are extremely difficult to recover due to their homogenous nature. Therefore, researchers have looked to tethering with both heterogeneous and homogeneous supports.[32] The heterogeneous systems allow for simple separation through filtration of the solid, but can suffer from mass transfer limitations and leaching of the metal, leading to reduced reaction efficiency and catalyst recycle. Other strategies involve homogeneous tethering to soluble polymer supports, such as poly(ethylene glycol) (PEG), and reaction in aqueous solutions, which allow for alkyl hydrocarbon extraction of the products.[31, 33] However, there is still a strong need for development of recyclable catalytic systems that can increase reaction efficiency and recycle of the expensive homogeneous catalysts.

Therefore, we applied our switchable solvents to the transformations, using the switchability to recover and reuse the organometallic catalyst. For this work, we focused on the ATH of acetophenone in piperylene sulfone with sodium formate and a homogeneous Ruthenium catalyst. The reaction is illustrated in Figure 2-15 with the catalyst and ligand pictured in Figure 2-16.

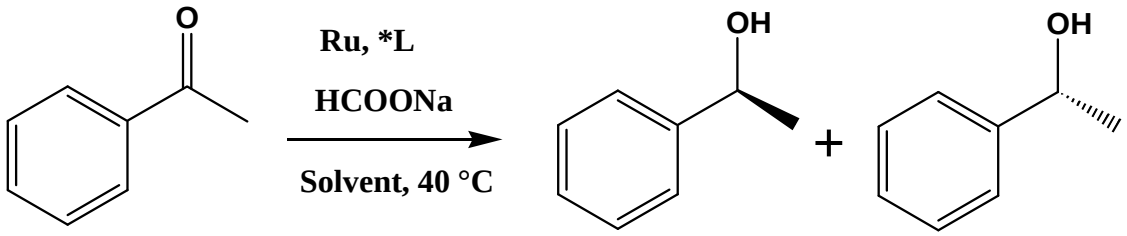

Figure 2-15 Asymmetric Hydrogenation of Acetophenone

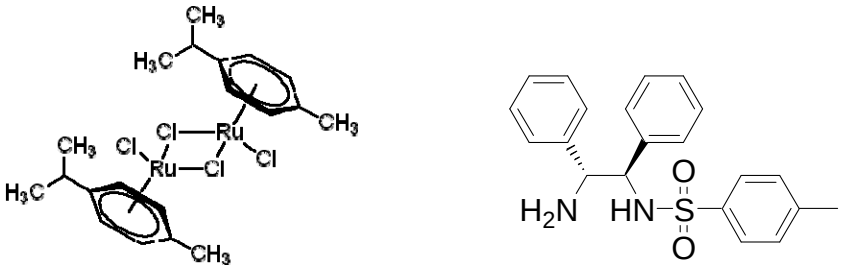

Figure 2-16 Ruthenium Catalyst (left) and Ligand (right) for Asymmetric Hydrogenation of Acetophenone

The asymmetric transfer hydrogenations were primarily carried out by another group member, who tested the reactions on various aryl ketones and investigated the recycle potential. We found excellent yields with high enantioselectivity, resulting in

>99% conversion with 97% enantiomeric excess after only one hour at 40ºC. We were able to recycle the catalyst and solvent three times with no loss in activity or enantioselectivity. However, the piperylene sulfone transformed from a liquid to a solid over the course of the recycle. We believe this occurred due to the isomerization of the piperylene sulfone, which can take place under strongly basic conditions, as shown in Figure 2-17. Such conditions arise in the reaction media due to formation of sodium hydroxide as a byproduct of the ATH. Thus, the focus for this research involves the development of a separation technique that can eliminate this detrimental compound.

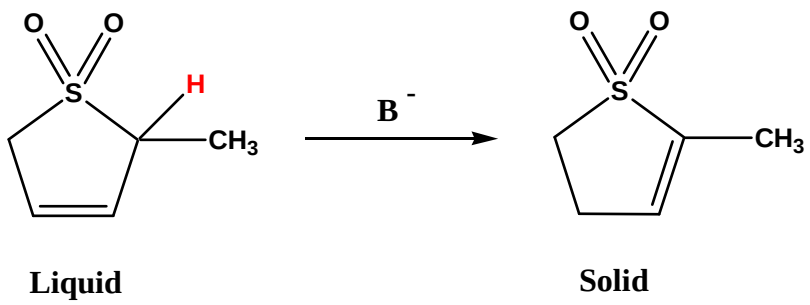

Figure 2-17 Isomerization of Piperylene Sulfone under Strong Basic Conditions

The solution for this problem came about from a vastly different area of research related to the sequestration of carbon dioxide. Due to increasing restrictions in greenhouse gas emissions, there has been expansive research into sequestration techniques that allow for removal of CO_2. One such technique involves the use of bases, such as sodium hydroxide, to remove CO_2 via reaction to a carbonate salt, as illustrated in

Figure 2-18. We utilized this technique to accomplish the reverse process, in which we capture and eliminate the sodium hydroxide by reaction with CO_2. The carbonate salt is highly insoluble in piperylene sulfone, allowing it to precipitate out of solution and enable recycle of the solvent without build-up of the negative material.

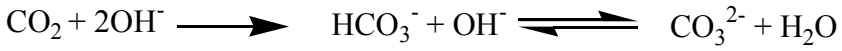

Figure 2-18 Formation of Carbonate Salt from Reaction of CO_2 with Hydroxide

We tested this on pure piperylene sulfone. In the control experiment, we added concentrated sodium hydroxide and stirred the mixture at room temperature. The solution immediately turned a pale yellow color. In the test experiment, we slowly bubbled CO_2 through the solution and then simultaneously added the sodium hydroxide. The solution remained clear and a white precipitate could be seen crashing out of the liquid. We have not yet applied this method to the recycle process, but the general strategy will involve reaction followed by product extraction and then CO_2 bubbling to remove the sodium hydroxide. We can then recycle the solvent and catalyst without byproduct issues. This technique also has a broader impact beyond the scope of ATH reactions. It could enable use of the switchable systems in other reactions that use or generate bases, expanding our solvent into realms that were not possible due to this harmful interaction.

2.3.3 Decomposition & Reformation

In order to prove the viability of the piperylene sulfone solvent system, it was necessary to demonstrate decomposition and reformation of the solvent. Figure 2-19

illustrates the thermal gravimetric analysis (TGA) data for the decomposition of piperylene sulfone.

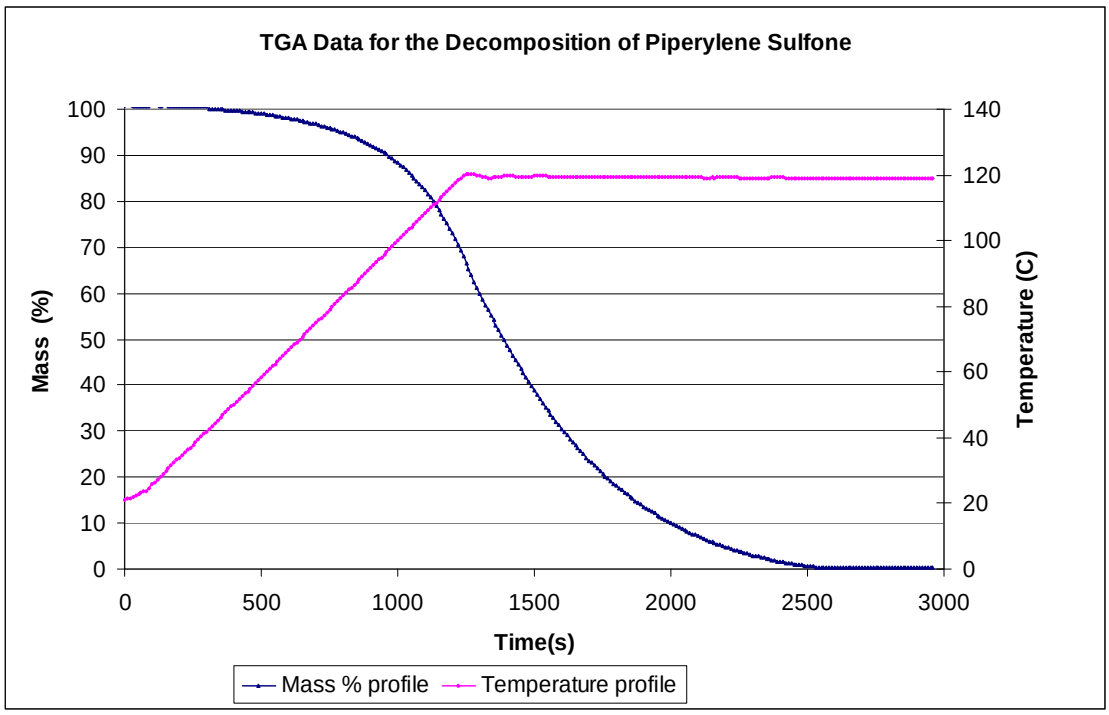

Figure 2-19. Thermal Gravimetric Analysis Data for the Decomposition of Piperylene Sulfone

This confirms complete loss of mass and indicates that we can achieve complete decomposition below 120ºC without polymerization of the diene. We then attempted to combine the decomposition with the reformation to show the recycle capability of the system. We ran the nucleophilic substitution of benzyl chloride with potassium thiocyanate in piperylene sulfone and then decomposed the solvent. The volatile decomposition products were collected and then reformed. The reaction products were recovered after the decomposition process and showed 96% yield. Without optimization, we were able to achieve 87% recovery of the solvent. We believe that through both

optimization and scale-up, the process can be significantly improved to increase the recovery efficiency.

The complete cycle for the reaction and separation process is shown in Figure 2-20. This process consists of the four main steps. The first involves reaction in piperylene sulfone as the solvent, followed by decomposition of the solvent at 110ºC. This allows for recovery of the products and reformation of the solvent at 25ºC for complete recycle.

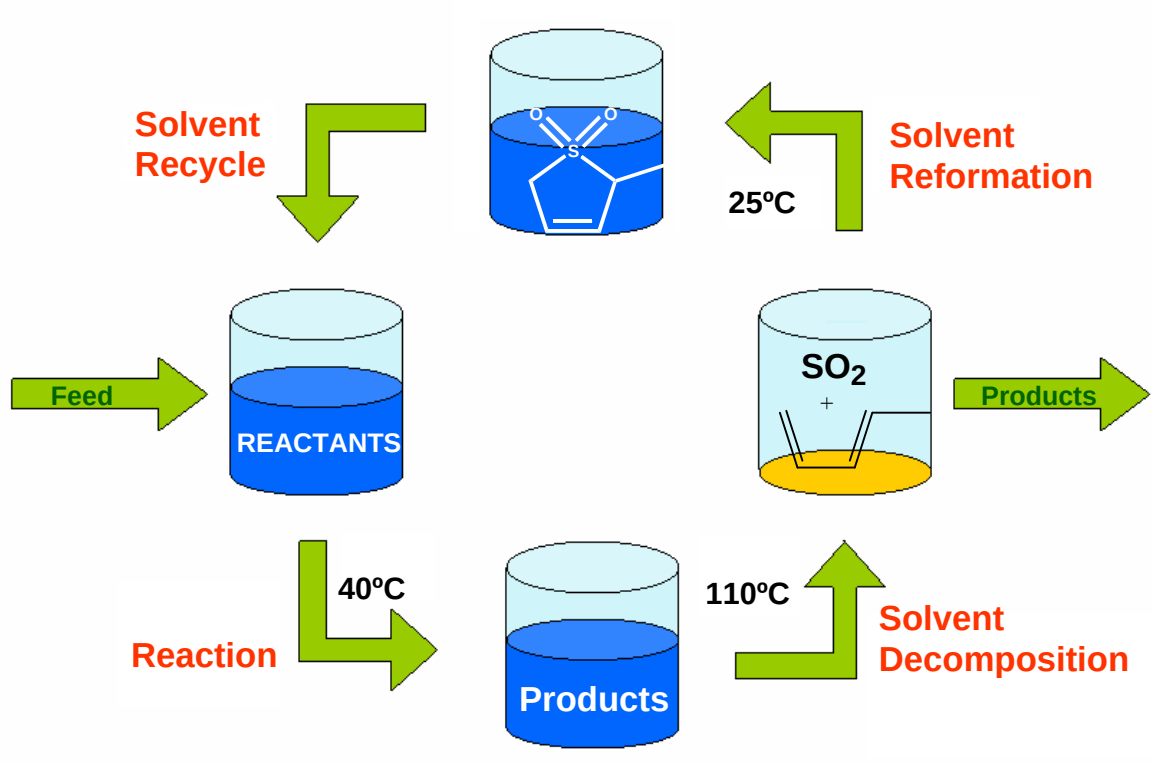

Figure 2-20 Complete Cycle for Use and Recovery of Piperylene Sulfone

2.4 Conclusions

Piperylene sulfone is representative of a novel class of switchable solvents that can enable efficient reaction and easy separation. This molecule is a polar, aprotic solvent and illustrates similar solvent properties to DMSO, indicating excellent solubility of solutes with widely varying properties. Unlike DMSO, piperylene sulfone has a built-in thermal switch, which allows for decomposition to volatile components. These can be efficiently removed and recombined to enable product and catalyst isolation.

We have investigated several applications of the solvent to important classes of reactions, including nucleophilic substitutions, Diels-Alder reactions, and organometallic-catalyzed reactions. The switchable solvent functioned well for the nucleophilic substitutions, enabling high product recovery and good solvent reformation. Due to interactions with reactants or catalysts, we could not apply the solvent to the Diels-Alder reaction or the telomerization of butadiene with water. However, proper selection of reactants or catalysts could allow the solvent to work quite effectively in these systems. The asymmetric transfer hydrogenation is an example of this, in which we were able to use the selected organometallic catalyst efficiently. In this work, we determined that the basic byproducts of the reaction needed to be removed from the solution to prevent isomerization of the solvent. Therefore, we separated the material through a simple reaction with CO_2, which generated a highly insoluble salt and increased the likelihood of solvent and catalyst recycle.

We have shown that piperylene sulfone can serve as a solvent replacement in applications that require good solvation of immiscible materials and easy separation and recycle of the solvent. We have published a paper on the nucleophilic substitutions[34]

and filed for a patent for the solvent. In Chapter 3, we describe further applications that take advantage of the equilibrium of the decomposition mechanism.

2.5 References

1. Beckman, E.J., *Supercritical and near-critical CO2 in green chemical synthesis and processing.* Journal of Supercritical Fluids, 2004. **28**: p. 121-191.

2. Jessop, P.G. and B. Subramaniam, *Gas-Expanded Liquids.* Chemical Reviews, 2007. **107**: p. 2666-2694.

3. Welton, T., *Room-Temperature Ionic Liquids. Solvents for Synthesis and Catalysis.* Chemical Reviews, 1999. **99**: p. 2071-2083.

4. West, K.N.H., Jason P.; Jones, Rebecca S.; Bush, David; Liotta, Charles L.; Eckert, Charles A., *CO2-Induced Miscibility of Fluorous and Organic Solvents for Recycling Homogeneous Catalysts.* Industrial and Engineering Chemistry Research, 2004. **43**(4827-4832).

5. Dunn, P.J., in *10th Green Chemistry and Engineering* 2006: Washington D.C.

6. Dehmlow, E.V. and S.S. Dehmlow, *Phase Transfer Catalysis*. 3rd ed. 1993, New York: VCH.

7. Strarks, C.M., C.L. Liotta, and M. Halpern, *Phase Transfer Catalysis: Fundamentals, Applications, and Industrial Perspectives*. 1994, New York: Chapman & Hall.

8. Loder, D.J. 1952: US.

9. Bhatt, A.I., et al., Green Chemistry, 2006. **8**: p. 161-171.

10. Phan, L.A.H., Loel K.; Edie, Colin F.; Luco, Aimee-Lee; Mirchandani, Anish; Darensbourg, Donald J.; Jessop, Philip G., *Switchable-Polarity Solvents Prepared with a Single Liquid Component.* Journal of Organic Chemistry, 2008. **73**: p. 127-132.

11. Jessop, P.G., et al., *Reversible non-polar-to-polar solvent.* Nature, 2005. **436**: p. 1102.

12. Phan, L., et al., *Switchable Solvents Consisting of Amidine/Alcohol or Guanidine/Alcohol Mixtures.* Industrial and Engineering Chemistry Research, 2007.

13. John, E., *Novel Switchable Systems and Applications*, in *Chemistry and Biochemistry*. 2007, Georgia Institute of Technology: Atlanta.

14. Drake, L.R., S.C. Stowe, and A.M. Partanksy, *Kinetics of the Diene Sulfur Dioxide Reaction.* Journal of the American Chemical Society, 1946. **68**: p. 2521-2524.

15. Krug, R.C. and J.A. Rigney, Journal of Organic Chemistry, 1959. **23**: p. 1697-1699.

16. Yamada, S.O., Hideto; Suzuki, Takayoshi; Takayama, Hiroaki, *Stereoselective synthesis of (E)-, (E,Z)- and (E,E)-conjugated dienes via alkylation of 3-sulfolenes as the key step.* Journal of Organic Chemistry, 1986. **51**(25): p. 4934-4940.

17. Chou, T.S.T., Hsi Hua; Chang, Lee Jean, *Study of the alkylation reactions of sulfol-3-enes.* Journal of the Chemical Society, Perkin Transactions 1: Organic and Bio-Organic Chemistry, 1985. **3**: p. 515-519.

18. Marcus, Y., Chemical Society Reviews, 1993: p. 409-416.

19. Reichardt, C., *Solvatochromic Dyes as Solvent Polarity Indicators.* Chemical Reviews, 1994. **94**: p. 2319-2358.

20. Taft, R.W.K., Mortimer J., *The solvatochromic comparison method. 2. The .alpha.-scale of solvent hydrogen-bond donor (HBD) acidities.* Journal of American Chemical Society, 1976. **98**(10): p. 2886-2894.

21. Kamlet, M.J.T., R. W., *The solvatochromic comparison method. I. The .beta.-scale of solvent hydrogen-bond acceptor (HBA) basicities.* Journal of American Chemical Society, 1976. **98**(2): p. 377-383.

22. Kamlet, M.J.A., Jose Luis; Taft, R. W., *The solvatochromic comparison method. 6. The .pi.* scale of solvent polarities.* Journal of American Chemical Society, 1977. **99**(18): p. 6027-6038.

23. Thompson, R.L., et al., *Rate Variations of Hetero-Diels-Alder Reaction in Supercritical Fluid CO2.* Industrial and Engineering Chemistry Research, 1999. **38**: p. 4220-4225.

24. Ford, J.W., et al., *Solvent Effects on the Kinetics of a Diels-Alder Reaction in Gas-Expanded Liquids.* Industrial and Engineering Chemistry Research, 2007.

25. Monflier, E.B., Paul; Couturier, Jean-Luc; Kervennal, Jacques; Mortreux, Andre, *Highly efficient telomerization of butadiene into octadienol in a micellar system: a judicious choice of the phosphine/surfactant combination.* Applied Catalysis A: General, 1995. **131**: p. 167-178.

26. *EP0436226*. 1988, Kuraray Company.

27. Lee, B.I.L., Kyung Hee; Lee, Jae Sung, *The effects of reaction variables on the palladium-catalyzed reactions of butadiene with water.* Journal of Molecular Catalysis A: Chemical, 2001. **166**: p. 233-242.

28. Albers, P.P., J.; Parker, S. F., *Poisoning and deactivation of palladium catalysts.* Journal of Molecular Catalysis A: Chemical, 2001. **173**(1-2): p. 275-286.

29. Mowery, D.L.G., Michael S.; Ohno, Tim R.; McCormick, Robert L. , *Deactivation of PdO–Al2O3 oxidation catalyst in lean-burn natural gas engine exhaust: aged catalyst characterization and studies of poisoning by H2O and SO2.* Applied Catalysis B: Environmental, 1999. **21**(3): p. 157-169.

30. Foley, J.M.K., James R.; Manogue, William H. , *Sulfur deactivation in nitric oxide reduction by ammonia. 1. Rates of reduction by ammonia and hydrogen.* Industrial & Engineering Chemistry Product Research and Development, 1979. **18**(3): p. 170-179.

31. Wu, X.X., Jianliang, *Aqueous-phase asymmetric transfer hydrogenation of ketones- a greener approach to chiral alcohols.* Chemical Communications, 2007: p. 2449-2466.

32. Liu, P.N.D., Jin Gen; Tu, Yong Qiang; Wang, Shao Hua, *Highly efficient and recyclable heterogeneous asymmetric transfer hydrogenation of ketones in water.* Chemical Communications, 2004(18): p. 2070-2071.

33. Liu, J.Z., Yougui; Wu, Yinuo; Li, Xingshu; Chan, Albert S.C., *Asymmetric transfer hydrogenation of ketones with a polyethylene glycol bound Ru catalyst in water.* Tetrahedron: Asymmetry, 2008. **19**: p. 832-837.

34. Vinci; Donaldson, M.; Hallett, J. P.; John, E. A.; Pollet, P.; Thomas, C. A.; Grilly, J. D.; Jessop, P. G.; Liotta, C. L.; Eckert, C. A., *Piperylene sulfone: a labile and recyclable DMSO substitute.* Chemical Communications, 2007. **14**: p. 1427-1429.

Chapter III: Switchable Solvents for *In-Situ* Acid Catalysis

3.1 Introduction

Catalytic systems represent an important area of development for reducing the environmental impact of reaction and separations. Acid catalysis is a key subset of this category, enabling a wide range of reactions such as hydrolyses, rearrangements, alkylations, acylations, condensations, and many more. Approximately 1 x 10^8 tons of products are generated each year from acid-catalyzed processes.[1] Generally, these processes involve homogeneous Bronsted acids, such as HCl, H_2SO_4, and HF, or Lewis acids, such as $AlCl_3$ and BF_3. These materials are cheap and effective, but generate large amounts of hazardous waste from neutralization of the acids. Neutralization creates salt byproducts that contaminate aqueous waste streams and must be processed to remove the hazardous materials.[2] One such example involves Friedel-Crafts acylations, which can use up to 20 kg of $AlCl_3$ for every kg of product produced.[3] The acid must be neutralized, creating huge amounts of the salt waste. Another example refers to the utilization of H_2SO_4 in alkylation processes, which uses up to 100 kg of acid per ton of alkylates formed for the reaction of isobutene and butylene. In this case, the acid can be regenerated through an energy intensive process, including decomposition to SO_2, reoxidation, and hydration.[4] This does indeed allow for acid recycle without neutralization, but has a large energy burden that limits its advantages over more typical processes.

Due to these key issues with conventional acid catalysis, there has been a great deal of research into the development of novel catalysts. These new materials primarily include solid acids, functionalized ionic liquids, carbon-dioxide expanded liquids, and nearcritical water. The first and most prevalent involves the development of solid, heterogeneous acid catalysts. These include a variety of systems, such as polymer supported acids, zeolites, and mesoporous materials.[1, 5] They have been used effectively in a wide array of reactions and offer simple separation through filtration of the solid.[6-10] However, they can suffer from mass transfer limitations that are frequently associated with heterogeneous systems. Therefore, these catalysts can sometimes require harsh conditions in order to achieve rates comparable to those with homogenous acids. Additionally, they can irreversibly bind with basic materials present in the reaction mixture, reducing their activity and recyclability. In one recent example involving the Beckmann rearrangement of cyclohexanone oxime, H_2SO_4/SiO_2 heterogeneous catalysts showed rapid deactivation due to irreversible poisoning related to the formation of hydroxylamine from a side reaction.[11]

The next system is part of the rapidly expanding world of ionic liquids. These have been defined and described in Chapter 2 of this thesis in relation to their development as novel solvent systems. Some ionic liquids contain inherent Lewis acidity, such as those containing chloroaluminate anions.[4, 12] However, these materials are generally functionalized with acidic tails, such as sulfonic acids, which can significantly improve their performance as acid catalysts. These materials have been used in numerous reactions, including rearrangements[13-15] and hydrolyses.[16] However, they still have a number of issues with separation and recyclability. First, product

separation is highly limited due to the low vapor pressure of the ionic liquids, which restricts the product isolation to few techniques, such as extraction and crystallization. Additionally, like the solid acid catalysts, these too can be deactivated in the presence of basic products.

Two recent areas in novel acid catalysis are related to some of the current research within our group. The first involves the formation of alkylcarbonic acids from carbon dioxide-expanded liquids. Essentially, these systems use the dissolution of CO_2 into alcohols to form weak acids, as illustrated in Figure 3-1. The acid forms in-situ under CO_2 pressure and can be eliminated by simply depressurizing the system. Hence, the acid can be removed without neutralization or regeneration.

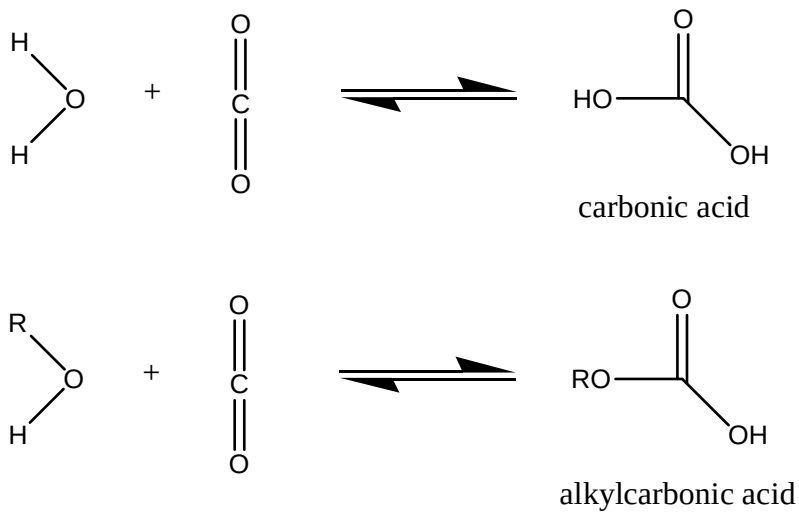

Figure 3-1 Formation of Carbonic/Alkylcarbonic Acid from Reaction of CO_2 with Water/Alcohols

This scheme has been used on several reactions, including the hydrolysis of β-pinene, diazotizations, Sandmeyer, and Ugi reactions.[17-21] This process is green, but has significant limitations due to the weak acidity of the alkylcarbonic acids. For example,

the hydrolysis of β-pinene shows excellent selectivity for the desired products with this system, but has extremely slow reaction times, requiring up to 24 hours to achieve yields similar to the current methods.

We have also worked extensively on novel acid catalysis involving nearcritical water. These systems are generally defined as water heated to 200-300ºC and saturation pressures of 15-90 bar.[21] At these conditions, the properties of water change drastically from those at atmospheric, causing it to behave more like a moderately polar solvent and allowing for dissolution of organic molecules. More importantly, the conditions cause a significant increase in the autodissociation constant, generating hydronium and hydroxide ions that can enable both acid- and base-catalyzed reactions. The dissociation can be reversed readily by simply cooling the system. This eliminates the need for neutralization and simplifies product separation. These systems have been studied extensively for a wide array of reactions, including hydrolyses, alkylations, condensations, and rearrangements.[22] These reactions are highly effective and notably green, but come at a high energy cost due to the elevated temperatures and pressures required in the system. Additionally, reaction selectivity has not always shown exceptional results. For example, in the hydrolysis of β-pinene, the reaction goes to complete conversion rapidly, but generates low selectivity for the desired products.[20]

The aforementioned catalytic systems represent several developments that have been explored over the last few decades. Overall, each system has advantages that are beneficial for product separation and waste reduction. However, they also have drawbacks that can limit their applicability to general acid catalysis, opening possibilities for further development of novel catalysts.

Therefore, we focused our research on development of switchable solvents that simultaneously act as both solvent and acid catalysts. For this work, we applied the retro-cheletropic solvents, butadiene sulfone and piperylene sulfone. In the previous Chapter, we looked at solvent properties and reaction applications for piperylene sulfone.[23, 24] These applications utilized the novel material's excellent properties and built-in thermal switch to enable reactions and separations. Essentially, these reactions explored the breadth of possibilities in which piperylene sulfone could be used as a solvent. In this Chapter, we incorporate additional applications, exploring a new aspect of the retro-cheletropic solvents: their use as acid catalysts. Importantly, the sulfolenes themselves cannot act as catalysts. It is the equilibrium of the retro-cheletropic reaction that can allow for the generation of the acid catalyst. This can be accomplished by using the thermodynamics of our thermoresponsive system. As shown in Figure 3-2, the sulfolene can be decomposed into sulfur dioxide and a diene through the retro-cheletropic equilibrium reaction.

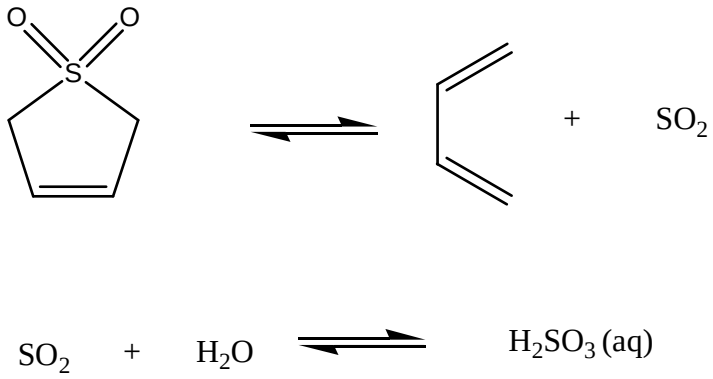

Figure 3-2 Formation of Sulfurous Acid Through Equlibrium Reaction between SO_2 and Water for Butadiene Sulfone

The equilibrium favors the solvent at temperatures under 100ºC, but shifts toward the decomposition constituents at temperatures that exceed this value. However, the equilibrium dictates that small amounts of the diene and sulfur dioxide will be present at solvent conditions. By adding water to the solvent, the available sulfur dioxide can dissolve and form sulfurous acid, creating an in-situ catalyst. Most importantly, the acid can be eliminated without neutralization by elevating the system to normal solvent decomposition temperatures at which the acid is highly unstable.[25] Hence, the retro-cheletropic solvents can function as both solvent and acid catalyst, combining excellent substrate solubility, easy product recovery, and simple acid elimination without wasteful neutralization. Figure 3-3 shows the general scheme for reaction and separation in the novel catalytic system.

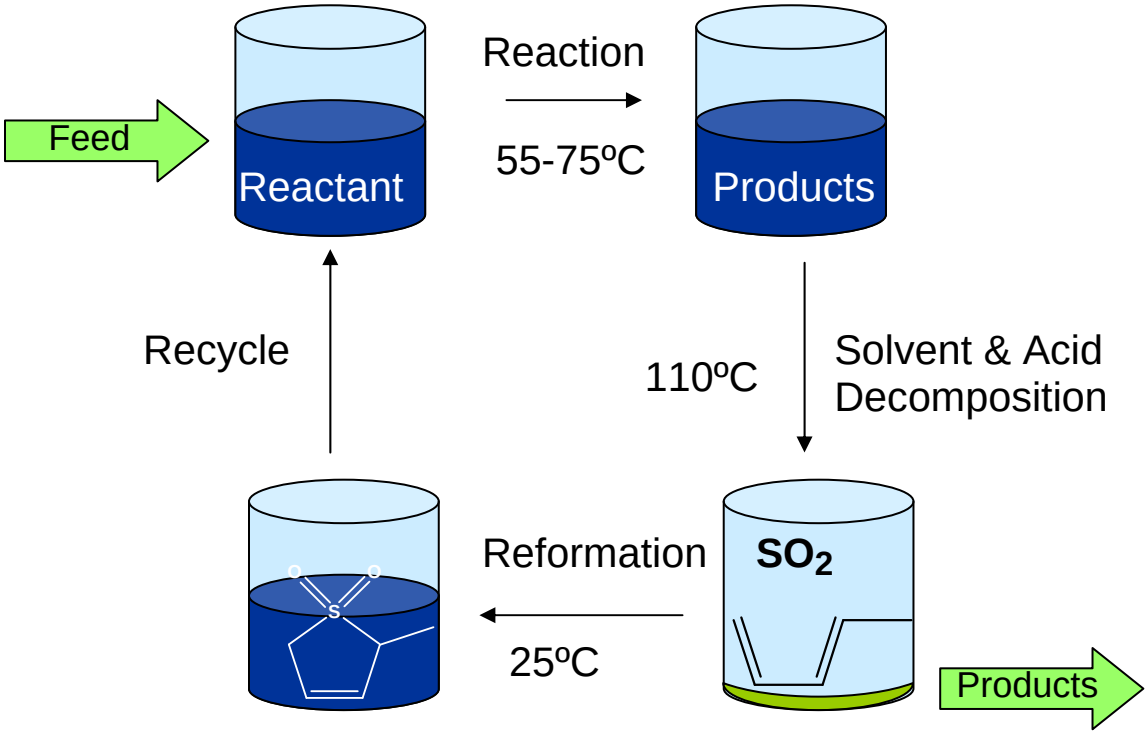

Figure 3-3 Cycle for the Use of Sulfolenes in Acid-Catalyzed Reactions and Separations

In order to assess the efficacy of the sulfolene system, we investigated a series of characteristic acid-catalyzed reactions. We focused the study on transformations involving hydrolyses and rearrangements. The first and primary application is the hydrolysis of β-pinene (**1**) to α-terpineol (**10**). Generally, the industrial method for catalyzing this reaction involves use of strong acids, such as H_2SO_4, that will require wasteful neutralization or regeneration processes.[20] Therefore, it represents an industrial example in which waste could be reduced significantly by development of a novel, recyclable acid catalyst. Also, the hydrolysis generates molecules that are important for the flavor and fragrance industry, resulting in floral or coniferous aromas useful in perfumes and cleaning materials.[16]

The mechanism for the hydrolysis of β-pinene (**1**) has been well studied as a model compound for carbocation rearrangements.[26] However, a large number of side products can result, as shown in the overall mechanism of the reaction in Figure 3-4. The reaction follows the general acid catalysis route, with the protonation of β-pinene (**1**) to the carbocation (**2**) as the rate determining step. The carbocation can then rearrange to (**3**), (**4**), or (**5**), leading to bicyclic alcohols, hydrocarbons, and α-terpineol (**10**). The rearranged carbocation (**3**) generates either borneol (**6**) from reaction with water or camphene from a Wagner-Meerwein rearrangement. The rearranged carbocation (**4**) reacts to form the main products of the reaction, generating terpinolene (**8**) and limonene (**9**) through proton elimination or α-terpineol (**10**) through interaction with water. The final avenue involves reaction of carbocation (**5**) with water to form fenchol (**12**) or a Wagner-Meerwein rearrangement to form fenchene (**11**).

Numerous systems have been developed to reduce the neutralization waste associated with the hydrolysis of pinene. In Table 3-1, we compare some of the novel catalysts described in literature with the typical systems used for the reaction. In the conventional process, sulfuric acid is the primary catalyst, illustrating high conversions for short reactions times and mild conditions.[27] However, the selectivity for terpineol is relatively low. The novel systems reflect the various types of catalysts discussed in the previous section, including solid acids, ionic liquids, gas-expanded liquids, and near-critical water. The solid acids overcome the separation difficulties associated with the homogeneous catalysts and have reasonable conversions at low times, but also suffer from low selectivity to the hydrolysis products.[6, 7] The ionic liquids vary depending upon the anion and cation, but generally require longer times to achieve similar yields to

the conventional acids.[16] In our recent work, we showed that gas-expanded liquids have excellent selectivity for the hydrolysis products, but call for significantly increased reaction times.[20] The opposite is true for the nearcritical water systems, which have high reactivity but low selectivity.[20] Therefore, the switchable solvents have the potential to improve both the efficiency and environmental aspects of the current technologies associated with this model reaction.

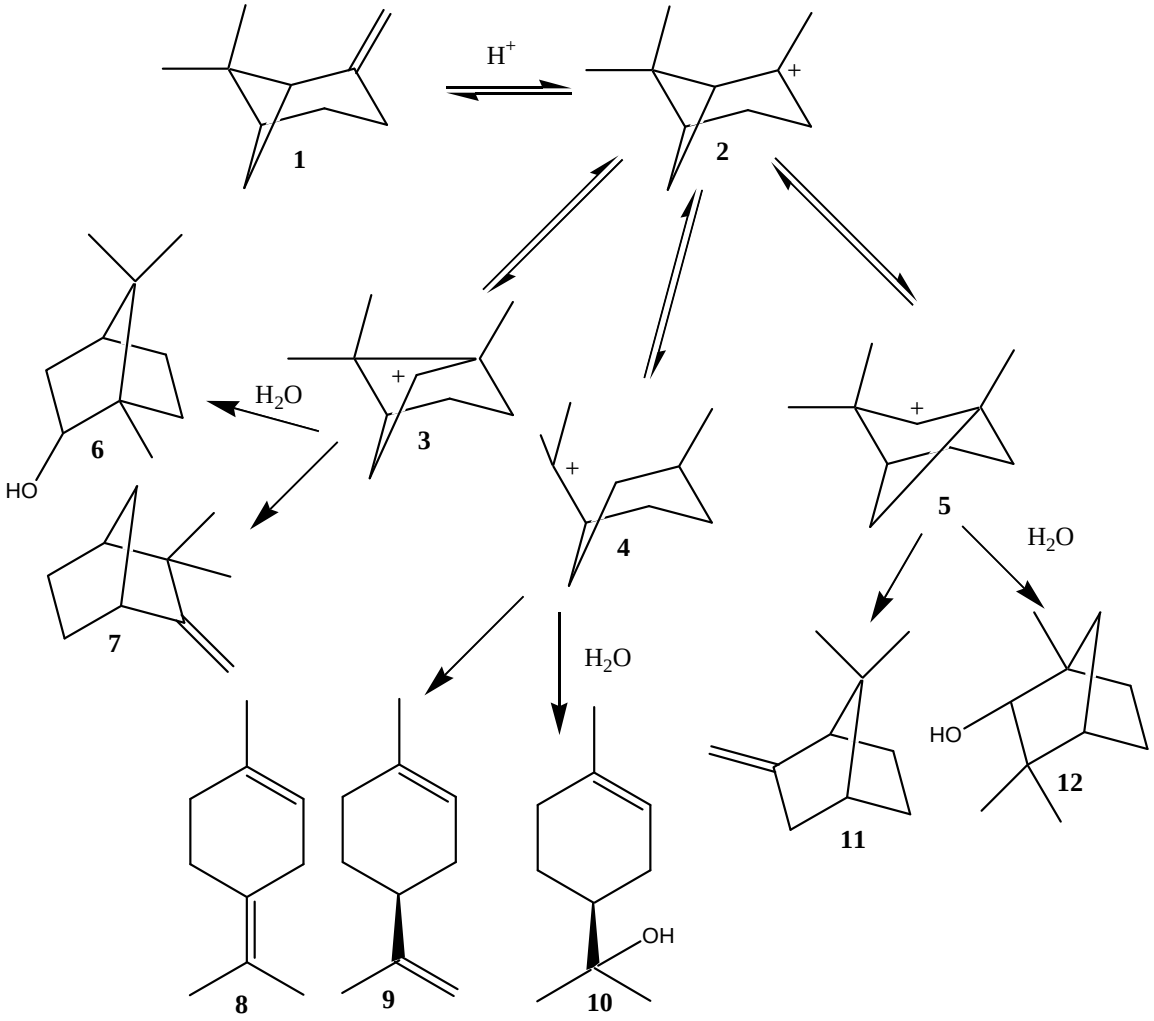

Figure 3-4 Mechanism for Acid-Catalyzed Hydrolysis of β-Pinene with Possible Side Reactions

Table 3-1 Comparison of Conversion & Selectivity for Hydrolysis of Pinene in Various Systems

Type	Acid Information	Conditions	Conversion	Selectivity[a]	Ref
Conventional	H_2SO_4	α-pinene, 0.075N acid, 95% acetone/water, 75ºC, 4 hr	91%	41%	[27]
Conventional	H_2SO_4	β-pinene, 0.073N acid, 95% acetone/water, 75ºC, 1 hr	88%	42%	[27]
Solid	Heteropoly Acid	β-pinene, 0.003M acid, acetic acid/water, 25ºC, 2 hr	92%	42%	[7]
Solid	Zeolites/polymeric membrane	α-pinene, 52.8% cat loading, acetone/water, 50ºC	50%	58%	[6]
IL	$[C_4mim]HSO_4$	α-pinene, 0.07M, IL/water, 80ºC, 8 hr	94%	34%	[16]
IL	$[Hmim]H_2PO_4$	α-pinene, 0.07M, IL/water, 80ºC, 8 hr	46%	54%	[16]
GXL	$MeOH/CO_2$	β-pinene, MeOH/water/CO_2 (30/67/3), 75ºC, 24 hr	71%	58%	[20]
NCW	Water	β-pinene, water, 200ºC, 0.33 hr	90%	16%	[20]
NCW	Water	β-pinene, water/isopropanol (50/50), 200ºC, 2.5 hr	90%	49%	[20]

[a] Selectivity for hydrolysis of β-pinene to terpineol

The primary studies for this work were carried out on the hydrolysis reaction. However, we also wanted to explore additional possible acid-catalyzed reactions to assess the breadth of applications feasible in our novel system. Therefore, we decided to investigate the Beckmann rearrangement of cyclohexanone oxime to ε-caprolactam and the rearrangement of pinacol and benzopinacol.

Beckmann rearrangements represent an important type of acid-catalyzed transformation.[28, 29] These reactions involve the rearrangement of ketoximes to amides. The Beckmann rearrangement of cyclohexanone oxime generates ε-caprolactam, as shown in Figure 3-5, which is an important intermediate for the production of nylon 6.[30] In 1995, the total world production of caprolactam reached 3.7 x 10^6 tons per year.[30] Over 90% of the current industrial processes use oleum as the homogenous acid catalyst, necessitating neutralization for product purification.[31] This is usually carried out with ammonium hydroxide, which leads to the production of ammonium sulfate as an undesired byproduct. Depending on the reference, it is estimated that between 1.7 and 5 kg of sulfates are produced for every 1 kg of caprolactam.[30, 32] In order to reduce generation of wasteful neutralization products, there has been a great deal of research into novel acid catalysts that eliminate the need for such additional processes. These include many of the systems discussed in the previous background section, such as solid acids, nearcritical water, and ionic liquids.[13, 14, 33]

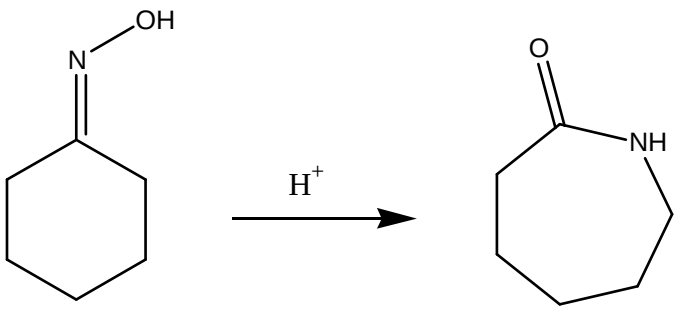

Figure 3-5 Beckmann Rearrangement of Cyclohexanone Oxime to ε-Caprolactam

The pinacol rearrangement represents another class of acid catalyzed reactions that have been extensively studied with both traditional and novel acids.[34] As illustrated in Figure 3-6, it allows for the transformation of 1,2 diols to carbonyls, enabling the production of aldehydes and ketones.[35] The reaction generally follows the rearrangement mechanism, which usually involves the loss of water and simultaneous 1,2 shift, but can also form side products through an elimination pathway.[34, 36] The reaction is usually carried out with sulfuric acid, which makes it an excellent target reaction for novel catalytic systems. Therefore, it serves as one of the primary model reactions for the development of new, recyclable acid catalysts.[35] We chose to test the switchable solvents on this reaction to expand our list of possible applications and compare its capabilities to the wide array of catalysts available.

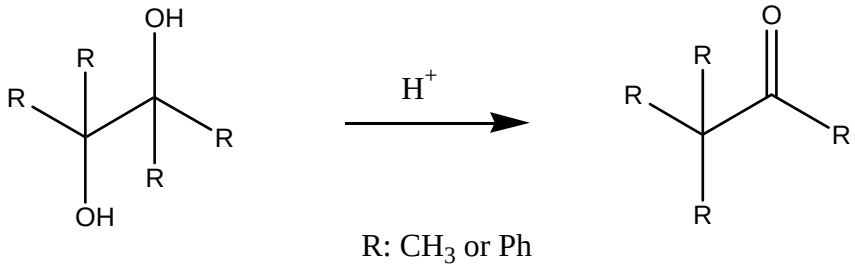

Figure 3-6 Pinacol Rearrangement (R=CH_3 for Pinacol and R=Ph for Benzopinacol)

3.2 Experimental

3.2.1 Materials

The following materials were used as obtained: butadiene sulfone (Aldrich, 98%), (−)−β-pinene (Aldrich, 99%), α-terpineol (Aldrich, Technical, 90%), terpinolene (Fluka, Technical, <85%), hexanes (BDH, ACS, 98.5%), dimethylsulfoxide (J.T. Baker, 99.9%), cyclohexanone oxime (Aldrich, 97%), pinacol (Alfa Aesar, Anhydrous, 99%), and benzopinacol (Alfa Aesar, 97%). Distilled water was obtained from the unit operations laboratory and piperylene sulfone was synthesized within our lab according to the procedures outlined in Chapter 2 and Appendix A of this thesis.

3.2.2 Experimental

3.2.2.1 Hydrolysis of β-Pinene

The hydrolysis reactions were performed in 15 mL glass pressure tubes equipped with PTFE threaded bushings and nitrile o-rings. These vessels were specifically chosen in order to reduce loss of both reactants and products, which can occur easily due to the high volatility of the flavor compounds. The tubes were loaded with 2.3 mL of sulfolene and water at varying concentrations and sealed tight with the bushing. The vessels were stirred with Teflon-coated magnetic stir bars and placed in an oil bath at the appropriate temperature. The system was equilibrated for a specified time, between three and twenty hours, in order to allow for generation of sulfurous acid. The reactant was weighed and added to the vessel with an Eppendorf pipette (0.4 mol/L). For the higher temperature reactions, the reactions were stopped after a given amount of time and then quenched by placing the entire vessel in an ice bath. After 30 minutes, the products were extracted

into 10 mL of hexane. The extraction was repeated two more times to ensure complete extraction of the products. For the kinetic experiments, aliquots were taken at various times and quenched in hexane.

The samples were analyzed by gas chromatography-mass spectroscopy. The analysis was completed on a GC-2010 Shimadzu GC with a GCMS-QP2010S MS and SHR5XLB column. The oven temperature had an initial value of 50.0ºC and was held for two minutes. The temperature was then ramped at 20.0ºC/min up to 300ºC, where it was held for an additional minute. The system was set to constant flow at 26.0 mL/min with an injection temperature at 275ºC and MS source temperature at 200ºC. β-pinene (**1**), α-terpineol (**10**), and limonene (**9**) were each calibrated for the response areas. All hydrocarbons were assumed to follow the calibration curve assigned to limonene (**9**), while all hydrolysis products were assumed to follow that of α-terpineol (**10**). The calibration curves in conjunction with the response areas allowed for direct determination of the concentrations, which were then used to determine conversion and selectivity.

The mass balances were calculated for each run in order to verify recovery of reactants and products. In each case, the total values were within ±10%, with an average recovery for all runs of 99%. However, the reaction mixture usually changed from a clear solution to a pale yellow, which is frequently indicative of oligomer formation.[7] This product can form from an additional side reaction of the pinene, but could not be detected by GC-MS or NMR. Therefore, oligomer formation was minimal at the conditions tested for this reaction, so it is not included in the selectivity calculations.

3.2.2.2 Rearrangements: Beckmann and Pinacol

In the Beckmann rearrangement of cyclohexanone oxime to ε-caprolactam, we completed the reactions in round bottom flasks equipped with magnetic stir bars. The flasks were filled with 2.3 mL of butadiene sulfone with 1% water by volume. The system was then equilibrated for up to six hours at the appropriate temperature in an oil bath. The cyclohexanone oxime was added at a similar concentration to the previous reactions and allowed to react for several hours. Aliquots were taken at regular intervals and analyzed via GC-MS at the same conditions described above to determine the conversion and selectivity.

For the pinacol rearrangements, the reactions were also carried out in round bottom flasks and stirred with magnetic stir bars. The vessels were filled with 2 mL of piperylene sulfone and place in an oil bath set at the desired temperature. In the low temperature reactions, the flasks were covered with rubber septa. For the high temperature conditions, condensers connected to cooling water were placed on the flasks to reduce solvent losses. After a short equilibration, the reactants were added and allowed to react for the set amount of time, ranging from hours to several days. After completion of the reaction, the pinacol samples were analyzed by GC-MS at the same conditions as previously described. The benzopinacol reaction could not be analyzed in this fashion due to the high melting point of the materials. Therefore, these reaction solutions were placed in a temperature controlled heating mantle set to 110ºC to decompose the piperylene sulfone. The remaining material was then analyzed by ^{1}H and ^{13}C NMR.

3.3 Results

3.3.1 Hydrolysis of β-Pinene

The model reaction was the hydrolysis of β-pinene in butadiene sulfone and piperylene sulfone. Due to the complex equilibrium for generation of the in-situ acid, it was necessary to evaluate a variety of conditions for the reaction. Hence, we focused this study on the characterization of several key effects, including solvent/water equilibration time, temperature, water concentration, time dependence, and ease of recycle. The vast majority of these studies were carried out in only butadiene sulfone. Generally, we prefer to use piperylene sulfone due to its superior handling properties (i.e. liquid at room temperature, lower decomposition temperature). However, as noted in the previous chapter, piperylene sulfone is not commercially available and, therefore, must be synthesized in our laboratory. Butadiene sulfone, on the other hand, is commercially available and illustrates the same retro-cheletropic properties found in piperylene sulfone. Hence, we decided to explore the potential of these switchable solvents on the molecule that was more readily available. Both solvents were used in the time dependent experiments to ensure that the reactions could be carried out in our preferred system.

3.3.1.1 Equilibrium Effect

The first effect we evaluated was the length of time for equilibration of the butadiene sulfone system. The formation of sulfurous acid results from two equilibrium reactions, as previously illustrated in Figure 3-2. The first is the equilibrium of the butadiene sulfone with the decomposition products, butadiene and sulfur dioxide. The next involves the dissolution of the sulfur dioxide into the water and the subsequent

equilibrium formation of the in-situ acid. The retro-cheletropic reaction is driven further due to the loss of sulfur dioxide to sulfurous acid. Effectively, the formation of the acid drives the decomposition process, but it is limited by the extremely low equilibrium constant for the acid formation and the concentration of water. The rate of reaction for the hydrolysis is in part dependent on this acid concentration, so variation in equilibration time could cause significant discrepancies in the concentration and, thus, the reaction rate for a given system.

In order to assess the equilibrium effect, we ran a series of tests to determine the required time for equilibration. The reactions were carried out at 65ºC for two hours at varying water concentration (based on volume percent) and equilibration time, including three hours and twenty hours. The results for this study are found in Figure 3-7 and Table 3-2. The study shows that the yields are much lower for the shorter equilibration time in the 5, 10, and 15% water cases. For the 20% water case, the conversions for both times are approximately equal. Therefore, at the low equilibration time, the systems with lower water concentration have not achieved equilibrium. This indicates that they have not generated the maximum possible acid concentration, causing the rates to decrease at the reduced time. However, at the highest water concentration, we see an almost equivalent yield, which means that the system produced enough acid to effectively catalyze the reaction at both times. With this information, it is difficult to interpret whether the system actually reaches equilibrium faster or it has simply generated enough acid to minimize the concentration effect on the reaction. Regardless, we chose to use the 20 hour, 20% water case to ensure that the equilibration did not influence the next set of experiments.

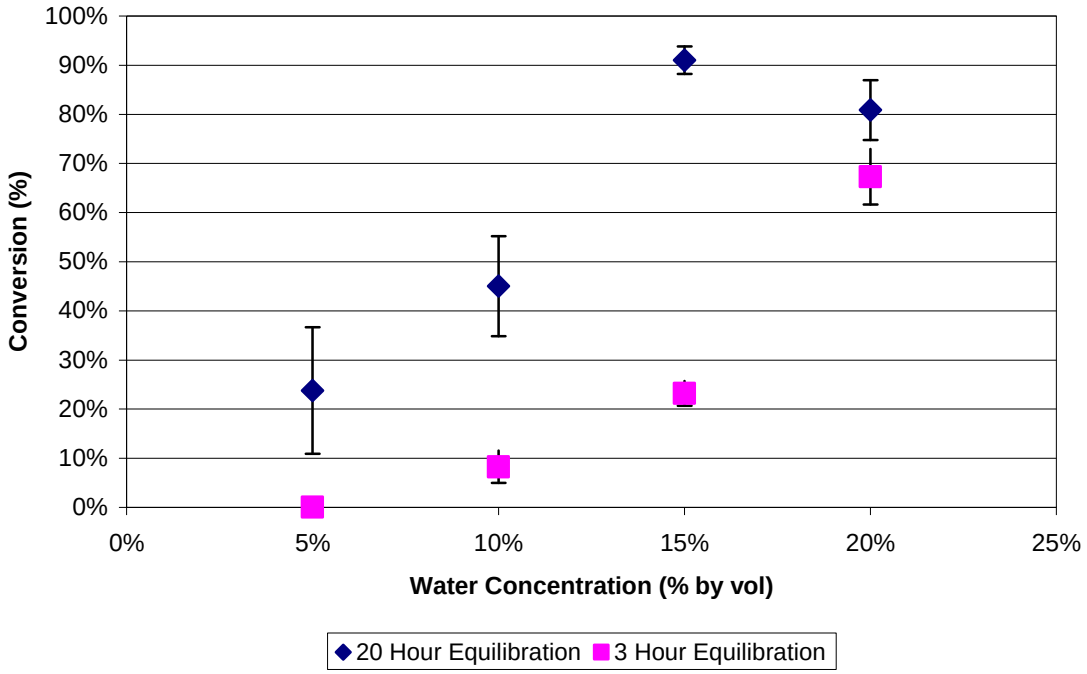

Figure 3-7 Effect of Equilibration on the Hydrolysis of β-Pinene at 65°C for 2 Hours in Butadiene Sulfone with Varying Concentrations of Water

Table 3-2 Effect of Equilibration on the Hydrolysis of β-Pinene at 65°C for 2 Hours in Butadiene Sulfone with Varying Concentrations of Water

Equilibration Time (hr)	Water Vol %	Conversion	Selectivity
20	20%	81% ±6%	65% ±4%
20	15%	91% ±3%	55% ±5%
20	10%	45% ±10%	32% ±3%
20	5%	24% ±13%	21% ±2%
3	20%	67% ±6%	61% ±6%
3	15%	23% ±3%	60% ±2%
3	10%	8% ±3%	36% ±5%
3	5%	0.1% ±0%	60% ±1%

3.3.1.2 Water Concentration Effect

The next effect we investigated was the influence of water concentration on the activity of the system and the selectivity toward the desired hydrolysis products. As described in the previous section, water concentration plays a pivotal role in the generation of the in-situ acid. Moreover, water is required in the hydrolysis reaction, so the selectivity can be significantly affected by the concentration.

These reactions were carried out at 65ºC for two hours in butadiene sulfone with varying concentrations of water, ranging from 5 to 20% based on volume. The results are illustrated in Figure 3-8, which shows both the conversion and the selectivity toward the three main categories of products, including terpineols, hydrocarbons, and bicyclic alcohols.

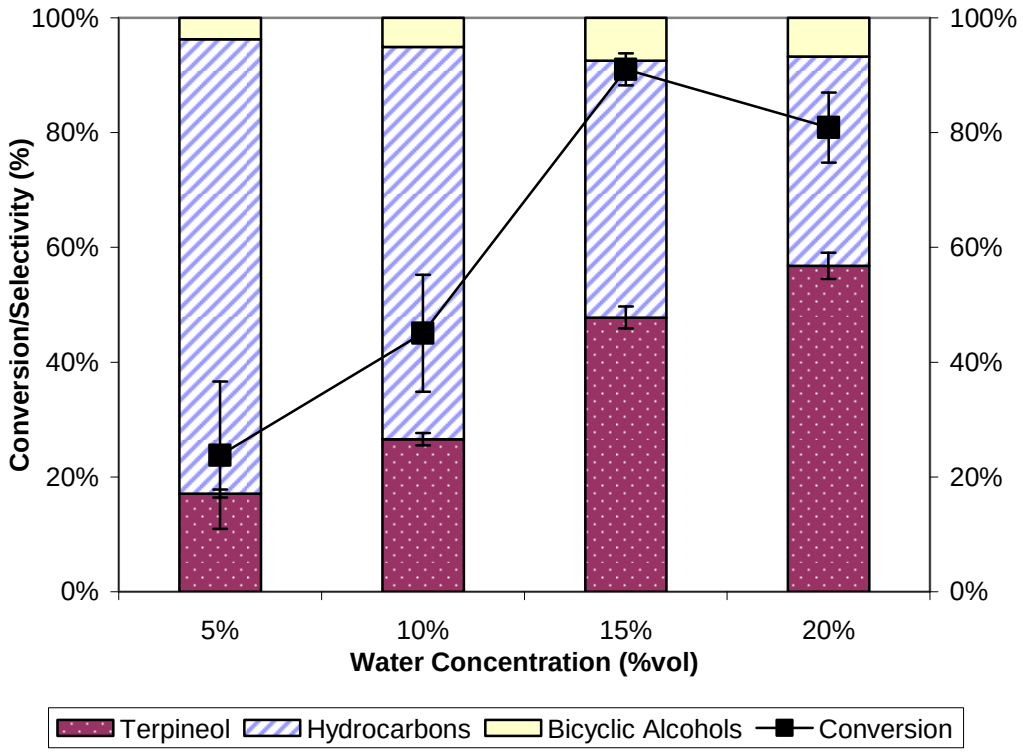

Figure 3-8 Effect of Water Concentration on the Hydrolysis of β-Pinene at 65ºC for 2 Hours in Butadiene Sulfone (20 Hour Equilibration)

Within the results, we can see that the conversion of β-pinene gradually increases over increasing water concentration until it reaches a maximum value of 91% at 15% water. It then decreases approximately 10% for the 20% water level. The selectivity for the hydrolysis reaction is also greatly affected by the concentration of water in the system. As expected, the selectivity for the total hydrolysis products, including both bicyclic alcohols and terpineols, increases with increasing water concentration, ranging from 21% at 5% water to 65% at the 20% water. At all concentrations, the bicyclic alcohols represent the smallest fraction, ranging between 5 and 10%. This value is on par with most literature systems.[20] The selectivity for the desired terpineols increases for increasing water concentration, reaching a maximum of 58% for the 20% water case. This causes the hydrocarbons to reduce to approximately 30%.

The maximum in the conversion data in Figure 3-8 indicates that there are two competing effects controlling the rate of reaction. The first effect stems from the concentration of acid produced in-situ within the reaction media. The total acid concentration is dictated by the dual equilibrium reactions that allow for formation of sulfurous acid. As discussed previously, the water acts as a driving force for the formation of the acid. Hence, at low water concentrations, the acid concentration will be reduced so the overall rate of reaction will slow down. At high water concentrations, there is enough acid to enable the reaction to proceed rapidly, but the rate slows down none the less. This is due to a possible countereffect related to the properties of the mixed solvent. We specifically designed the sulfolene switchable solvents to mimic many of the properties of polar, aprotic solvents like DMSO and DMF. Hence, these materials have excellent solvent properties and can easily dissolve both water and the

highly hydrophobic β-pinene, bringing the vastly varying reactants into a single phase. As the water concentration increases, the solvent power for the organic component strongly decreases, making the medium less favorable for the reaction. This, in turn, limits the benefit of water for the reaction rate, so the system must be optimized for these two effects. The selectivity results have a relatively simple and expected explanation for the increased yields. Essentially, in the higher water concentrations, more water is available for the hydrolysis reactions, so the reaction follows the path to the hydrolysis products instead of the hydrocarbons.

3.3.1.3 Temperature Effect

The next effect we studied involved the impact of temperature on the conversion and selectivity of the hydrolysis of β-pinene in the switchable solvents. In our system, temperature plays a role in both the generation of the in-situ acid and the rate and selectivity of the reaction. As shown in Table 3-3, the equilibrium constant for the retro-cheletropic reaction is highly dependent on temperature.[37] In butadiene sulfone, the constant remains relatively high at 90ºC, indicating that the decomposition products make up a minimal fraction of the system. In piperylene sulfone, the equilibrium constants are significantly lower, which illustrates the reduced stability of the molecule and, hence, its lower decomposition temperature. In our catalytic system, we are utilizing the sulfur dioxide from the equilibrium to generate sulfurous acid. Thus, at greater temperatures, more sulfur dioxide will be available for production of the acid, allowing for an increase in the acid concentration and, thereby, the rate of the reaction. Additionally, the rate and

selectivity are also a function of the temperature in their own right, as with most typical reactions.

Table 3-3 Equilibrium Constant for Retro-Cheletropic Reactions of Butadiene Sulfone and Piperylene Sulfone at Various Temperatures

Butadiene Sulfone	
K	T (C)
0.67	170
1.2	160
2.5	150
5.3	140
18.5	120
128	100
304	90

Piperylene Sulfone	
K	T (C)
0.41	140
0.98	120
2.87	100
8.03	80

The studied reactions were carried out in butadiene sulfone with 20% water by volume for one and two hours at temperatures ranging from 55 to 75ºC. The conversion and selectivity results are shown in Figure 3-9 and enumerated in Table 3-4. In the two hour case, the conversions increased with increasing temperature, from 48% at 55ºC to 100% at 75ºC. On the other hand, the selectivity for the hydrolysis products remained equal for the 55 and 65ºC cases at approximately 66%, but then dropped significantly at 75ºC to 45%.

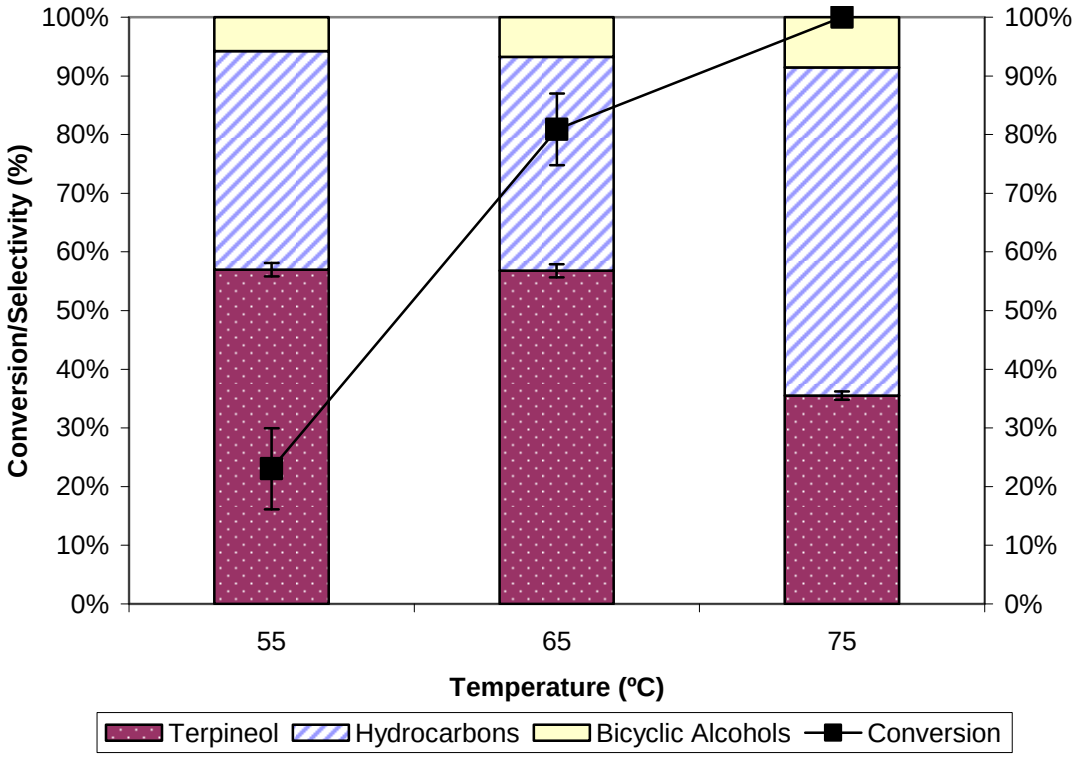

Figure 3-9 Effect of Temperature on the Hydrolysis of β-Pinene at 65ºC for 2 Hours in Butadiene Sulfone with 20% Water (20 Hour Equilibration)

Table 3-4 Effect of Temperature on the Hydrolysis of β-Pinene at 65ºC for 1 and 2 Hours in Butadiene Sulfone (20 Hour Equilibration)

Reaction Time (hr)	Temp (ºC)	Conversion	Selectivity
1	55	11% ±6%	60% ±8%
1	65	69% ±15%	59% ±2%
1	75	99% ±1%	47% ±6%
2	55	23% ±7%	63% ±7%
2	65	81% ±6%	65% ±4%
2	75	100% ±0%	44% ±3%

The data obtained show increasing conversion and decreasing selectivity for elevating temperatures. However, it is difficult to decouple the two effects at work in our system. The acid concentration should increase at elevated temperatures, which will cause an increase in the reaction rate. On the other hand, the rate itself is dependent on temperature, so the effects are essentially additive in this scenario.

3.3.1.5 Recyclability

In order to demonstrate the full potential of our novel solvents, it is necessary to illustrate that the solvent/catalytic system is entirely recyclable. Thus, the final effect we investigated is the activity and selectivity of our catalyst over five recycles for the hydrolysis of β-pinene. In this reaction, we cannot use the decomposition mechanism of our solvent to recover the products. This is due to their high volatility, which causes them to be carried away with the decomposition products. Hence, we decided to prove the recycle with a slightly different mechanism, similar to the asymmetric transfer hydrogenations discussed in Chapter 2. We use a hexane extraction to remove the products and leave the solvent with the acid catalyst intact, allowing for its re-use in another reaction. The series of reactions were carried out at two different conditions with butadiene sulfone and 20% water (by volume). The first reactions took place at 65ºC for two hours, while the second ran at 55ºC for six hours. The conversions and selectivities for the five recycles are shown in Figures 3-10 and 3-11.

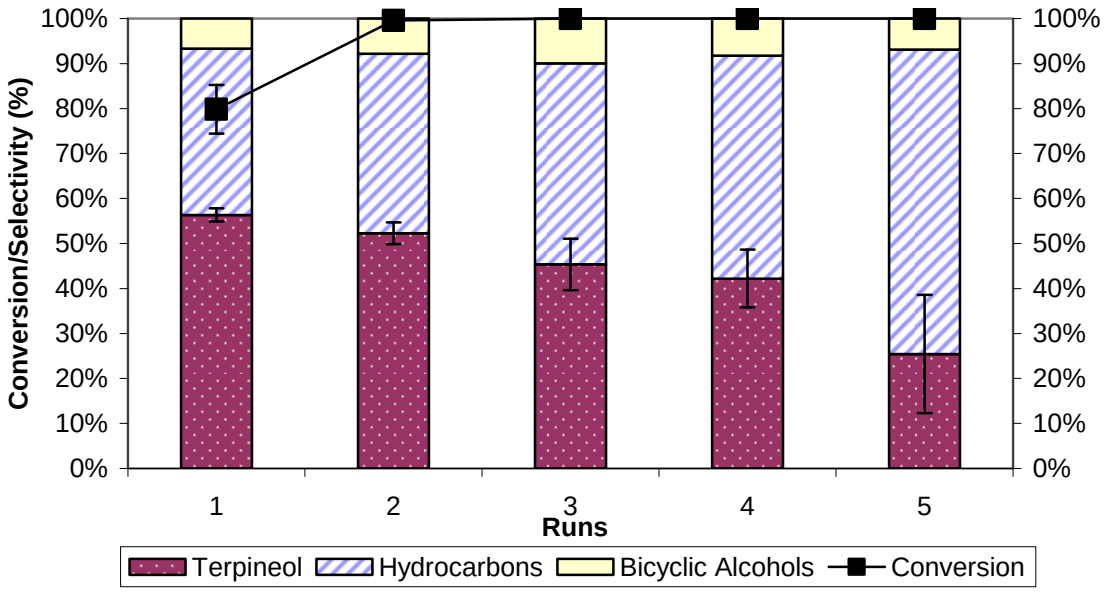

Figure 3-10 Recycle of Butadiene Sulfone with 20% Water (by volume) for the Hydrolysis of β-Pinene at 65ºC for 2 Hours (20 Hour Equilibration)

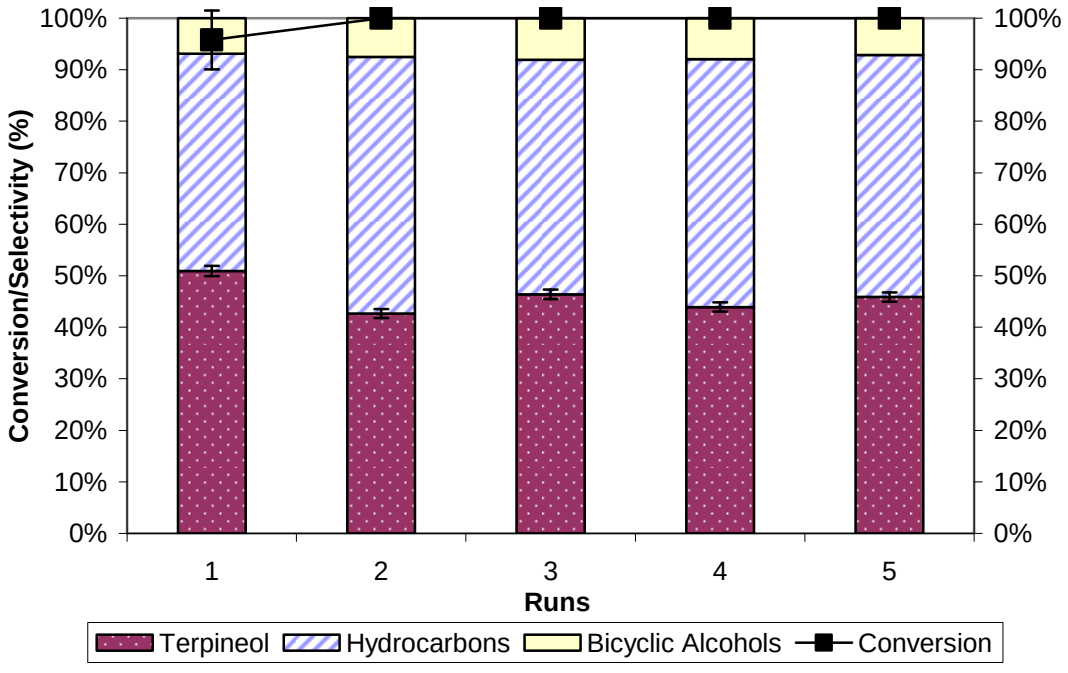

Figure 3-11 Recycle of Butadiene Sulfone with 20% Water (by volume) for the Hydrolysis of β-Pinene at 55ºC for 6 Hours (20 Hour Equilibration)

As shown in Figure 3-10, the system shows excellent recyclability at the first conditions. The activity of the catalytic system remains high over the course of the five recycles, actually elevating from 85% conversion in the first run to 100% throughout the remaining runs. This increase in conversion can be attributed to the further decomposition of the butadiene sulfone, leading to additional generation of the acid and increased rates. Earlier we discussed the effect of equilibration on the system, which illustrated significant discrepancies between the three hour case and the twenty hour for most water concentrations. However, at 20% water, the conversions converge to approximately equal values, presumably indicating that the system has come to some semblance of equilibrium. On the other hand, the elevated water concentrations can lead to additional decomposition of the sulfolenes, as greater amounts of water are available to couple with the sulfur dioxide and form the acid. This, in turn, drives the decomposition further than the initial rapid equilibrium associated with the retro-cheletropic reaction. Essentially, this effect leads to increased concentrations of acid over the course of the recycles, causing the activity to actually increase. On the other hand, the selectivity for the hydrolysis products decreases significantly over the five runs, reducing from approximately 60% to 30% by the final run. This observation can also be attributed to the increase in the acid concentration, which usually leads to greater production in the hydrocarbon byproducts.

While high activity is important, we would like to maintain maximum selectivity for the hydrolysis products. Therefore, we decided to explore additional conditions to attempt to improve the overall selectivity for the recycle. The second reaction condition is lower in temperature, but greater in time, which should lead to reduced acid

concentrations and slower rates. As the plot indicates, the activity remains high for all five runs, remaining above 95% conversion throughout the recycle. This is consistent with the first set of conditions. The selectivity, however, deviates from the initial behavior by staying constant at approximately 50% over the five runs. This illustrates the profound effect the conditions have upon the solvent equilibrium and acid formation. The lower temperature shifts the retro-cheletropic equilibrium further to the sulfolene, slowing the decomposition and reducing the amount of acid that can be formed during the recycles. Thus, the system can achieve high, consistent activity and selectivity toward the desired products for at least five recycles of the solvent system.

In order to prove that the system is completely recyclable, we tested the decomposition of recycled butadiene sulfone. This is important for the overall life cycle assessment of our system, because most solvents and catalysts have a limited number of recycles, leading to disposal or regeneration of the material. Conventional acids systems can actually be recycled in this very manner, but at the end of their life, they must be neutralized or regenerated. In our system, we can simply decompose the acid and solvent and then reform the solvent molecule, creating an entirely recyclable system. To illustrate this point, we used TGA to decompose both the recycled butadiene sulfone and pure material. The plot is shown in Figure 3-12, which shows the temperature profile increasing at 10ºC/min up to 130ºC. The mass loss proceeds steadily to approximately 1% mass remaining, indicating that we have excellent and almost complete decomposition of our catalytic system. The remaining material appears for both cases and could possibly be attributed to the impurities in the solvent. In this case, we did not

prove the regeneration of the solvent, because we have already validated this in the previous chapter, with at least 86% recovery for piperylene sulfone.

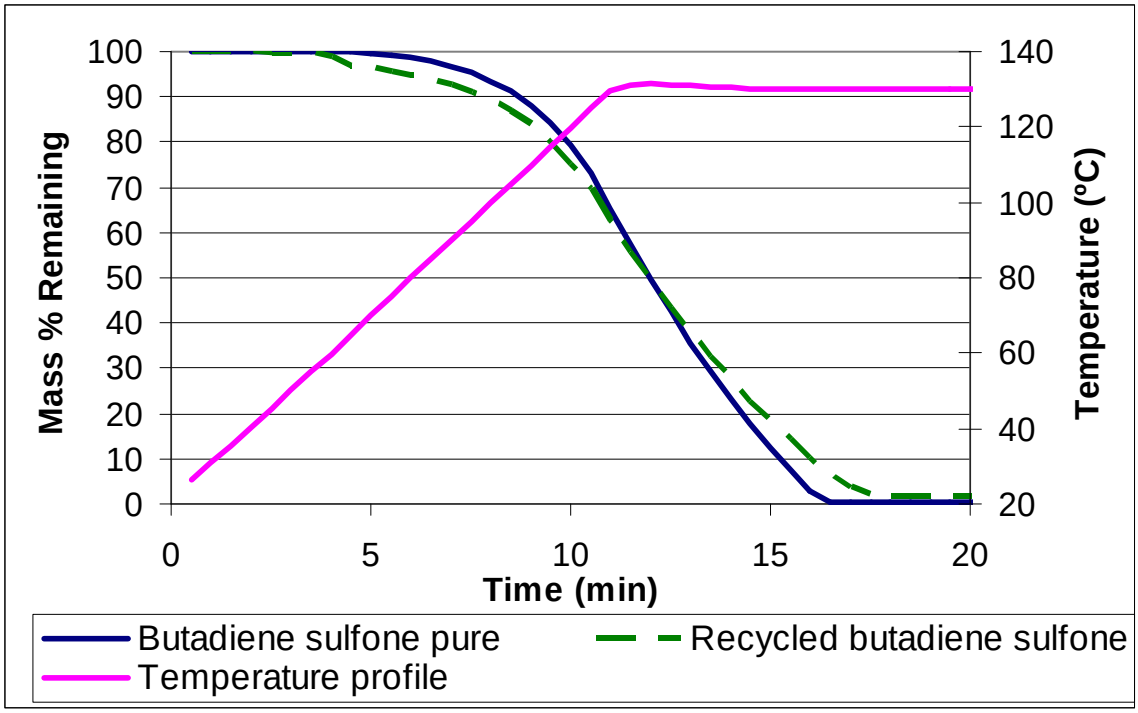

Figure 3-12 TGA for Decomposition of Recycled Butadiene Sulfone

3.3.1.4 Time Dependence

In most of the preceding work, we analyzed the hydrolysis reaction at specified times. We chose not to get kinetic data for these experiments due to the high volatility of the reactants and products involved in this reaction. This made it extraordinarily difficult to remove aliquots without releasing additional material at the high temperature conditions. However, the time dependent behavior of these systems is important for the overall understanding of the reaction within our novel catalytic solvent. Thus, we completed a kinetic study of the hydrolysis in butadiene sulfone and piperylene sulfone at lower temperatures, which minimized losses of the reaction materials. We ran the hydrolysis reaction at 45ºC in piperylene sulfone with 10% water and at 55ºC in butadiene sulfone with 20% water. These conditions are slightly different due to several factors. The first is related to the solubility of water in piperylene sulfone, which is well below the 20% (by volume) concentration used in the majority of these studies. The temperature was also reduced due to the decreased stability of the piperylene sulfone. We ran the reaction in butadiene sulfone at 20% concentration and 55ºC due to the elevated melting point of the solvent, which limits its use within the lower temperature regions. The time dependent behavior for piperylene sulfone and butadiene sulfone are illustrated in Figure 3-13 and 3-15, respectively. The first order kinetic plots for the data are shown in Figures 3-14 and 3-16.

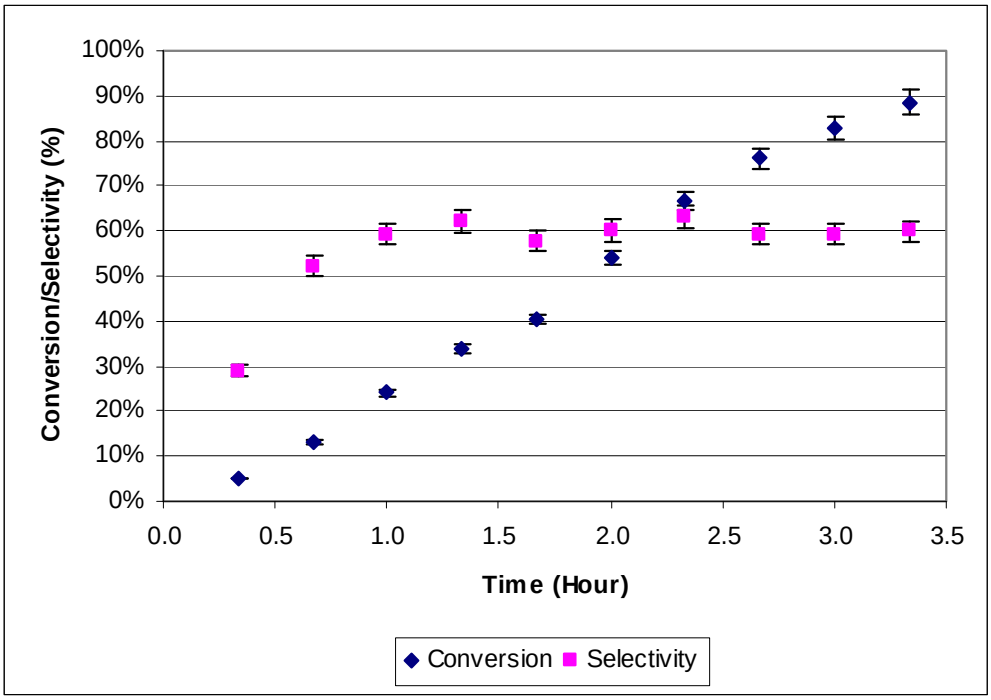

Figure 3-13 Time Dependence of the Hydrolysis of β-Pinene in Piperylene Sulfone (10% H_2O) at 45°C

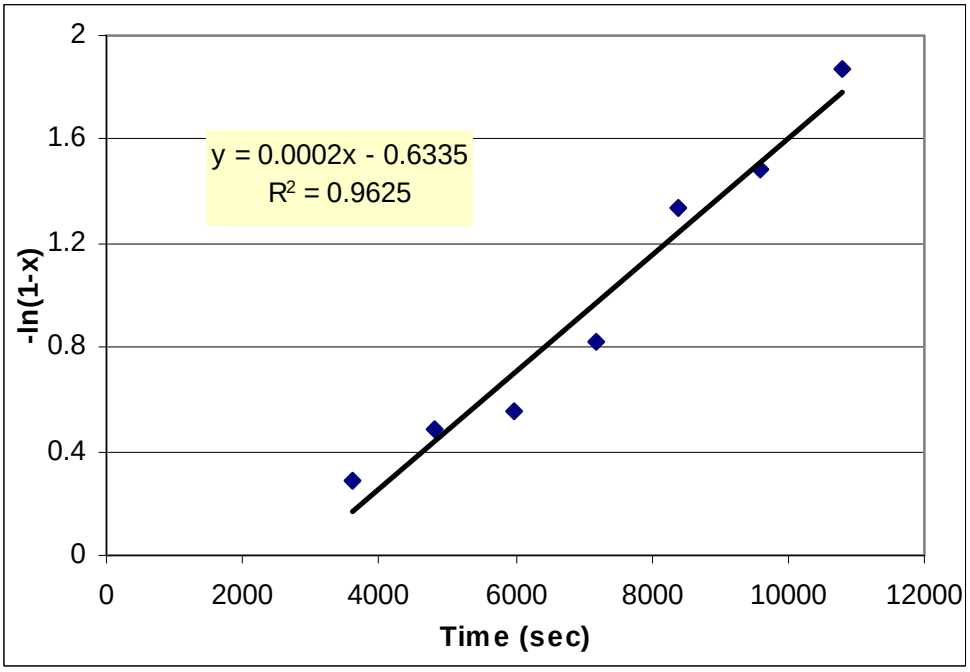

Figure 3-14 First Order Rate Plot for Hydrolysis of β-Pinene in Piperylene Sulfone (10% H_2O) at 45°C

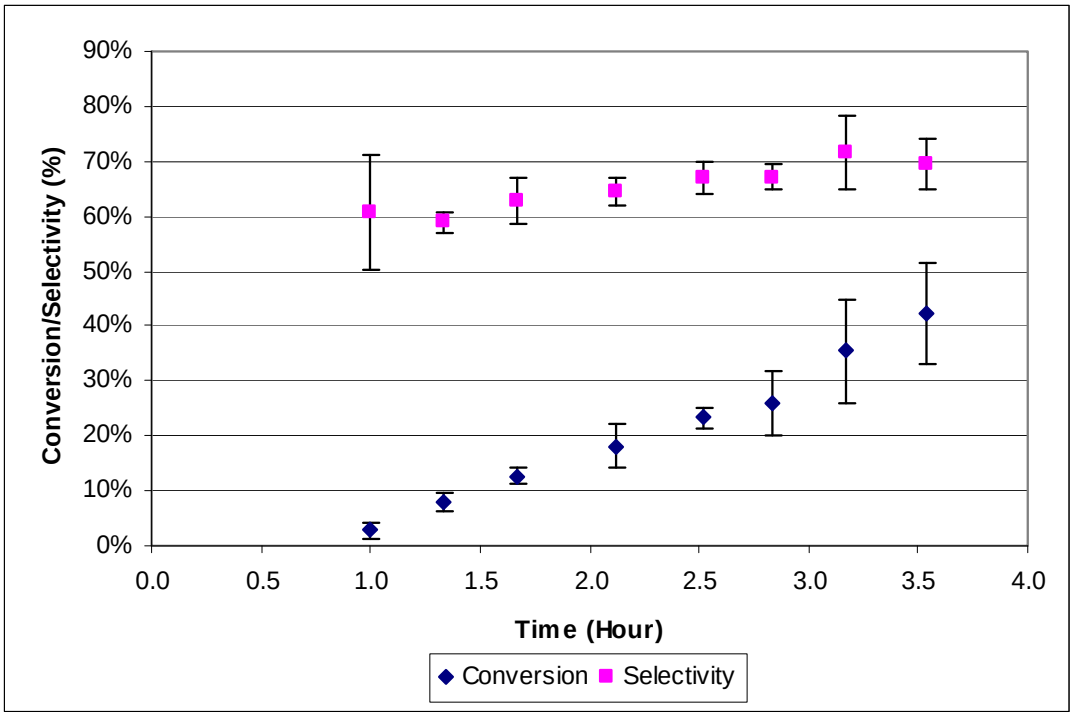

Figure 3-15 Time Dependence of the Hydrolysis of β-Pinene in Butadiene Sulfone (20% H_2O) at 55ºC

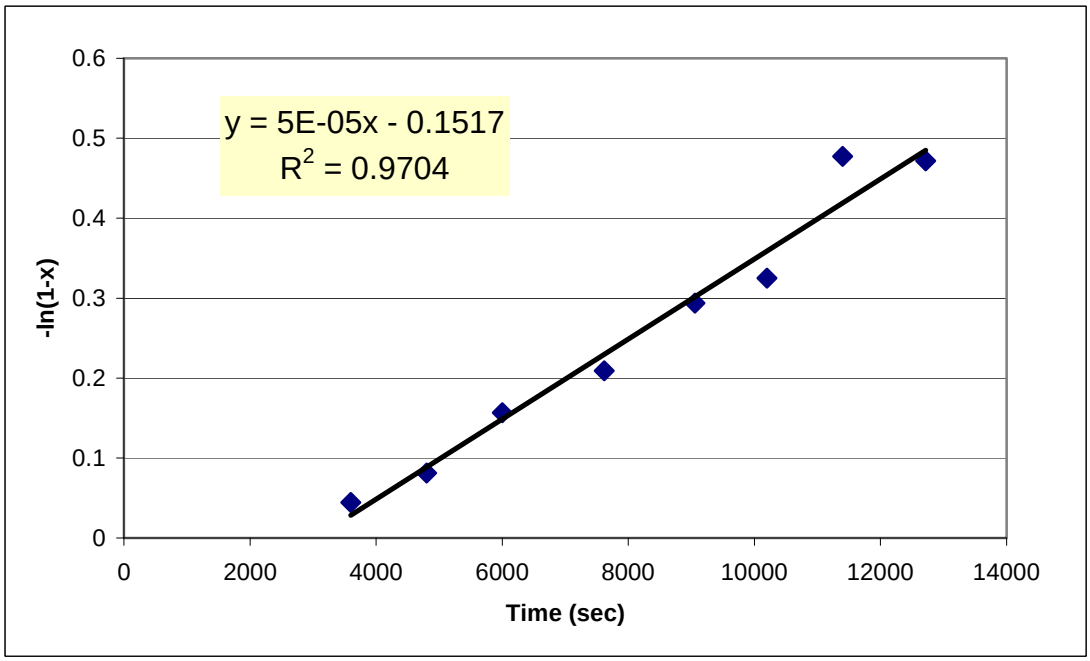

Figure 3-16 First Order Rate Plot for Hydrolysis of β-Pinene in Butadiene Sulfone (20% H_2O) at 55ºC

As seen in Figure 3-13, the conversion increases to approximately 90% in 3.5 hours for the 10% water case at 45ºC in piperylene sulfone. The selectivity for hydrolysis products starts out low at 30%, but then increases steadily for the first 30 minutes until the value reaches about 60%. It then stabilizes at this level for the remainder of the reaction. The first order rate plot for piperylene sulfone illustrates the appropriate linear behavior and generates a rate constant of $2.1\pm0.22 \times 10^{-4}$ s^{-1}. The butadiene sulfone rate plot in Figure 3-15 for 20% water and 55ºC shows slower conversion, increasing to just over 40% within 3.5 hours. The selectivity remains constant between 60 and 70% for the entirety of the run. As predicted from the reduced acid concentration, the rate constant for this system is an order of magnitude slower than the piperylene sulfone case at $5.7\pm1.5 \times 10^{-5}$ s^{-1}.

The rate plots can be correlated with a linear trend line quite well, but it is difficult to ensure that the system meets all the conditions of first order behavior. This is due to the fact that first order rates for catalytic systems assume that the catalyst remains at a constant concentration throughout the reaction. In our system, this is not necessarily guaranteed, as illustrated in the first set of recycle runs. Therefore, under certain conditions, it is possible for the concentration of acid to actually increase over the course of the reaction, which would invalidate the first order rate law. If this were the case, we would most likely observe deviations in the linear behavior of the rate plot. In both plots, however, the trends exhibit excellent linearity, with R^2s above 95%, which indicates that the acid concentration remains relatively constant and first order behavior is most likely applicable at these conditions.

3.3.2 Additional Reactions

The hydrolysis of β-pinene represents just one class of acid catalyzed reactions, but serves as an excellent model reaction for the study of our novel solvent systems. However, we wanted to investigate additional reactions that can illustrate the full potential of our switchable solvent/acid. In order to accomplish this, we completed two brief studies on acid-catalyzed rearrangements – Beckmann and pinacol.

3.3.2.1 Beckmann Rearrangement

The first reaction is the Beckmann rearrangement of cyclohexanone oxime to ε-caprolactam. This represents a model reaction for industrially significant processes that could be greatly improved by development of alternative acid catalysts. For this investigation, we studied the rearrangement in butadiene sulfone with 1% (by volume) water at 65 and 100ºC. We chose butadiene sulfone as the sulfolene due to its enhanced stability at elevated temperatures. After monitoring the reactions for several hours, only starting material and cyclohexanone were detected. Cyclohexanone is a byproduct that can be formed from the hydrolysis of cyclohexanone oxime, as illustrated in the complete mechanism in Figure 3-17. This side reaction can often occur with low levels of acidity and has been widely reported in the literature.[11] For example, in the rearrangement of acetophenone oxime, hydrolysis products were favored in solutions containing less than 70% sulfuric acid.[38] In order to obtain the rearrangement product, it is necessary to ensure high levels of acidity, which is difficult to achieve in our current system. Therefore, the butadiene sulfone does not appear to be a viable option for replacement of oleum in the production of ε-caprolactam. However, we have completed only a

preliminary investigation on this reaction, so varied conditions, such as temperature or water concentration, could improve the selectivity of the reaction to the desired product.

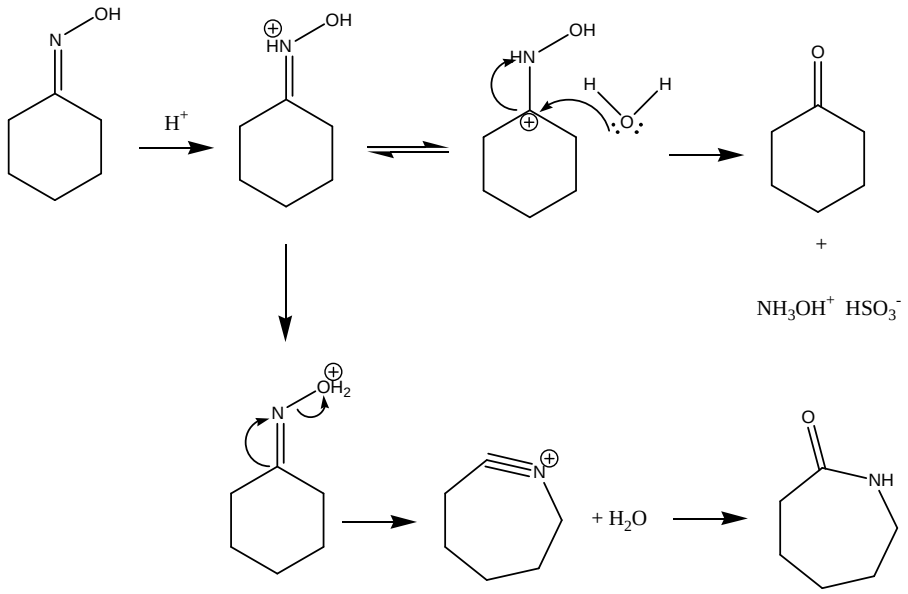

Figure 3-17 Mechanism for Beckmann Rearrangement and Hydrolysis of Cyclohexanone Oxime

3.3.2.2 Pinacol Rearrangement

The final test reaction for our novel solvent system is the acid-catalyzed pinacol rearrangement as previously seen in Figure 3-6. We tested the rearrangement on both pinacol and benzopinacol in piperylene sulfone with 1% water at 40 and 80ºC. For the pinacol reactions, we did not see any rearrangement to pinacolone. However, in the benzopinacol rearrangement, we saw slow reaction, but could not immediately identify the products. We then allowed the reaction to proceed over 48 hours at 40ºC and then decomposed the solvent. The solid material remaining was then analyzed by ^{1}H NMR and identified as the desired product, benzopinacolone.

The results for this reaction are preliminary, but indicate that this could be a new opportunity for the application of the switchable solvents. This is an important step toward in the development of these materials, because the process uses all the characteristics that have been designed into the solvent. It takes advantage of the excellent solvent properties associated with the polar, aprotic molecule, its ability to create an in-situ acid, and the built-in separation mechanism. Therefore, it takes the process one step beyond the initial work on the hydrolysis of β-pinene. This reaction uses the first two characteristics, but cannot apply the last due to the high volatility of the products. The future of this work and other applications will be discussed further in the final chapter.

3.4 Conclusions

In this work, we have expanded the application of our novel switchable solvents to acid-catalyzed reactions. We can use the thermodynamics of the sulfolene molecules to generate sulfurous acid, which allows us to utilize this material as both solvent and catalyst. The entire system is completely reversible, because the solvent and the catalyst can be decomposed and fully recycled. This eliminates the need for wasteful neutralization processes that are often required for conventional homogenous acid solutions. Through utilization of the in-situ acid, we can effectively recycle the homogeneous catalyst and avoid excessive and hazardous neutralization waste. Consequently, we have been able to combine the superior solvent properties of the

molecules with their ability to catalyze certain reactions in one completely recyclable system.

We have applied this work to several types of reactions, including hydrolyses and rearrangements. For the hydrolysis of β-pinene, we have analyzed a number of properties associated with the model reaction and the solvent system. The results show excellent reaction in both butadiene sulfone and piperylene sulfone at mild reaction conditions. We can achieve similar activity to conventional sulfuric acid systems, with slight improvements in the selectivity for the desired hydrolysis products. The study indicates that the system can be recycled at least five times without loss in activity or selectivity, depending on the reaction conditions.

Finally, we have extended the applications to the Beckmann rearrangement and the pinacol rearrangement. This work showed that the system may not be very effective in reactions that require strong acid concentrations, such as in the Beckmann reaction. However, it has proven to be effective for the rearrangement of benzopinacol. In this reaction, we can combine all elements of the switchable solvent, using its excellent solvent power, acid catalyst, and separation mechanism to recover the products.

3.5 References

1. Corma, A., *Solid Acid Catalysts.* Current Opinion in Solid State & Material Science, 1997. **2**: p. 63-75.

2. Clark, J.H., *Green Chemistry: Challenges and Opportunities.* Green Chemistry, 1999(1): p. 1-8.

3. Dartt, C.B.D., Mark E., *Catalysis for Environmentally Benign Processing.* Industrial and Engineering Chemistry Research, 1994. **33**: p. 2887-2899.

4. Busca, G., *Acid Catalysts in Industrial Hydrocarbon Chemistry.* Chemical Reviews, 2007. **107**: p. 5366-5410.

5. Clark, J.H., *Solid Acids for Green Chemistry.* Accounts of Chemical Research, 2002. **35**: p. 791-797.

6. Vital, J.R., A.M.; Silva I.F., Valente, H., Castanheiro, J.E., *Hydration of a-pinene over zeolites and activated carbons dispersed in polymeric membranes.* Catalysis Today, 2000. **56**: p. 167-172.

7. Robles-Dutenhefner, P.A.d.S., Kelly A.; Siddiqui, M. Rafiq H.; Kozhevnikov, Ivan V.; Gusevskaya, Elena V., *Hydration and acetoxylation of monoterpenes catalyzed by heteropoly acid.* Journal of Molecular Catalysis A: Chemical, 2001. **175**: p. 33-42.

8. Forni, L.T., C.; Fornasari, G.; Trifiro, F.; Vaccari, A.; Nagy, J.B., *Vapour-Phase Beckmann rearrangement of cyclohexanon-oxime over Al-MCM-41 type mesostructured catalysts.* Journal of Molecular Catalysis A: Chemical, 2004. **221**: p. 97-103.

9. Li, L.Y., Shitao; Liu, Fusheng; Yang, Jinzong; Zhaug, Shufen, *Reactions of terpentine using Zr-MCM-41 family of mesoporous molecular sieves.* Catalysis Letters, 2005. **100**(3-4): p. 227-233.

10. Castanheiro, J.E.R., A.M., Fonseca, I.; Vital, J., *The acid-catalysed reaction of a-pinene over molybdophosphoric acid immobilised in dense polymeric membranes.* Catalysis Today, 2003. **82**: p. 187-193.

11. Marziano, N.C.R., L.; Tortato, C.; Vavasori, A.; Badetti, C., *Catalyzed Beckmann rearrangement of cyclohexanone oxime in heterogeneous liquid/solid system, Part 1: Batch and continuous operation with supported acid catalysts.* Journal of Molecular Catalysis A: Chemical, 2007. **277**: p. 221-232.

12. Welton, T., *Room-Temperature Ionic Liquids. Solvents for Synthesis and Catalysis.* Chemical Reviews, 1999. **99**: p. 2071-2083.

13. Guo, S.D., Zhengyin; Zhang, Shiguo; Li, Dongmei; Li, Zuopeng; Deng, Youquan, *Clean Beckmann rearrangement of cyclohexanone oxime in caprolactam-based Bronsted acidic ionic liquids.* Green Chemistry, 2006. **8**: p. 296-300.

14. Du, Z.L., Zuopeng; Gu, Yanlong; Zhang, Juan; Deng, Youquan, *FTIR study on deactivation of sulfonyl chloride functionalized ionic materials as dual catalysts and media for Beckmann rearrangement of cyclohexanone oxime.* Journal of Molecular Catalysis A: Chemical, 2005. **237**: p. 80-85.

15. Cole, A.C.J., Jessica L; Ntai, Ioanna; Tran, Kim Loan T.; Weaver, Kristin J.; Forbes, David C.; Davis, James H. Jr., *Novel Bronsted Acidic Ionic Liquids and Their Use as Dual Solvent-Catalysts.* Journal of the American Chemical Society, 2002. **124**: p. 5962-5963.

16. Liu, S.-W.Y., Shi-Tao; Liu, Fu-Sheng; Xie, Cong-Xia; Li, Lu; Ji, Kai-Hui, *Reactions of a-pinene using acidic ionic liquids as catalysts.* Journal of Molecular Catalysis A: Chemical, 2008. **279**: p. 177-181.

17. Xie, X., Liotta, Charles L.; Eckert, Charles A., *CO2-Catalyzed Acetal Formation in CO2-Expanded Methanol and Ethylene Glycol.* Industrial and Engineering Chemistry Research, 2004. **43**: p. 2605-2609.

18. West, K.N., Wheeler, Christy; McCarney, Jonathan P.; Griffith, Kris N., Bush, David; Liotta, Charles L.; Eckert, Charles A., *In Situ Formation of Alkylcarbonic Acids with CO2.* Journal of Physical Chemistry A, 2001. **105**: p. 3947-3948.

19. Weikel, R.R.H., Jason P.; Liotta, Charles L.; Eckert, Charles A., *Self-neutralizing in situ acid catalysts from CO2.* Topics in Catalysis, 2006. **37**(2-4): p. 75-80.

20. Chamblee, T.S., Weikel, Ross R.; Nolen, Shane A.; Liotta, Charles L.; Eckert, Charles A., *Reversible in situ acid formation for b-pinene hydrolysis using CO2 expanded liquid and hot water.* Green Chemistry, 2004. **6**: p. 382-386.

21. Hallett, J.P.P., Pamela; Liotta, Charles L.; Eckert, Charles A., *Reversible in Situ Catalyst Formation.* Accounts of Chemical Research, 2008.

22. Kruse, A.D., E., *Hot compressed water as reaction medium and reactant: Properties and synthesis reactions.* Journal of Supercritical Fluids, 2007. **39**: p. 362-380.

23. Vinci, D.D., M.; Hallett, J. P.; John, E. A.; Pollet, P.; Thomas, C. A.; Grilly, J. D.; Jessop, P. G.; Liotta, C. L.; Eckert, C. A., *Piperylene sulfone: a labile and recyclable DMSO substitute.* Chemical Communications, 2007. **14**: p. 1427-1429.

24. Jiang, N.V., Daniele; Liotta, Charles L.; Eckert, Charles A.; Ragauskas, Arthur J., *Piperylene Sulfone: A Recyclable Dimethyl Sulfoxide Substitute for Copper-Catalyzed Aerobic Alcohol Oxidation.* Industrial and Engineering Chemistry Research, 2008. **47**(3): p. 627-631.

25. Voegele, A.F.T., Christofer S.; Loerting, Thomas; Hallbrucker, Andreas; Mayer, Erwin; Liedl, Klaus R., *About the Stability of Sulfurous Acid (H2SO3) and its Dimer.* Chemistry: A European Journal, 2002. **8**(24): p. 5644-5651.

26. Indyk, H.W., David, *Rearrangements of Pinane Derivatives. Part V. The Influence on Rearrangements of Neutral Nucleophiles associated with the Carbonium Ion.* Journal of the Chemical Society Perkin II, 1974: p. 313-317.

27. Williams, C.M.W., D., *Rearrangements of Pinane Derivatives. Part I. Products of Acid Catalysed Hydrations of a-Pinene and b-Pinene.* Journal of the Chemical Society B, 1971: p. 668-672.

28. Beckmann, E., Chem. Ber., 1886. **19**: p. 988.

29. Jones, B., *Kinetics and Mechanism of the Beckmann Rearrangement.* Chemical Reviews, 1944. **35**: p. 335.

30. Weissermel, K.A., H.J., *Components for Polyamides*, in *Industrial Organic Chemistry*, K. Sora, Editor. 1997, VCH Publishers, Inc: New York. p. 251-262.

31. Petrini, G.L., G.; Mantegazza, M.A.; Pignataro, F., *Caprolactam via Ammoximation*, in *Green Chemistry: Designing Chemistry for the Environment*, P.T.W. Anastas, Tracy C., Editor. 1996, American Chemical Society: Washington D.C.

32. Hashimoto, M.O., Yasushi; Sakaguchi, Satoshi; Ishii, Yasutaka, *Beckmann Rearrangement of Ketoximes to Lactams by Triphosphazene Catalyst.* Journal of Organic Chemistry, 2008. **73**: p. 2894-2897.

33. Ikushima, Y.H., Kiyotaka; Sato, Osamu; Yokoyama, Toshirou; Arai, Masahiko, *Acceleration of Synthetic Organic Reactions Using Supercritical Water: Noncatalytic Beckmann and Pinacol Rearrangements.* Journal of American Chemical Society, 2000. **122**: p. 1908-1918.

34. Molnar, A., *The Pinacol Rearrangement*, in *Fine Chemicals through Heterogeneous Catalysis*, R.A.v.B. Sheldon, H., Editor. 2001, Wiley-VCH: New York.

35. Upadhyaya, D.J.S., Shriniwas D., *A facile and effiecient pinacol-pinacolone rearrangement of vicinal diols using ZnCl2 supported on silica as a recyclable catalyst.* Applied Catalysis A: General, 2008. **340**: p. 42-51.

36. Lezaeta, M.D.S., Wajiha;Svoronos, Paris; Karimi, Sasan; Subramaniam, Gopal, *Effect of various acids at different concentrations on the pinacol rearrangement.* Tetrahedron Letters, 2002. **43**: p. 9307-9309.

37. Drake, L.R., S.C. Stowe, and A.M. Partanksy, Journal of the American Chemical Society, 1946. **68**: p. 2521-2524.

38. Gregory, B.J.M., R.B.; Schofield, K., *Kinetics and Mechanism of the Beckmann Rearrangement of Acetophenone Oximes in Sulphuric Acid.* Journal of the Chemical Society B, 1970: p. 338-346.

Chapter IV: Phase Behavior of Polyethylene Glycol and CO_2 with Common Organic Solvents

4.1 Introduction

Due to increasing concern over the environmental impact of solvents, researchers have been working on the development of novel sustainable materials, including ionic liquids[1], supercritical fluids[2], and fluorous compounds[3]. The general goal for this work involves the replacement of volatile organic compounds (VOCs) with new materials that are environmentally benign. One such area of research has to do with polyethylene glycol (PEG), which has a number of important properties that make it appealing for solvent replacement. At low molecular weights (200-600), it is inexpensive, non-toxic, food-safe, miscible with water and many organics, and has low volatility.[4] We are now utilizing this novel solvent to enable separation processes that ease product recovery and catalyst recycle. In this work, we will explore the liquid-liquid equilibria of PEG with several common organic solvents and carbon dioxide. By determining the phase behavior of these systems, we can define the appropriate conditions for application to homogenous reactions with heterogeneous separations. We then illustrate the utilization of this separation technique to the industrial production of phenols.

4.1.1 Properties & Applications of PEG

PEG has been used for a multitude of applications, including synthesis, drug delivery, and catalysis. For example, it has been used extensively in the modification of proteins and peptides for use in drug delivery.[5] This process, known as PEGylation, makes the molecules more robust, allowing them to stay in the body longer and become less immunogenic. The modification takes advantage of the non-toxic and water soluble nature of PEG and allows proteins and peptides to become more effective drugs. Numerous reviews have explored the breadth of PEG applications to the biomedical arena.[6, 7] However, the primary focus for this research is related to its use as a solvent or catalyst-modifier within synthetic reactions.

Due to its benign nature, PEG has become one of the prime molecules in the field of sustainable solvent development. Much of this research has focused on using PEG as a recyclable solvent or catalyst for numerous reactions. We will look at three of the key areas for its utilization in reactions, including its replacement of volatile organic solvents, use as a phase transfer catalyst, and application as a homogeneous tether for catalyst recycle.

As a reaction medium, PEG offers numerous advantages over the current industrial systems. These systems rely heavily on VOCs as solvents in both reactions and separations, contributing to the negative environmental impacts and high cost of these processes. PEG, on the other hand, has low volatility and minimal toxicity, making it a benign alternative to the current solvents. Also, it's cheaper and more readily available than many of the novel systems under recent review, such as ionic liquids and fluorinated compounds. It exists as a liquid below 600 MW, but can still be used as a solvent above

this value at elevated temperatures.[4] Also, PEG has a wide range of solubility with numerous compounds, including water, organics such as toluene and acetone, and some salts. However, it is insoluble with aliphatic hydrocarbons and diethyl ether, which allows for the majority of the product purification and catalyst recycle methods used within the numerous applications. The structure of PEG is illustrated in Figure 4-1.

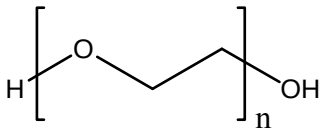

Figure 4-1 Structure of Polyethylene Glycol (PEG)

Rogers *et al.* provide a detailed review on the wide array of reactions that have been carried out in PEG.[4] These include substitutions, oxidations, reductions, and polymerizations. We will look at several examples that characterize the solvent properties and recyclability of PEG, such as Michael additions and Heck reactions. In the Michael addition of amines and conjugated alkenes, the reaction was carried out in low molecular weight PEG at room temperature without additional base or acid.[8] The transformation proceeds rapidly, using the interaction of PEG with one of the reactants to enhance the reaction rate. The products were easily separated by cyclohexane extraction, which allowed for three solvent recycles with minimal loss in activity.

In the following reactions, PEG enables excellent recycle of expensive catalytic systems by immobilization of the catalysts in the solvent. The first transformation is the palladium-catalyzed Heck reaction between bromobenzene and ethyl acrylate by Chandrasekhar *et al.*[9] Using high molecular weight PEG at elevated temperatures, the

researchers achieved good yields with improved regioselectivity over ionic liquids or conventional systems. The recycle was carried out by extracting the products into ether and reducing the temperature to 0ºC, which allowed for solidification of the PEG and sequestration of the catalyst. This enabled five recycles with only small losses in activity. Similar activity and catalyst recycle have been explored for the Suzuki-Miyaura reaction and the Sonogashira coupling.[10, 11]

The next application of PEG in synthesis involves its use as a phase transfer catalyst (PTC). In the next Chapter, we shall describe the PTC process in depth, but it basically uses catalysts to shuttle reactants into the same phase, allowing for a monophasic reaction in a multiphasic system.[12] PEG represents a cheap class of catalysts that behave similarly to the more expensive crown ethers. These catalysts can complex with metal cations, which, in turn, bring along an anion that can become available for reaction.[4] The reaction efficiency can be tuned by manipulating the molecular weight of the PEG. This area has been extensively explored, so many types of reactions have been tested, including nucleophilic substitutions and redox reactions. The technique has also been extended to PEG-supported PTCs, which enable rate enhancements and improved catalyst recovery through solid precipitation.

PEG supports have been applied not only to PTCs, but also to numerous other types of catalysts. These types of support offer homogenous reaction with built-in separation, allowing the catalysts to overcome the typical mass transport and leaching problems associated with heterogeneous supports. PEG-supported catalysts are usually separated by adding large amounts of poor solvent, such as ether or carbon dioxide, which cause the catalyst to precipitate.[13] The separation can also be induced

thermomorphically, similar to other soluble polymers, such as polyethylene and poly(N-isopropylacrylamide) (PNIPAM).[14] Berbreiter *et al.* used a liquid-liquid biphasic system to enable PEG-supported catalyst recovery using N,N-dimethylacetamide and heptane as solvents, which are immiscible at low temperatures and completely miscible at high.[15] They were able to recycle the system three times in the Pd-catalyzed Heck reaction of aryl iodides with alkenes.

4.1.2 Gas-Expanded Liquids

Most of the preceding applications of PEG in synthetic reactions involve the use of organic solvents during the separation steps. This necessity reduces the benefits of using an environmentally benign solvent, because we revert back to the problems associated with conventional solvents. However, recent developments have improved this situation by replacing the organic solvents with supercritical fluids. The most commonly used supercritical fluid is carbon dioxide, which is benign and cheap and has relatively low critical points.[2] There has been a great deal of research into its properties, and it has shown wide ranging applications in both reactions and separations.

This work has been extended through the combination of carbon dioxide with organic solvents, known as gas-expanded liquids (GXLs).[16] These novel materials are generated by the dissolution of a gas, usually carbon dioxide, into the totally miscible solvent, causing the liquid to expand and the solvent properties to vary. Carbon dioxide is a poor, non-polar solvent and the dissolution is highly dependent on temperature and pressure, so the properties of a solvent can be tuned by simply modifying the system

conditions. The solvent properties combine those of supercritical fluids and liquids, as illustrated in Figure 4-2.

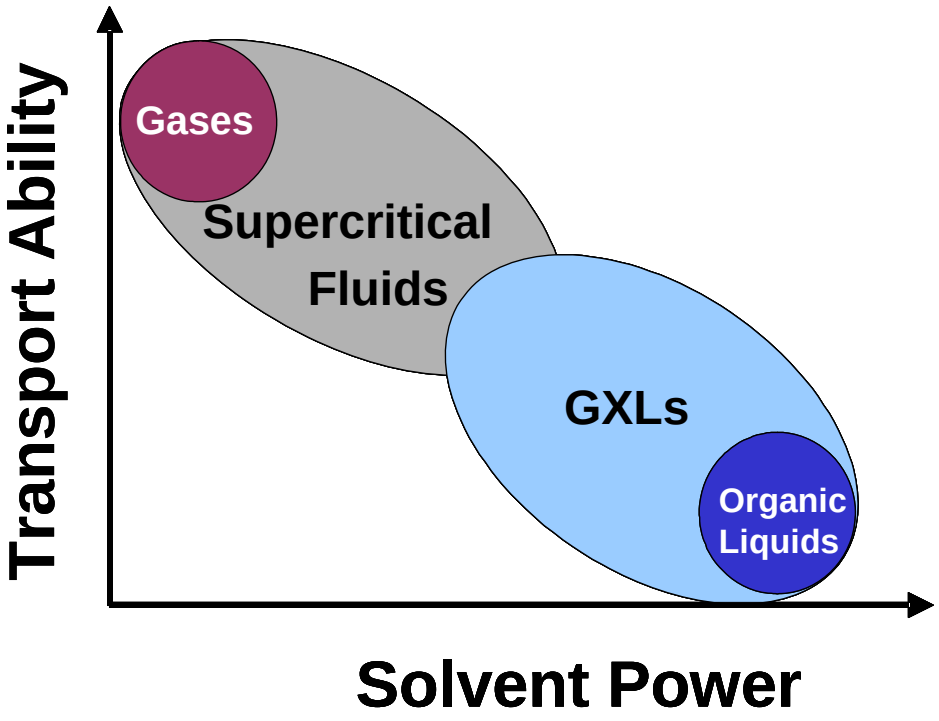

Figure 4-2 Qualitative Relationship between Solvents for Transport Ability and Solvent Power

GXLs have improved mass transport over liquids and elevated solvent power over supercritical fluids. This leads to improved substrate solubility and reduced transport issues related to multiphasic system, such as in PTC reactions. These novel solvents have been applied to many processing applications, including gas antisolvent (GAS) processes, particle deposition, and homogenous reactions coupled with heterogeneous separations to name just a few.[16] GAS uses carbon dioxide as a poor solvent to induce the precipitation of solutes, and has been applied to a variety of processes, including crystallization. Roberts *et al.* have used GXLs to enable nanoparticle deposition, using

carbon dioxide pressure to selectively precipitate nanoparticles of a specific size. Additionally, numerous reactions have been carried out in GXLs, ranging from hydrogenations and hydroformylations to acid-catalyzed reactions and polymerizations. In most of our work, we use GXLs to induce phase separations that allow for product purification and catalyst recycle.

Researchers have used carbon dioxide with PEG in a variety of reactions and separations, and have studied its effect on the solvent properties. The properties of these modified systems show interesting and useful effects, such as reduction of viscosity and melting point depression under carbon dioxide pressure. Jessop *et al.* developed the first PEG/scCO_2 scheme in the rhodium-catalyzed hydrogenation of styrene to ethyl benzene.[17, 18] In this system, they allowed the reaction to proceed at 40ºC and then used sweeping scCO_2 to remove the products. The catalyst was immobilized in the PEG phase and recycled five times with no loss in activity. Similar systems were used for the aerobic oxidation of styrene by $PdCl_2$/CuCl.[19] Another interesting extension of this work involves the lipase-catalyzed acylation of 2-phenylethanol by vinyl acetate. Wiesenhofer *et al.* were able to use a continuous reaction/separation process with scCO_2 and recycle the catalytic system 11 times.[20] This application broadens the capabilities of PEG as a solvent system beyond simple reactions and organometallic-catalyzed transformations into the extensive realm of enzyme-catalyzed synthesis.

GXLs have been employed in reaction and separations for several systems. In most of these scenarios, researchers use mixed solvents to enable homogenous reaction and then add carbon dioxide to induce phase separation, allowing for heterogeneous separation. In our group, we have primarily focused on organic-aqueous tunable solvents

(OATS), investigating phase behavior and numerous reaction/separation applications.[21] We use these systems to facilitate homogenously-catalyzed reactions, which allow for improved activity and selectivity over heterogeneous systems. These homogeneous catalysts eliminate mass transfer limitations, leaching, and deactivation that can often occur with heterogeneous catalysts. However, due to their homogeneous nature, they are difficult to recycle, which is extremely important for reactions that involve expensive and/or toxic catalysts and ligands. Therefore, we couple this technique with heterogeneous separations by using GXL-induced phase separation, allowing for catalyst recycle and easy product recovery. We create the homogeneous reaction system through use of water and a soluble organic, such as dioxane, acetonitrile, or THF. After completion of the reaction, we add the carbon dioxide, which preferentially partitions into the organic phase, creating a GXL that reduces in polarity and induces phase separation. The phase separation requires only 30 bar of carbon dioxide for the THF system, significantly reducing the pressure needed for good separation as compared to supercritical systems.[22, 23] Through proper design of OATS, we are able to use carbon dioxide as a phase switch to partition the hydrophobic products into the organic phase and the hydrophilic catalysts into the aqueous phase. The effect is easily reversible through depressurization of CO_2, which allows for continuation of the reaction cycle. We have worked on several reaction systems, including hydroformylations, epoxidations, and enzymatic reactions.[24-26]

Similar systems have been developed for ionic liquid separation. These systems closely resemble OATS, but exchange the aqueous phase for an ionic liquid. Scurto *et al.* demonstrated the carbon dioxide induced switch for a solution containing methanol and

[Bmim][PF_6].[27] Like OATS, the two solvents are miscible at atmospheric conditions, but then phase separate upon addition of 50-80 bar carbon dioxide, depending on the concentration of ionic liquid. This technique represents an important development in ionic liquid separations, which are often difficult to remove due to their low volatility. We have also developed separation systems with fluorinated solvents. The mechanism for these separations operates in a different manner since the fluorinated materials are immiscible with polar organic solvents at atmospheric conditions. Through dissolution of 30 bar carbon dioxide, the GXL reduces in polarity, causing it to become miscible with the fluorous solvent.[3] Hence, the process works in reverse, with the heterogeneous state at atmospheric conditions and the homogenous under elevated pressures and temperatures. These have applications to fluorinated catalytic systems, allowing for recovery of these materials in the fluorous phase. We have applied several reactions to this system, including a hydrogenation and epoxidation.[3]

4.1.3 PEG-Tunable Systems

We would like to modify the OATS technique to replace the water phase with a low molecular weight PEG. The key advantage to the PEG-tunable systems is the elimination of the aqueous phase. The cosolvents for the original system are limited by the organic solubility in water, which must have complete miscibility at atmospheric conditions. Due to the organic character of low molecular weight PEGs, we are able to expand the list of available organic cosolvents. More importantly, these new systems create additional applications for reactions involving water-sensitive compounds or

water-unfavorable equilibrium. The scheme for this reaction and separation system is illustrated in Figure 4-3.

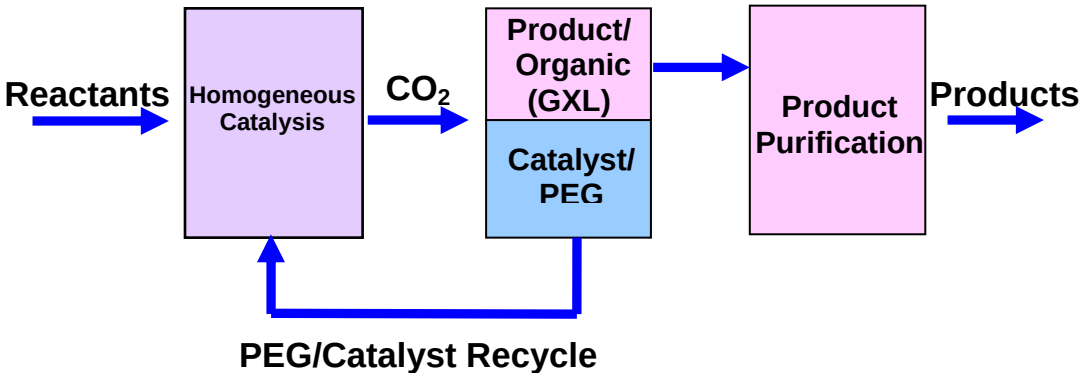

Figure 4-3 Scheme for Homogenous Reaction with Heterogeneous Separation for Catalyst Recycle

The current focus of this study involves the determination of the liquid-liquid equilibrium between PEG 400, various organic solvents, and carbon dioxide. In order to design these systems, we must understand the phase behavior of PEG, a largely unexplored area of fluid phase equilibria. However, there have been several studies on the binary phase behavior of low molecular weight PEGs with carbon dioxide. Gourgouillon *et al.* used a sapphire-cylinder equilibrium cell with sampling to obtain the binary phase behavior of PEG 200, 400, and 600 with carbon dioxide.[28] Guandagno *et al.* took a different approach to obtain the binary data for PEG 400 and carbon dioxide,

using in-situ near-IR spectroscopy.[29] Generally, the only ternary studies related to PEG involve aqueous biphasic systems, in which significant amounts of salt are added to the PEG and water mixture to induce phase separation. The technique has been used for applications such as protein purification, creating the need for a number of phase behavior studies in order to help with the design of new systems. Unlike our technique, these systems are not reversible, limiting the environmental benefits and reducing the possibility of recycle. Besides the aqueous biphasic research, very few studies have looked into ternary systems, with even less related to mixtures containing PEG, organic solvents, and carbon dioxide. Recently, though, there have been reports on the phase behavior of PEG with alcohols and carbon dioxide, such as ethanol, 1-pentanol, and 1-octanol.[30, 31] The authors have identified the possible use of these materials for separation but have not completed an in-depth analysis with different solvents or developed any applications. We will explore the phase behavior for PEG 400 and carbon dioxide with 1,4-dioxane and acetonitrile at 25 and 40ºC. Then, we will lay the groundwork for application of the reaction/separation system for the production of phenols, which will be discussed in detail after the liquid-liquid equilibria.

4.2 Experimental

4.2.1 Materials

All chemicals used in this work were used as received from the supplier. They include: poly(ethylene glycol) (average molecular weight 300 and 400, Aldrich), poly(ethylene glycol) dimethyl ether (average molecular weight 250, Aldrich), 1,4-

dioxane (Sigma-Aldrich, anhydrous, 99.8%), acetonitrile (Sigma-Aldrich, anhydrous, 99.8%), isopropanol (Acros Organic, anhydrous), tetrahydrofuran (Sigma-Aldrich, HPLC grade, inhibitor-free, ≥99.9%), 2,5-dimethylphenol (Aldrich, 99+%), and ditertbutylphenol (Alfa Aesar, 97%). The carbon dioxide was SFC grade (Air Gas, 99.999%) and further purified to remove trace water and other impurities with a Matheson gas purifier and filter cartridge (Model 450B, Type 451 filter).

4.2.2 Experimental Methods

4.2.2.1 Vapor-Liquid-Liquid Equilibrium

The ternary phase equilibria were determined with the apparatus shown in Figure 4.4. The apparatus and procedure were described in great detail in Lazzaroni *et al.*[23] The system consists of a precision bored, hollow sapphire cylinder (50.8 mm O.D. x 25.4±0.0001 mm I.D. x 203.2 mm length) with stainless steel end caps and movable piston. The ends and the piston are sealed with an o-ring (75 Viton, size 210) and back-up ring (90 Nitrile, size 210). The piston divides the system into two chambers, in which the upper portion contains the equilibrium composition and the lower contains water as the pressurizing fluid. The temperature was controlled with an air bath and digital temperature controller (Omega CN76000) combined with an overtemperature controller (Omega CN375) to ensure safe operation. The controller temperature was monitored with thermocouples (Omega type K), while the cell vapor temperature was determined by RTD (Omega). The thermocouples and RTD were calibrated against a platinum RTD (Omega PRP-4) with DP251 Precision RTD Benchtop Thermometer (DP251 Omega),

providing an accuracy of ±0.2K. The pressures were measured with a Druck pressure transducer and read-out (DPI 260, PDCR 910), and were calibrated against a hydraulic piston pressure gauge (Ruska). The error associated with the pressure is estimated at ±0.01 MPa. Stirring was accomplished with a rotating shaft attached to the cell body, allowing for manual end-over-end rotation of the apparatus. The schematic for the apparatus is shown in Figure 4-4.

After assembly of the apparatus, the cell was vacuumed to remove any traces of air. The liquid phase material was then weighed and added through a gas-tight syringe. The CO_2 was added via a syringe pump (ISCO, model 500D) connected to an ethylene glycol chiller for constant pressure and temperature. The exact amount of CO_2 was determined by using the Span-Wagner EOS.[32] Height measurements of each phase were taken with a micrometer cathetometer. These values could then be correlated to volumes with knowledge of the inner diameter of the cell.

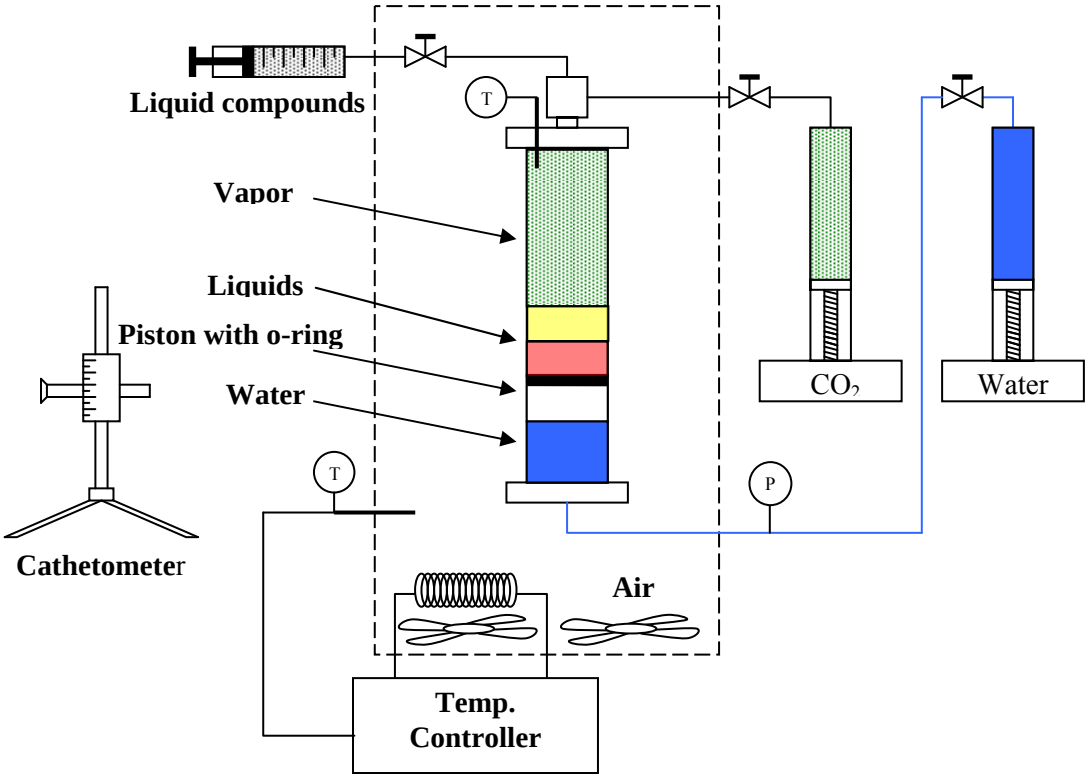

Figure 4-4 Apparatus for High Pressure, Variable-Volume Sapphire Cell

The sapphire cell procedure allows for determination of the ternary phase equilibria without sampling, eliminating the errors associated with normal sampling techniques. This procedure is a synthetic method that uses material balances to determine the compositions of each phase. The following equations represent the balances required for solving a three component system, where N represents moles, V the volume, v the molar volume, and x the mole fraction.

$$N_T = \frac{V^\alpha}{v^\alpha} + \frac{V^\beta}{v^\beta} + \frac{V^\nu}{v^\nu} \quad 4\text{-}1$$

$$N_1 = \frac{x_1^\alpha V^\alpha}{v^\alpha} + \frac{x_1^\beta V^\beta}{v^\beta} + \frac{x_1^\nu V^\nu}{v^\nu} \quad 4\text{-}2$$

$$N_2 = \frac{x_2^\alpha V^\alpha}{v^\alpha} + \frac{x_2^\beta V^\beta}{v^\beta} + \frac{x_2^\nu V^\nu}{v^\nu} \quad 4\text{-}3$$

From each experiment, both the individual and total number of moles can be determined, while the volumes are calculated from the cathetometer readings. Since the mole fractions and molar volumes are independent of concentration in a three component, three phase system, we can use three independent loadings to generate nine equations and nine unknowns to solve for the composition of each phase. In this case, at least four loadings were completed to increase precision. Due to the low amount (<2 mol%) of impurities in the vapor phase, the value of the molar volume for this phase was determined by the pure CO_2 density at the given pressure and temperature based on the Span-Wagner EOS. The composition of the vapor phase was estimated based on the binary organic/CO_2 system as modeled by the Peng-Robinson EOS.

4.2.2.2 Partitioning Experiments

In order to assess the partitioning of various solutes in the PEG tunable systems, we used a sampling technique to measure directly the compositions. We used a high

pressure Jerguson cell equipped with a sample valve to remove a 0.5 mL sample from the two liquid phases for analysis. The schematic for the sample valve and complete cell apparatus are shown in Figure 4-5 and 4-6. The apparatus involves similar peripheral components to those contained in the sapphire cell set-up, such as temperature controller, air bath, syringe pump, and thermocouple. In the measurement of the solute partitioning, PEG-400, 1,4-dioxane, and either 2,5-dimethylphenol or 2,4-ditertbutylphenol, were added and the system was pressurized with CO_2 until it reached the cloud point, where the two phases split. We then continued to add CO_2 until the system reached the desired measurement conditions. We analyzed the partitioning by using the sample valve to collect samples from each phase and then analyzed them via UV-vis spectroscopy. The solute concentrations were determined directly with calibration curves, and then compared to derive the partition coefficient. We tested the solute composition in both phases for various conditions, and then altered the solvent slightly by adding small quantities of salt and water to test the effect of additional solutes.

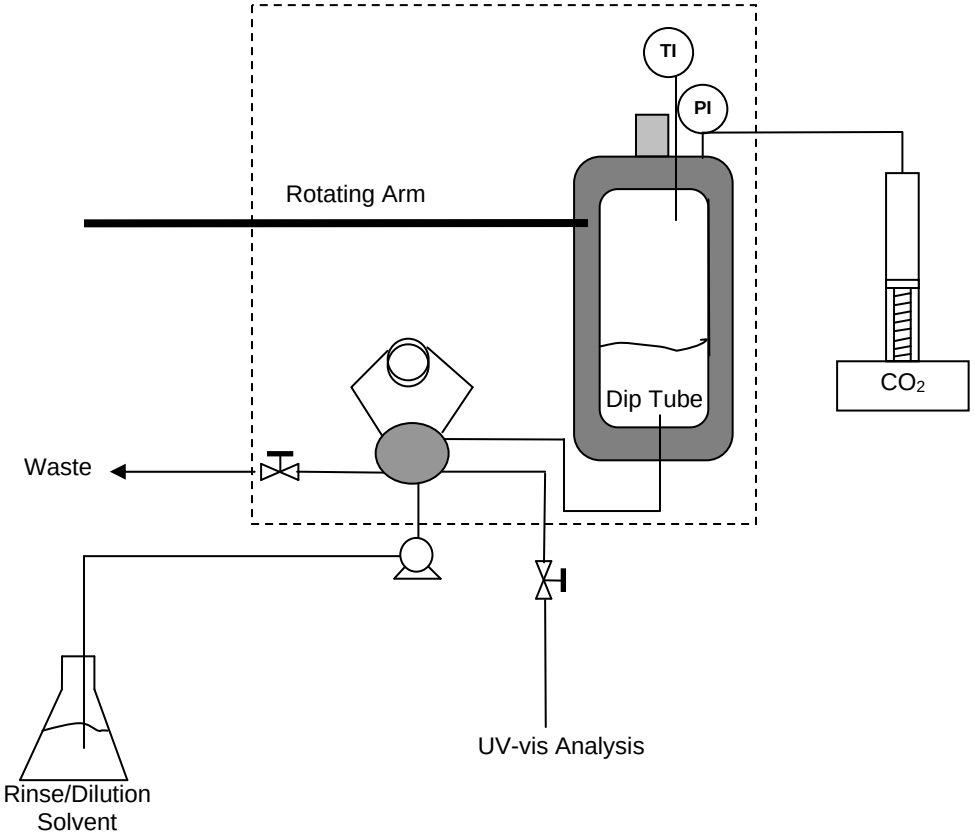

Figure 4-5 Apparatus for High Pressure Jerguson Cell with Sample Loop

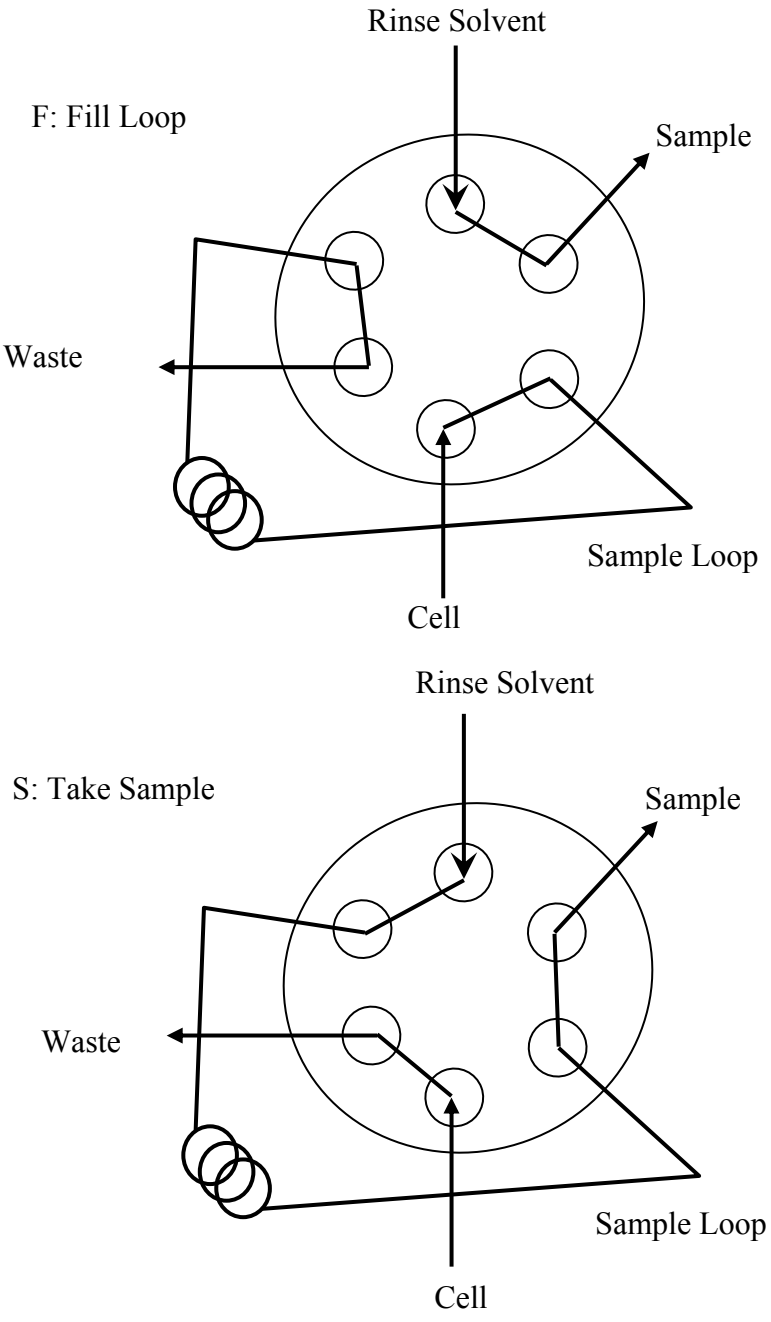

Figure 4-6 Internal Mechanics of Sample Loop for Jerguson Cell Sampling Method

4.3 Modeling

We chose to model the LLE data with the Sanchez-Lacombe equation of state (SL-EOS).[33] In our earlier work, Lazzaroni *et al.* have found that the Peng-Robinson with Stryjeck and Vera modification (PRSV) with Huron-Vidal mixing rules[34] work best for OATS.[23] However, with a polymer system, the modeling could yield significantly different results from our previous efforts with the OATS phase behavior. Thus, it is necessary to test the theories that have been successfully applied to non-ideal, polymeric solutions. Numerous models have been completed for polymer solutions in the literature, including molecular theories like UNIQUAC and NRTL and group contribution theories like UNIFAC.[35] However, for the binary phase behavior of PEG-400 and carbon dioxide, Gourgouillon *et al.* used the SL-EOS, which was successfully applied to the polymer phase behavior.[28] This model has been successfully applied to numerous polymeric systems, so it represents an excellent starting point for modeling the data.

The Sanchez-Lacombe equation of state uses lattice fluid (LF) theory to predict the thermodynamics of polymeric systems. It expands upon the classical lattice theory developed by Flory and Huggins for modeling molecules of vastly varying sizes, such as polymers and solvents. The LF theory deviates from the original by allowing for vacancies to exist within the lattice.[36, 37] This factor causes the theory to incorporate compressibility, significantly enhancing the predictive capabilities of the model. By accounting for compressibility, the model can predict entropically driven phenomena, such the lower critical solution temperature (LCST) commonly found in polymeric solutions.[33] The model uses only one adjustable parameter to characterize the behavior.

4.3.1 Parameter Calculation

In the SL-EOS model, the lattice defines a system of N_1r_1-mers, N_2r_2-mers, ….N_ir_i-mers with N_0 vacant sites, in which an r-mer represents a molecule that occupies r sites. The EOS uses three key parameters to describe the pure component properties. The first parameter is r, the average number of sites that a molecule occupies on the lattice. It is used to define the composition of one r_i-mer on the lattice, or the site fraction:

$$\phi_i = \frac{r_i N_i}{\sum_{i=1}^{n} r_i N_i} \qquad 4\text{-}4$$

This equation can be rewritten in terms of site fraction to yield a simple formula for determining r:

$$\frac{1}{r} = \sum_{i=1}^{n} \frac{\phi_i}{r_i} \qquad 4\text{-}5$$

The next parameter is ε*, which represents the average site to site interaction energy:

$$\varepsilon^* = \sum_{i=1}^{n}\sum_{j=1}^{n} \phi_i \phi_j \varepsilon_{ij}^* \qquad 4\text{-}6$$

The mixed energy parameter, ε_{ij}*, is determined by the geometric mean rule and the binary interaction parameter, ζ_{ij}:

$$\varepsilon_{ij}^{\ *} = \left(\varepsilon_{ii}^* \varepsilon_{jj}^*\right)^{1/2} \zeta_{ij} \qquad 4\text{-}7$$

The energy parameter is also useful for determining the Flory-Huggins interaction parameter, which will be required in later calculations:

$$\chi_{ij} = \frac{\varepsilon_{ii}^{*} + \varepsilon_{jj}^{*} - 2\varepsilon_{ij}^{*}}{kT} \tag{4-8}$$

The final parameter is v*, the average volume of the molecular segments, which is calculated with quadratic mixing rules:

$$v^{*} = \sum_{i=1}^{n}\sum_{j=1}^{n}\phi_i\phi_j v_{ij}^{*} \tag{4-9}$$

$$v_{ij}^{*} = \left(\frac{v_{ii}^{*1/3} + v_{jj}^{*1/3}}{2}\right)^3 \tag{4-10}$$

The above parameters can be used to calculate the characteristic temperature (T*), pressure (P*), and density (ρ*) or their reduced properties:

$$\widetilde{T} \equiv \frac{T}{T^{*}} = \frac{kT}{\varepsilon^{*}} \tag{4-11}$$

$$\widetilde{P} \equiv \frac{P}{P^{*}} = \frac{Pv^{*}}{\varepsilon^{*}} \tag{4-12}$$

$$\widetilde{\rho} \equiv \frac{1}{\widetilde{v}} \equiv \frac{\rho}{\rho^{*}} = \rho\frac{rv^{*}}{M} \tag{4-13}$$

In the reduced properties equations, k is defined as the Boltzmann constant and M is the average molecular weight, which is calculated linearly with the mole fraction (y_i)::

$$M = \sum_{i=1}^{n} y_i M_i \qquad 4\text{-}14$$

$$y_i = \frac{\phi_i r}{r_i} \qquad 4\text{-}15$$

4.3.2 Equation of State Calculations

The equation of state can be derived by approximating a large lattice coordination number (z), and the following related to the Gibbs free energy:

$$\left.\frac{\partial G}{\partial \tilde{v}}\right|_{T,P,\phi} = 0 \qquad 4\text{-}16$$

This yields the Sanchez-Lacombe EOS:

$$\tilde{\rho}^2 + \tilde{P} + \tilde{T}\left[\ln(1-\tilde{\rho}) + \left(1 - \frac{1}{r}\right)\tilde{\rho}\right] = 0 \qquad 4\text{-}17$$

The final equation for development of the lattice fluid EOS requires the derivation of the Gibbs free energy with respect to N_i at constant T, P, and N_j to give the chemical potential of the species in each phase:

$$\frac{\mu_i^{LF}}{kT} = \ln\phi_i + \left(1 - \frac{r_i}{r}\right) + r_i\tilde{\rho}\left(\sum_{j=1}^{n}\phi_j\chi_{ij} - \sum_{j=1}^{n}\sum_{k=j+1}^{n}\phi_j\phi_k\chi_{jk}\right) + r_i\left[-\frac{\tilde{\rho}}{\tilde{T}_i} + \frac{\tilde{P}_i\tilde{v}}{\tilde{T}} + (\tilde{v}-1)\ln(1-\tilde{\rho}) + \frac{1}{r_i}\ln\tilde{\rho}\right] \quad 4\text{-}18$$

4.3.3 Equilibrium Composition Calculations

In order to determine the equilibrium compositions, we use the equation of state to find the density of each phase at a given temperature and pressure, and then use that value to calculate the chemical potential of the components in each phase. The system is constrained by the following conditions, in which the chemical potential of one component in one phase must be equivalent to that same component in the other phase:

$$-\frac{\mu_1^{l_1}}{kT} = -\frac{\mu_1^{l_2}}{kT} \text{ and } -\frac{\mu_3^{l_1}}{kT} = -\frac{\mu_3^{l_2}}{kT} \quad 4\text{-}19$$

We solved for the compositions with a procedure involving the Generalized Reduced Gradient non-linear algorithm used in the solver function of Microsoft Excel. The Visual-Basic code for the model is presented in Appendix D. In order to characterize the accuracy of the model, we calculated an average absolute relative deviation (AARD) for each binary and ternary system. The following equation represents the method of calculation:

$$AARD = average\left(\frac{x_i^{\exp} - x_i^{calc}}{x_i^{\exp}}\right) x\ 100\% \quad 4\text{-}20$$

4.3.4 Pure Component Parameters

The parameters for the Sanchez-Lacombe EOS were obtained from several sources. The organic solvent parameters were derived from application of the SL-EOS to the pure vapor pressure data. Those for 1,4-dioxane were obtained directly from Sanchez *et al.*, while those for acetonitrile were fit to the vapor pressure data from Ochoa *et al.*[38] The parameters for acetonitrile were fit according to the procedure outlined in Sanchez *et al.*[33] Polymer parameters are determined in a different fashion due to their low volatility. They are usually fit by nonlinear least-squares analysis of liquid density data.[36] The parameters for carbon dioxide are also fit differently due to its high compressibility. Therefore, most researchers model the PVT data to determine the values. However, depending on the range of the data, the parameters can vary widely, resulting in many sets of values for this single component. We chose to use parameters fit by Garg *et al.*, because they model CO_2 for a wide range of PVT data, allowing for its broadest application.[39] The parameter values are displayed in Table 4-1.

Table 4-1 Parameters for Sanchez-Lacombe EOS Model

Molecule	MW (g/mol)	ε* (kJ/mol)	v* (cm^3/mol)	r	References
CO_2	44.01	2.73	5.88	5.25	Garg *et al.*[39]
1,4-dioxane	88.11	4.31	8.05	9.42	Sanchez, Panayiotou[33]
acetonitrile	41.05	4.70	6.40	7.62	Calculated
PEG 400	400	5.47	11.28	30.00	Harrison *et al.*[40]

4.3.5 Binary Interaction Parameters

The binary interaction parameters (ζ_{ij}) were determined from the binary phase behavior for CO_2 with the various solvents. In order to validate the model, we first determined the binary interaction parameter for a known system, acetone and CO_2, from the binary data generated by Day *et al.*[41] The model generated a parameter (ζ_{ij}) equivalent to 1.048 with an AARD of <1%, which closely matches the values reported in literature.[41] The plot illustrating the binary data and the model is shown in Figure 4-7. We then applied the model to the test systems and determined the parameters listed in Table 4-2. Figure 4-8 illustrates an example of one of the binary plots with the fitted model. The remaining plots are located in Appendix E. We were unable to determine the binary interaction parameter for PEG-400 at 25ºC due to a lack of binary phase behavior. However, according to recent literature, the values remain fairly constant over a large temperature range, allowing us to apply the 40ºC value to all the models.

Generally, the binary interaction parameters for CO_2 and the solvents fall within the typical range for these types of systems. However, the PEG-400 value at 1.134 slightly contradicted one literature study, which determined the parameter to be 0.973.[28] The difference could be attributed to variations in the mixing rules or SL-EOS parameters for CO_2, which vary widely within the literature depending on the method of calculation. The final binary interaction parameters are for the PEG-400-organic solvent relationship. These are used as adjustable parameters for the ternary system. Also, it must be noted that the model is extremely sensitive to small changes in these parameters, so minute variations lead to vastly different results.

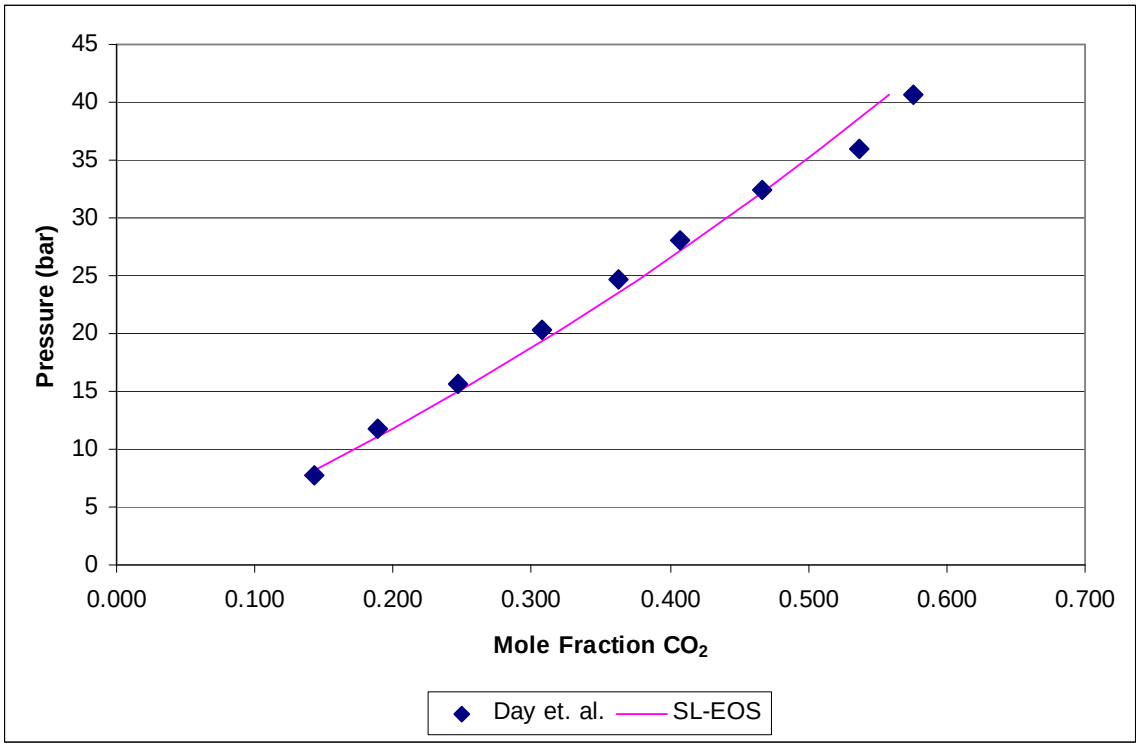

Figure 4-7 Validation of Sanchez-Lacombe EOS on Acetone/CO_2 VLE at 40°C, , ζ=1.048

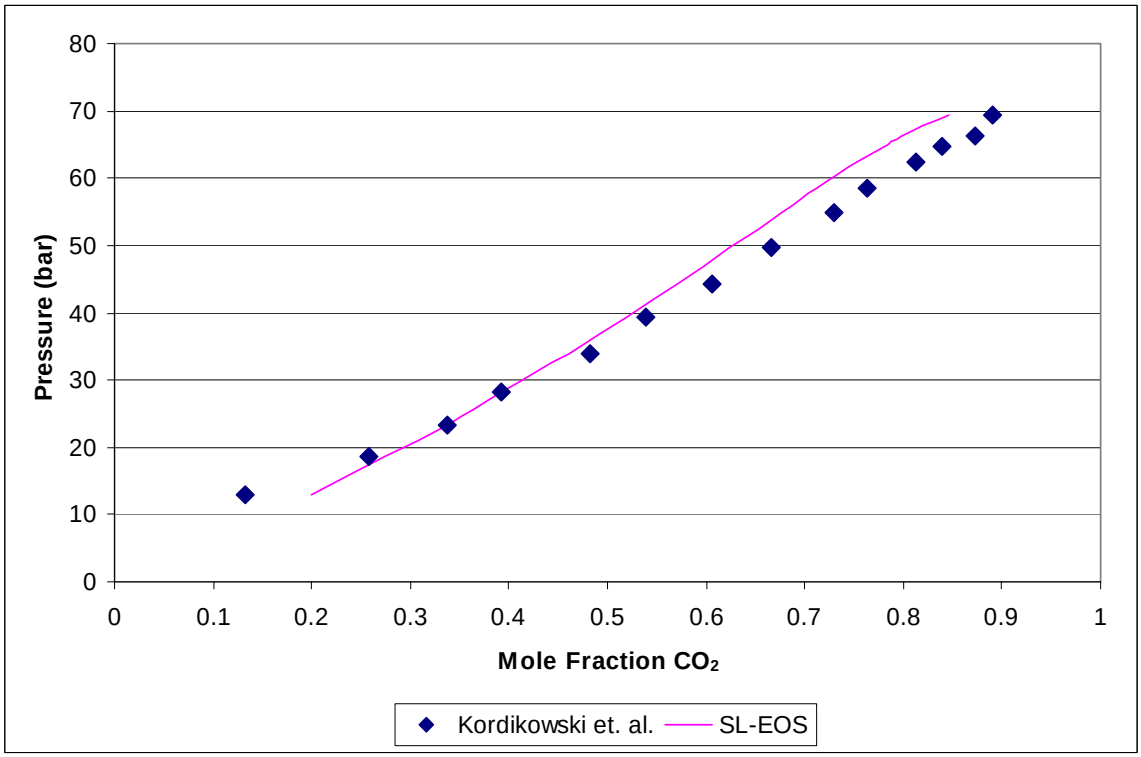

Figure 4-8 Application of Sanchez-Lacombe EOS to 1,4-Dioxane/CO_2 Binary Data at 40°C, ζ=1.049

Table 4-2 Binary Interaction Parameters for CO_2-Cosolvent VLE

Cosolvent	T (K)	ξ_{12}	AARD (%)	References
1,4-dioxane	298	1.044	7%	Kordikowski *et al*.[42]
	313	1.049	9%	Kordikowski *et al*.[42]
acetonitrile	298	1.054	3%	Kordikowski *et al.*[42]
PEG 400	313	1.134	3%	Gourgouillon *et al.*[28]

4.4 Results

4.4.1 Binary Studies

In order to verify the accuracy of the phase behavior measurement technique for systems containing PEG, we first measured the binary data for PEG 300 and 400 with carbon dioxide. Based on literature, it was assumed that there was no PEG in the vapor phase, which is accurate up to approximately 11.0 MPa. Figure 4-9 illustrates the results and shows that the technique works well for this system, since the experimental data closely match the literature.[43]

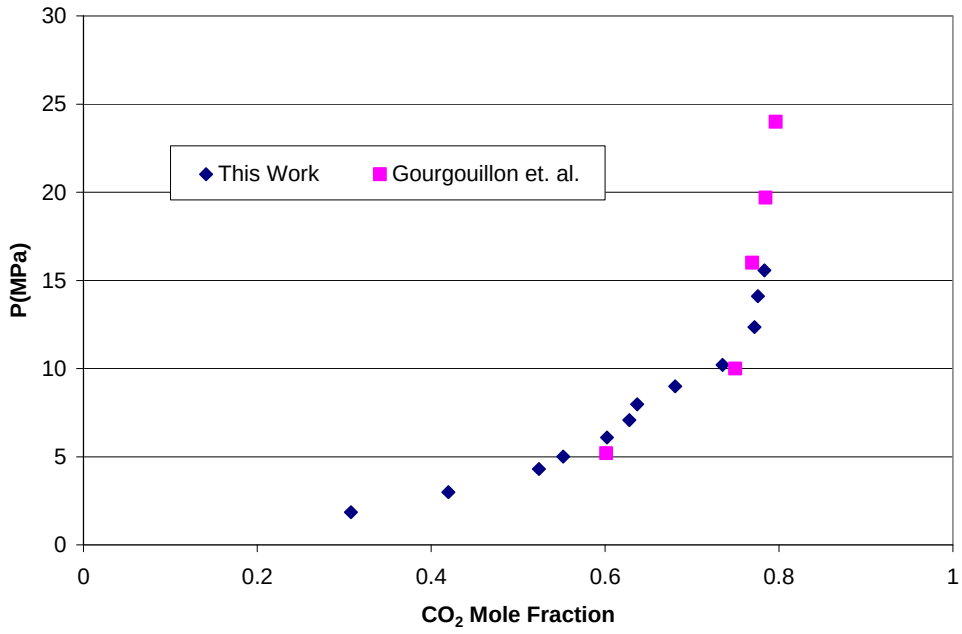

Figure 4-9 Validation of Sapphire Cell Technique on Binary PEG400/CO_2 Data at 40ºC

4.4.2 Ternary System Cloud Point Analysis

The next effect we investigated involves cloud point testing to determine the pressure at which PEG, CO_2, and the various organic solvents change from a two phase system into a three phase system. This represents the cloud point for the mixture at a given temperature. As illustrated in Figure 4-10, the results indicate that the cloud points have minimal variability between several organic solvents, including dimethylsulfoxide, acetonitrile, toluene, 1,4 dioxane, tetrahydrofuran, and methyl isobutyl ketone (MIBK). The carbon dioxide required for the phase split is relatively high (4.5-6.0 MPa) in comparison to most organic/aqueous systems, indicating that the PEG systems will require higher pressure ranges to attain good partitioning.

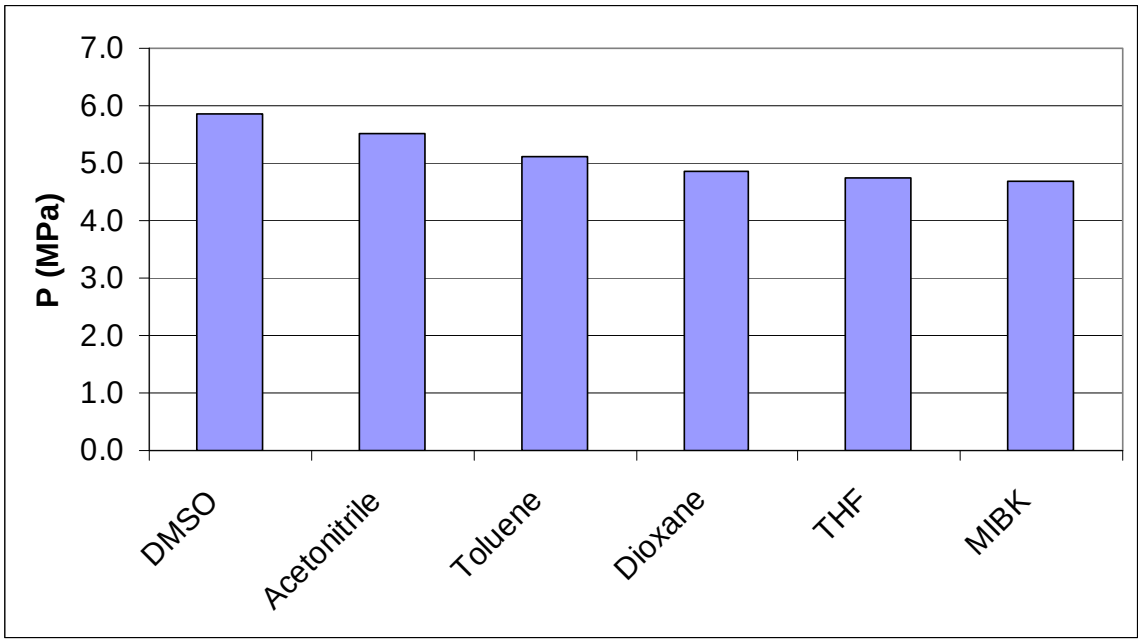

Figure 4-10 Cloud Points for Various Organic Solvents with PEG 300 at 25ºC

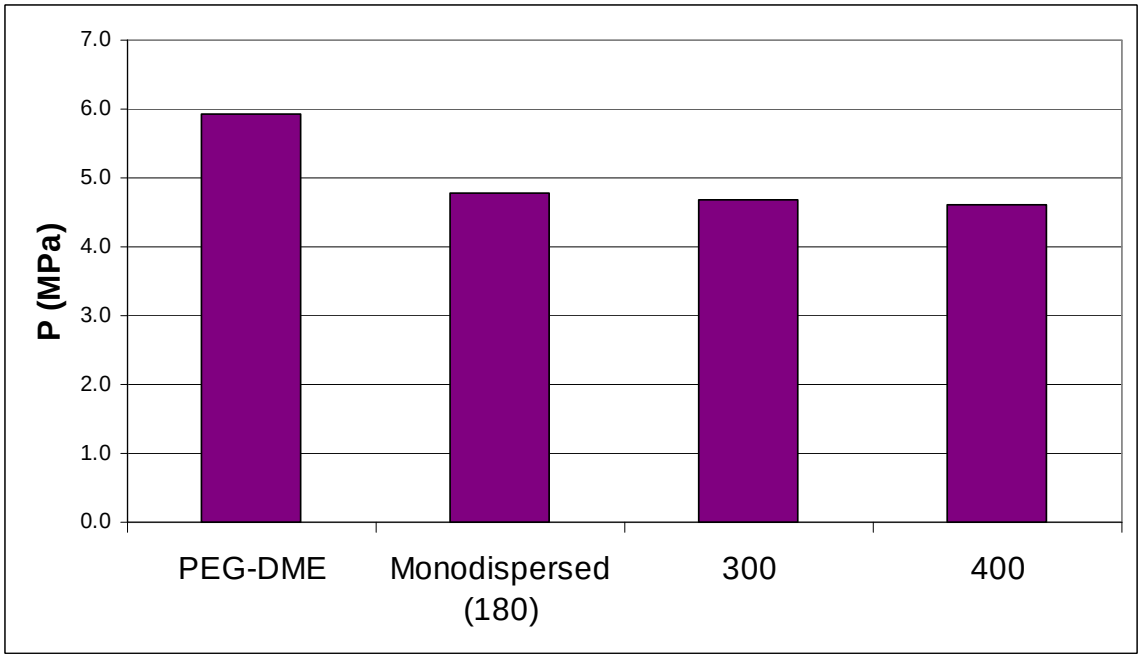

Figure 4-11 Cloud Points for Methyl isobutyl ketone (MIBK) with Various PEGs at 25ºC

Next, we examined the effect of molecular weight on the cloud points with MIBK, as shown in Figure 4-11. We chose this solvent in order to minimize the amount of pressure required to achieve the phase split, and MIBK had the lowest cloud-point value from the previous tests. The results showed negligible differences between PEG 300, 400, tetraethylene glycol (MW 180), and a methyl capped version, known as PEG-dimethyl ether (MW 250). This shows that the cloud point for PEG is not greatly impacted by changing molecular weight or modifying the end group. However, our study was limited to liquid PEGs, so there may be much larger differences with higher molecular weight materials.

4.4.3 Ternary Phase Behavior

The liquid-liquid phase behavior plots for PEG-400 and CO_2 with the organics are shown in Figures 4-13 through 4-15. The tables enumerating the data can be found in Tables 4-3 through 4-5. Due to the significant differences in molecular weight, the ternary plots use weight percent for the compositions to illustrate the data more clearly. In general, the liquid-liquid equilibria show type II behavior. Hence, the systems transition from liquid-vapor equilibrium to liquid-liquid-vapor, generating the third phase upon increased CO_2 pressure. The system consists of two liquid phases, a PEG-rich lower and an organic-rich upper, as well as a CO_2-rich vapor phase. At elevated pressures, the system can reach the critical point for the organic/CO_2 mixture, leading to loss of the organic-rich phase and generation of liquid-fluid equilibrium. Figure 4-12 illustrates the transitions that take place within the PEG-tunable systems.

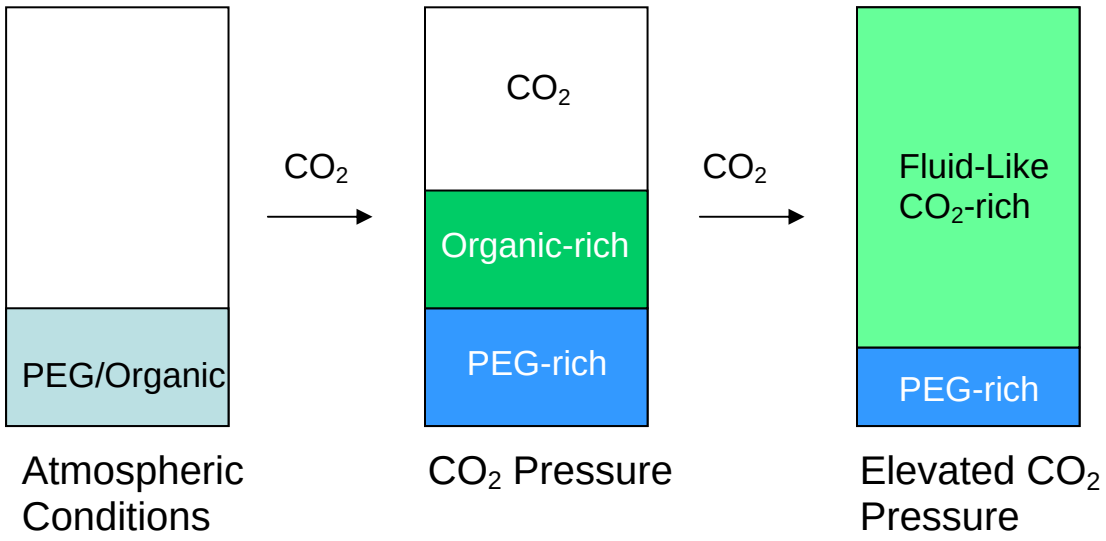

Figure 4-12 Schematic of Phase Transitions in PEG-Tunable Systems

For these experiments, we focused on the three-phase system only, so the compositions reflect only this region of the phase behavior. Only the liquid-liquid equilibria are shown in the ternary diagrams, but, in each case, the systems also contained a vapor phase consisting of >95 mol% CO_2, as estimated by the Peng-Robinson EOS.

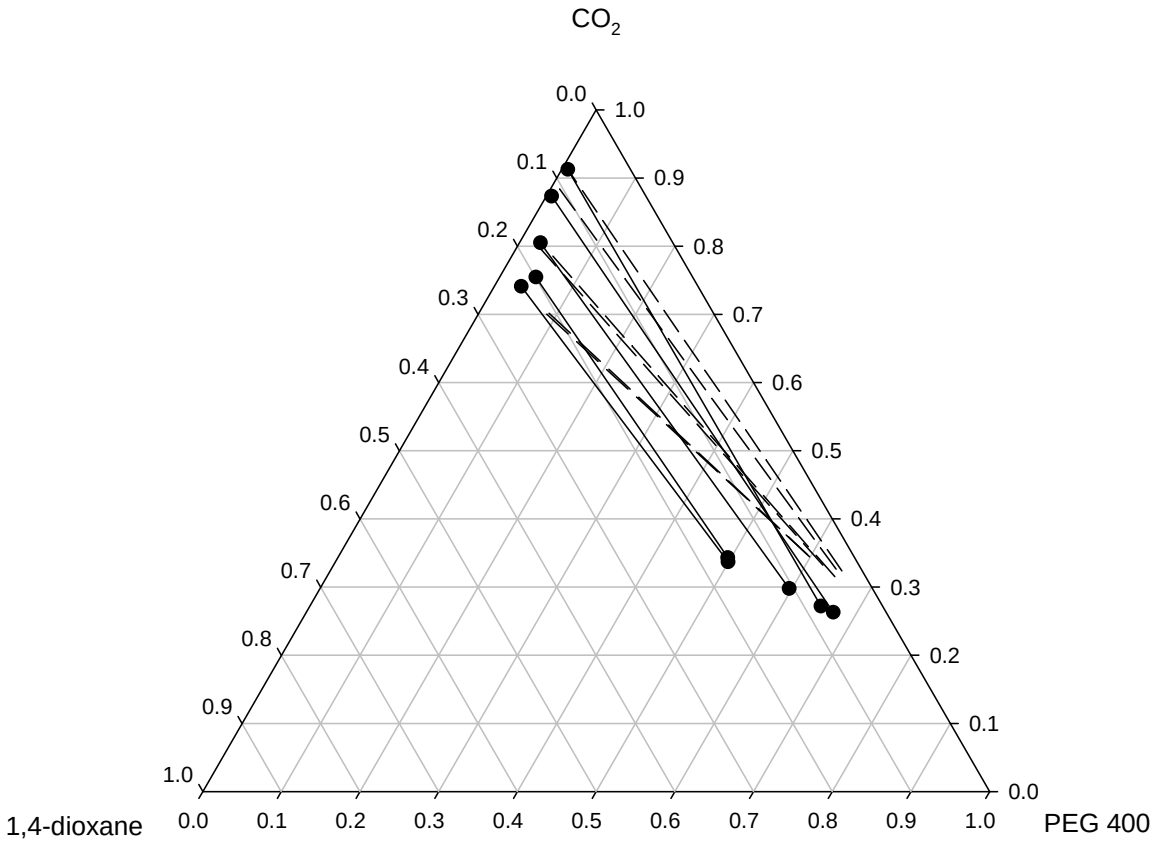

Figure 4-13 LLE PEG 400/CO_2/1,4-Dioxane at 25ºC (Experimental: Solid Lines, Sanchez-Lacombe Model: Dashed Lines)

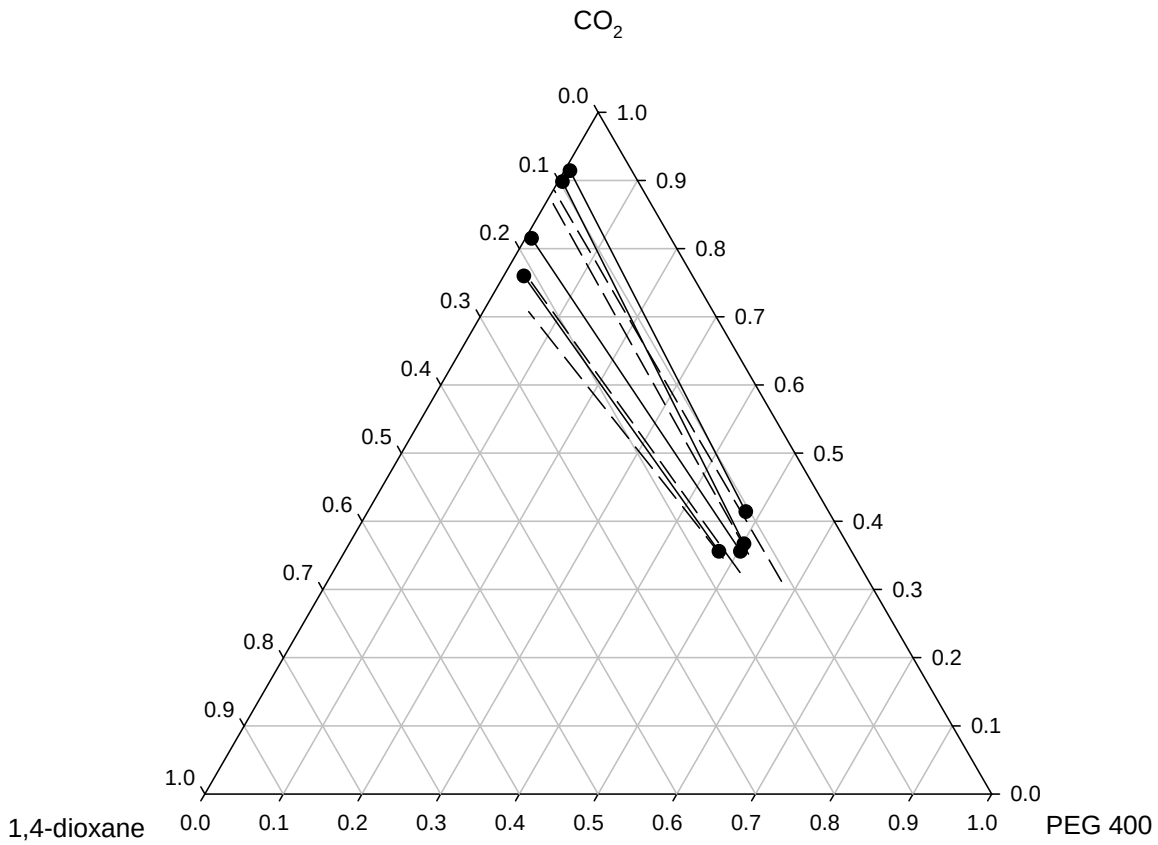

Figure 4-14 LLE PEG 400/CO_2/1,4-Dioxane at 40ºC (Experimental: Solid Lines, Sanchez-Lacombe Model: Dashed Lines)

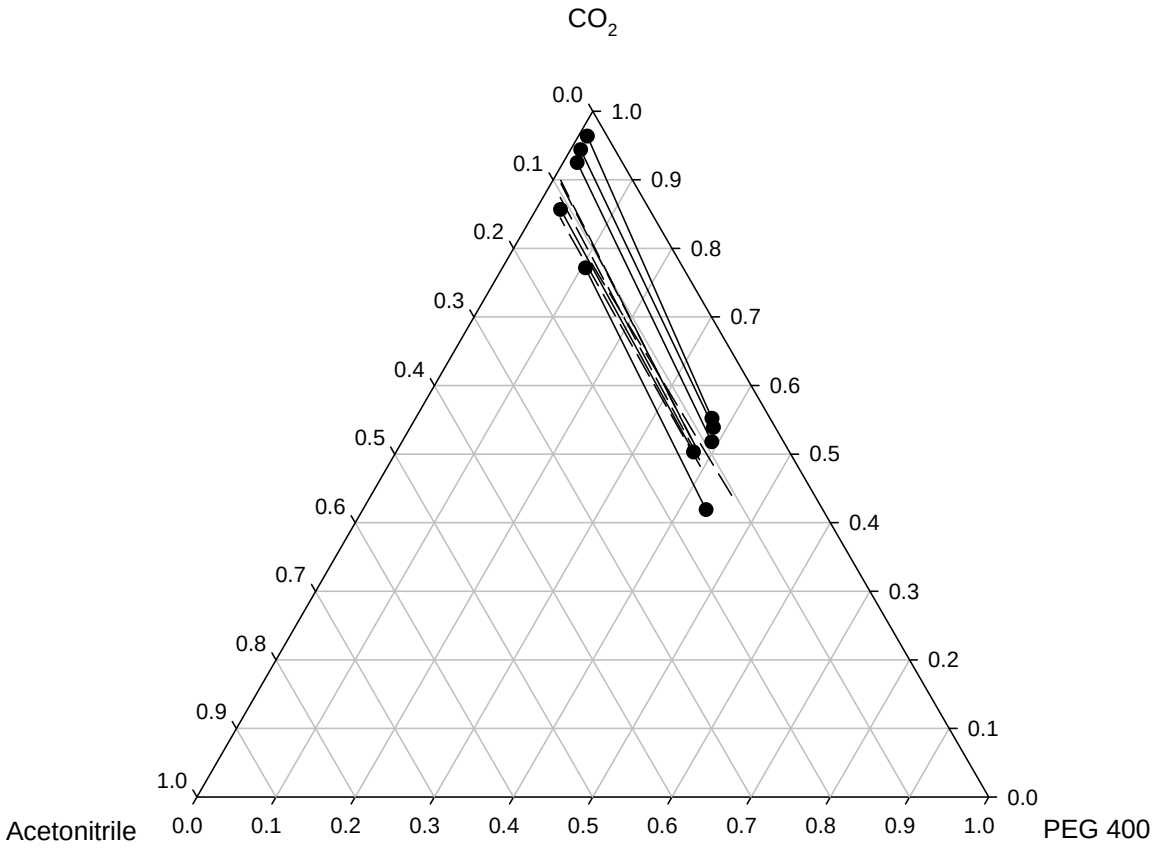

Figure 4-15 LLE PEG 400/CO_2/Acetonitrile at 25ºC (Experimental: Solid Lines, Sanchez-Lacombe Model: Dashed Lines)

Table 4-3 PEG-400 (1) + CO_2 (2) + 1,4-Dioxane(3) at 298K

	Liquid Phase 1 (L_1)				Liquid Phase 2 (L_2)				Vapor
P(MPa)	x_1	x_2	x_3	v (cm^3/mol)	x_1	x_2	x_3	v (cm^3/mol)	v (cm^3/mol)
5.24	0.499	0.337	0.164	83.0	0.034	0.741	0.225	51.4	308.6
5.34	0.496	0.343	0.161	81.4	0.046	0.755	0.199	51.5	298.4
5.53	0.596	0.298	0.106	100.0	0.027	0.805	0.168	49.9	278.3
5.78	0.670	0.263	0.067	112.1	0.007	0.873	0.120	50.4	253.3
5.90	0.650	0.272	0.079	100.6	0.008	0.913	0.080	52.2	240.8
6.03	0.670	0.282	0.048	100.7	0.005	0.940	0.056	54.1	228.2

Table 4-4 PEG-400 (1) + CO_2 (2) + 1,4-Dioxane(3) at 313K

	Liquid Phase 1 (L_1)				Liquid Phase 2 (L_2)				Vapor
P(MPa)	x_1	x_2	x_3	v (cm^3/mol)	x_1	x_2	x_3	v (cm^3/mol)	v (cm^3/mol)
7.11	0.475	0.356	0.169	74.1	0.026	0.760	0.215	57.5	215.1
7.38	0.503	0.356	0.141	72.2	0.008	0.815	0.177	61.1	197.8
7.67	0.502	0.367	0.131	65.0	0.006	0.898	0.096	61.3	179.6
7.90	0.481	0.414	0.106	54.7	0.007	0.914	0.079	68.2	164.7

Table 4-5 PEG-400 (1) + CO_2 (2) + Acetonitrile(3) at 298K

	Liquid Phase 1 (L_1)				Liquid Phase 2 (L_2)				Vapor
P(MPa)	x_1	x_2	x_3	v (cm^3/mol)	x_1	x_2	x_3	v (cm^3/mol)	v (cm^3/mol)
5.52	0.434	0.419	0.147	64.5	0.105	0.771	0.124	41.3	279.7
5.69	0.376	0.503	0.121	39.7	0.031	0.856	0.112	61.1	262.3
5.86	0.391	0.518	0.091	37.5	0.018	0.925	0.057	46.6	245.0
6.03	0.383	0.539	0.078	33.2	0.013	0.944	0.043	56.7	227.5
6.21	0.375	0.552	0.073	30.6	0.011	0.963	0.025	56.3	209.3

The plot for the 1,4-dioxane system at 25ºC shows pressures ranging from 5.2 to 6.0 MPa. With increasing pressure, the compositions in the PEG-rich phase show increasing PEG content with decreasing amounts of both CO_2 and dioxane. The dioxane-rich phase illustrates opposite trends, showing a modest decrease in PEG content and significant increase in CO_2. The increase in CO_2 causes the dioxane content to decrease, which allows CO_2 to enhance its lead as the primary component of the second liquid phase at >90 wt%. Most importantly, the composition of PEG-400 in the dioxane phase reduces to 0.5 wt%, while the dioxane in the PEG phase decreases to 5 wt%. This indicates high purity of the phases, which is necessary for optimum phase separation of the products and catalysts. Also, it is worthwhile to note that the PEG-rich phase contains a relatively high amount of CO_2, ranging from 25 to 35 wt%. In most of the OATS phase behavior, we see less than 2 mol% CO_2 in the aqueous phase due to extremely low solubility. Polymers expand much more readily so the higher CO_2 content follows expected trends.

The ternary diagram for 1,4-dioxane at 40ºC has elevated pressures, ranging from 7.1-7.9 MPa. The composition of the dioxane-rich phase shows similar behavior with comparable values to the previous study at 25ºC. However, the PEG-rich phase illustrates different behavior, with the PEG content remaining approximately equal over the pressure range. The CO_2 actually increases slightly and the dioxane decreases modestly. This contradictory behavior for the CO_2 trend could be attributed to solubility effects. The dioxane has increased solubility at the elevated temperatures, as evidenced by the need for higher pressures to attain the phase separation. Thus, the increased levels of dioxane will allow for greater CO_2 solubility within the PEG phase. Also, the

solubility of CO_2 in PEG-400 increases with increasing pressures even without the cosolvent effect. These two effects are additive and could lead to the variation in the trends for the different conditions. In general, this system has good overall phase behavior for the separation process. The PEG-rich phase contains additional impurity from the elevated levels of dioxane, but the dioxane-rich phase is extremely pure with only 0.8 wt% PEG.

The phase behavior for acetonitrile ranges between 5.5 and 6.2 MPa. The compositions in the PEG-rich phase show minimal change in the PEG content, with increasing CO_2 and decreasing acetonitrile. The lowest pressure shows approximately equal amounts of PEG and CO_2, with relatively high amounts of acetonitrile. The acetonitrile-rich phase shows similar behavior to the previous dioxane systems, illustrating decreasing PEG and acetonitrile and increasing CO_2. The PEG decreases to 1.1 wt% in the acetonitrile phase, while the acetonitrile remains above 7 wt% in the PEG phase. Additionally, over half the composition in the PEG phase is CO_2, which makes it the predominant component of both liquid phases. Therefore, the combination of high CO_2 content and increased cross-contamination could lead to poor separation properties. This is due to the fact that the phases have relatively similar compositions, which generally leads to poor partitioning of catalysts and products.

The SL-EOS models the phase behavior well for the 1,4-dioxane system at 25ºC, exhibiting excellent calculation of the dioxane-rich phase. It provides a binary interaction parameter of 0.936. The model, however, under represents the significant changes that take place in the PEG-rich phase. It shows compositions comparable to the final pressure point for the entire range of data, but cannot capture the variation that takes

place. However, the SL-EOS provides a good overall fit for the phase behavior at these conditions, with an AARD of 9%. At 40ºC, the SL-EOS models both liquid phases very well with an AARD of 8%. The model has a binary interaction parameter of 0.991. Unlike the previous system, the model closely represents the PEG-rich phase, which shows relatively little change as compared to the first conditions. However, the model predicts similar behavior at both 25 and 40ºC, indicating that it may not be capturing the temperature induced solubility effects for the PEG-rich phase. Finally, the SL-EOS models the acetonitrile system quite poorly, underestimating the amount of change that takes place in the compositions for the given pressures. The binary interaction parameter is similar to the previous case at 0.994. In the prior cases, only the PEG-rich phase was under represented. However, both phases show this trend with acetonitrile, but the AARD is only 4%. This indicates the difficulty in capturing the small changes that take place over such a limited pressure range.

4.5 Application: Partitioning of Phenol

In order to test our novel PEG tunable systems, we applied the reaction/separation method to the production of phenol. This material is an industrially important intermediate for the generation of polymers and pharmaceuticals. The world production of phenol was 4.9 x 10^6 tons/yr in 1996, with over 90% generated from the hazardous cumene process.[44] This process involves a two step synthesis, including the oxidation of cumene to hydroperoxide and acid-catalyzed cleavage to phenol and acetone, as shown in Figure 4-16.

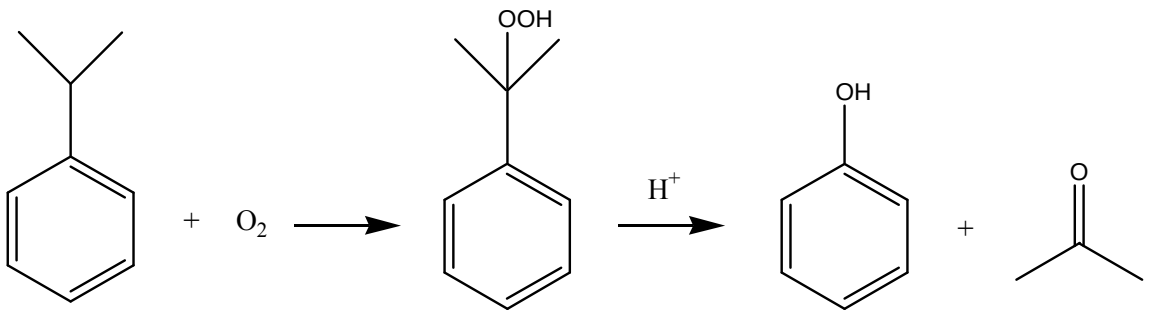

Figure 4-16 Cumene Process for Production of Phenol and Acetone

The initial reaction requires relatively harsh conditions and involves the highly unstable hydroperoxide intermediate, which must be limited to low yields for safety and selectivity.[45] Therefore, researchers have sought new reaction pathways to improve the safety and efficiency of the process. Buchwald *et al.* used palladium catalysts coupled with bulky, biphenyl phosphine ligands to synthesize phenol from aryl halides, as shown in Figure 4-17 and 4-18.[46] They were able to produce both phenols and ethers with their system for a variety of aryl halide derivatives. They used a mixed solvent consisting of water and dioxane, but failed to address the recycle method for the homogenous catalyst. Hence, we saw this reaction as an excellent opportunity to apply our novel tunable solvents to improve the recyclability of this system.

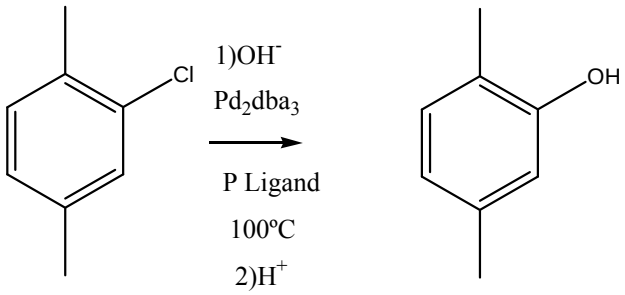

Figure 4-17 Palladium-Catalyzed Synthesis of Phenols from Aryl Halides and Salts

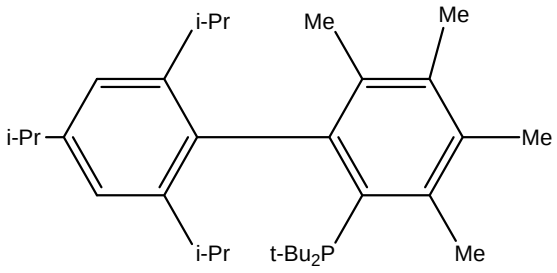

Figure 4-18 Biphenyl Phosphorus Ligand for Synthesis of Phenols

At this time, another group member is assessing the potential of this reaction in PEG-400. The preliminary results show excellent yields in short times. However, the focus for the present work here involves only the potential for the PEG tunable systems in the separation portion of the research. Therefore, we have focused this work on the partitioning of the solute in the heterogeneous system.

The primary study involves the determination of the partition coefficient between the 1,4-dioxane-rich phase and the PEG-rich phase. In order to attain good product recovery, we would like to find the optimal conditions for maximizing the partition coefficient. The coefficient is defined as the ratio of the concentration of the solute in the dioxane-rich phase to that in the PEG-rich phase. In the actual separation, the PEG phase will be used to immobilize the catalyst and allow for its recycle. Hence, we would like to extract the majority of the product into the dioxane phase.

The first study involved the primary target molecule, 2,5-dimethylphenol. For this case, we tested the partitioning in the PEG-400/dioxane system with small amounts of water and potassium chloride. We chose to add the latter components due to the fact that they are generated as reaction byproducts, which causes the materials to be present during the separation and may have a significant effect on the results. In this system, we were unable to attain good partitioning, with a coefficient below one for 25º C and 5 MPa

CO_2 pressure. We believe the poor results are a consequence of hydrogen bonding between the phenol and the PEG. Hydrogen bonding plays a significant role in the interactions associated with PEG, leading to its excellent solubility in water, for example. Phenol also has high solubility in water, which is generally attributed to this effect. Hence, the interactions of the solute with PEG limit its ability to transfer into the dioxane phase for product purification.

Undeterred by the previous results, we altered the target molecule to 2,4-ditertbutylphenol, which should have improved solubility in the dioxane phase. This is due to the high CO_2-philicity of molecules containing tert-butyl functionality and the fact that the dioxane-rich phase contains a far more significant fraction of CO_2. For these studies, we tested the partitioning at different temperatures with and without the presence of the salt/water byproducts. The results are illustrated Table 4-6.

Table 4-6 Partition Coefficient of 2,4-ditertbutylphenol in PEG-400/CO_2/1,4-Dioxane at Various Conditions

T (K)	P (Mpa)	Salt?	K ($C_s^{dioxane}/C_s^{PEG}$)
298	5.3	N	0.19
313	7.2	N	0.13
298	4.0	Y	7.0

They show that the partition coefficient is quite poor without the presence of the reaction byproducts. We had originally expected the salt and water to have a slight influence on the phase behavior, resulting in a reduction in the cloud point. However, we found that the byproduct influence on the phase behavior was only modest, while the effect on the partitioning was significant, shifting the coefficient from below one to approximately

seven. This proves that we can achieve excellent recovery of the phenol product at room temperature with relatively low pressures. We also studied the temperature effect in the byproduct-free solution, which resulted in a slight decrease in the partition coefficient. Therefore, the optimal condition studied thus far is 25ºC with the presence of the reaction byproducts. However, it is clear from the limited data points that we need to explore additional conditions to fully optimize the product recovery.

4.6 Conclusions

We have described a novel tunable solvent system consisting of PEG, carbon dioxide, and a number of common organic solvents. The system allows for homogeneous reaction and heterogeneous separation, enabling good activity with easy product and catalyst recovery. In order to characterize the heterogeneous system, we determined the liquid-liquid equilibria for mixtures of PEG-400, CO_2, and either 1,4-dioxane or acetonitrile. The best system for catalyst and product recovery is dioxane at 25ºC. It shows the greatest separation, generating exceptionally pure phases that can maximize the immobilization of the catalyst in the PEG-rich phase and partitioning of the products into the dioxane-rich phase. The Sanchez-Lacombe EOS models the dioxane phase behavior generally well, but under predicts the large changes that take place within the acetonitrile system over a small pressure range. We have also shown that we can achieve good partitioning of 2,4-ditertbutylphenol into the dioxane-rich phase, which lays the groundwork for application of the novel solvent system to an industrially significant reaction and separation. We will discuss further developments and future work for this application in Chapter 6: Conclusions and Recommendations.

4.7 References

1. Welton, T., *Room-Temperature Ionic Liquids. Solvents for Synthesis and Catalysis.* Chemical Reviews, 1999. **99**: p. 2071-2083.

2. Beckman, E.J., *Supercritical and near-critical CO2 in green chemical synthesis and processing.* Journal of Supercritical Fluids, 2004. **28**: p. 121-191.

3. West, K.N.H., Jason P.; Jones, Rebecca S.; Bush, David; Liotta, Charles L.; Eckert, Charles A., *CO2-Induced Miscibility of Fluorous and Organic Solvents for Recycling Homogeneous Catalysts.* Industrial and Engineering Chemistry Research, 2004. **43**(4827-4832).

4. Chen, J.S., Scott K.; Huddleston, Jonathan G., Rogers, Robin D., *Polyethylene glycol and solutions of polyethylene glycol as green reaction media.* Green Chemistry, 2005. **7**: p. 64-82.

5. Veronese, F.M.P., Gianfranco, *PEGylation, successful approach to drug delivery.* Drug Discovery Today, 2005. **10**(21): p. 1451-1458.

6. Filpula, D.Z., Hong, *Releasable PEGylation of proteins with customized linkers.* Advance Drug Delivery Reviews, 2008. **60**(1): p. 29-49.

7. Khandare, J.M., Tamara, *Polymer-drug conjugates: Progress in polymeric prodrugs.* Progress in Polymer Science, 2006. **31**(4): p. 359-397.

8. Kumar, R.C., Preeti; Nimesh, Surendra; Chandra, Ramesh, *Polyethylene glycol as a non-ionic liquid for Michael addition reaction of amines to conjugated alkenes.* Green Chemistry, 2006. **8**: p. 356-358.

9. Chandrasekhar, S.N., Ch.; Shameem Sultana, S.; Ramakrishna Reddy, N., *Poly(ethylene glycol) (PEG) as a Reusable Solvent Medium for Organic Synthesis. Application in the Heck Reaction.* Organic Letters, 2002. **4**(25): p. 4399-4401.

10. Corma, A.G., Hermenegildo; Leyva, Antonio, *Comparison between polyethylene glycol and imidazolium ionic liquids as solvents for developing a homogeneous and reusable palladium catalytic system for the Suzuki and Sonogashira coupling.* Tetrahedron 2005. **61**: p. 9848-9854.

11. Li, J.-H.L., Wen-Jie; Xie, Ye-Xiang, *Recyclable and Reusable Pd(OAc)2/DABCO/PEG-400 System fo Suzuki-Miyaura Cross-Coupling Reaction.* Journal of Organic Chemistry, 2005. **70**: p. 5409-5412.

12. Strarks, C.M., C.L. Liotta, and M. Halpern, *Phase Transfer Catalysis: Fundamentals, Applications, and Industrial Perspectives*. 1994, New York: Chapman & Hall.

13. Osburn, P.L.B., David E., *Molecular engineering of organic reagents and catalysts using soluble polymers.* Progress in Polymer Science, 2001. **26**: p. 2015-2081.

14. Bergbreiter, D.E.L., Yun-Shan; Osburn, Philip L., *Thermomorphic Rhodium (I) and Palladium (0) Catalysts.* Journal of American Chemical Society, 1998. **120**: p. 4250-4251.

15. Bergbreiter, D.E.O., Philip L.; Wilson, Allan; Sink, Erin M., *Palladium-Catalyzed C-C Coupling under Thermomorphic Conditions.* Journal of American Chemical Society, 2000. **122**: p. 9058-9064.

16. Jessop, P.G.S., Bala, *Gas-Expanded Liquids.* Chemical Reviews, 2007. **107**: p. 2666-2694.

17. Heldebrant, D.J.J., Philip G., *Liquid Poly(ethylene glycol) and Supercritical Carbon Dioxide: A Benign Biphasic Solvent System for Use and Recycling of Homogeneous Catalysts.* Journal of American Chemical Society, 2003. **125**: p. 5600-5601.

18. Heldebrant, D.J.W., Heather N.; Walsh, Sarah M.; Ellis, Taryn; Rauscher Japheth; Jessop, Philip G., *Liquid polymers as solvents for catalytic reductions.* Green Chemistry, 2006. **8**: p. 807-815.

19. Wang, J.-Q.C., Fei; Wang, Er; He, Liang-Nian, *Supercritical carbon dioxide and poly(ethylene glycol): an environmentally benign biphasic solvent system for aerobic oxidation of styrene.* Green Chemistry, 2007. **9**: p. 882-887.

20. Reetz, M.T.W., Wolfgang, *Liquid poly(ethylene glycol) and supercritical carbon dioxide as a biphasic solvent system for lipase-catalyzed esterification.* Chemical Communications, 2004: p. 2750-2751.

21. Lu, J.L., Michael J.; Hallett, Jason P.; Bommarius, Andreas S.; Liotta, Charles L.; Eckert, Charles A., *Tunable Solvents for Homogeneous Catalyst Recycle.* Industrial and Engineering Chemistry Research, 2004. **43**: p. 1586-1590.

22. Lazzaroni, M.J.B., David; Brown, James S.; Eckert, Charles A.. *High-pressure vapor-liquid equilibria of some carbon dioxide + organic binary systems.* Journal of Chemical and Engineering Data, 2005. **50**(1): p. 60-65.

23. Lazzaroni, M.J.B., D; Jones, Rebecca; Hallet, Jason P.; Liotta, Charles L.; Eckert, Charles A., *High-pressure phase equilibria of some carbon dioxide-organic-water systems.* Fluid Phase Equilibria, 2004. **224**: p. 143-154.

24. Hallett, J.P.F., Jackson W.; Jones, Rebecca S.; Pollet, Pamela; Thomas, Colin A.; Liotta, Charles L.; Eckert, Charles A.. , *Hydroformylation Catalyst Recycle with Gas-Expanded Liquids.* Industrial and Engineering Chemistry Research, 2008. **47**(8): p. 2585-2589.

25. Hill, E.M.B., James M.; Hallett, Jason P.; Bommarius, Andreas S.; Liotta, Charles L.; Eckert, Charles A., *Coupling chiral homogeneous biocatalytic reactions with benign heterogeneous separation.* Green Chemistry, 2007. **9**(8): p. 888-893.

26. Broering, J.M.H., Elizabeth M.; Hallett, Jason P.; Liotta, Charles L.; Eckert, Charles A.; Bommarius, Andreas S., *Biocatalytic reaction and recycling by using CO2-induced organic-aqueous tunable solvents.* Angewandte Chemie, 2006. **45**(28): p. 4670-4673.

27. Scurto, A.M.A., Sudhir N.V.K.; Brennecke, Joan F., *CO2 as a Separation Switch for Ionic Liquid/Organic Mixtures.* Journal of American Chemical Society, 2002. **124**: p. 10276-10277.

28. Gourgouillon, D. and M. Nunes da Ponte, *High pressure phase equilibria for poly(ethylene glycol)s + CO2: experimental results and modelling.* Physical Chemistry Chemical Physics, 1999. **1**: p. 5369-5375.

29. Guadagno, T.K., S.G., *High-Pressure CO2-Expanded Solvents: Simultaneous Measurement of CO2 Sorption and Swelling of Liquid Polymers with in-Situ Near-IR Spectroscopy.* Journal of Physical Chemistry B, 2004. **108**: p. 13995-13999.

30. Hou, M.L., Shuguang; Zhang, Zhaofu; Song, Jiyuan; Jiang, Tao; Han, Buxing, *Determination and modeling of solubility of CO2 in PEG200+1-pentanol and PEG-200+1-octanol mixtures.* Fluid Phase Equilibria, 2007. **258**: p. 108-114.

31. Matsuyama, K.M., Kenji, *Phase behavior of CO2 +polyethylene glycol + ethanol at pressures up to 20 MPa.* Fluid Phase Equilibria, 2006. **249**(1-2): p. 173-178.

32. Span, R.W., W., *A new equation of state for carbon dioxide covering the fluid region from the triple-point temperature to 1100K at pressures up to 800MPa.* Journal of Physical and Chemical Reference Data, 1996. **25**(6): p. 1509-1596.

33. Sanchez, I.C. and C.G. Panayiotou, *Equation of State Thermodynamics of Polymer and Related Solutions*, in *Models for Thermodynamic and Phase Equilibria Calculations*, S.I. Sandler, Editor. 1994, Marcel Dekker: New York.

34. Huron, M.J.V., J., *New Mixing Rules in Simple Equations of State for Representing Vapor-Liquid Equilibria of Strongly Non-ideal Mixtures.* Fluid Phase Equilibria, 1979. **3**: p. 225.

35. Haghtalab, A.E., Reza, *A new model and extension of Wong-Sandler mixing rule for prediction of (vapour+liquid) equilibrium of polymer solutions using EOS/GE.* Journal of Chemical Thermodynamics, 2004. **36**: p. 901-910.

36. Sanchez, I.C. and R.H. Lacombe, *An Elementary Molecular Theory of Classical Fluids. Pure Fluids.* The Journa of Physical Chemistry, 1976. **80**(21): p. 2352-2362.

37. Sanchez, I.C. and R.H. Lacombe, *Statistical Thermodynamics of Polymer Solutions.* Macromolecules, 1978. **11**(6): p. 1145-1156.

38. Ewing, M.B.O., J.C. Sanchez. *Vapour Pressure of Acetonitrile Determined by Comparative Ebulliometry*. in *Fifteenth Symposium of Thermophysical Properties*. 2003. Boulder, Colorado, USA.

39. Garg, A.G., Esin; Manke, Charles W., *Thermodynamics of Polymer Melts Swollen with Supercritical Gases.* Macromolecules, 1994. **27**(20): p. 5643-5653.

40. Harrison, K.L.J., Keith P.; Sanchez, Isaac C., *Effect of Surfactants on the Interfacial Tension between Supercritical Carbon Dioxide and Polyethylene Glycol.* Langmuir, 1996. **12**(11): p. 2637-2644.

41. Day, C.-Y.C., Chiehming J.; Chen, Chiu-Yang, *Phase Equilibrium of Ethanol + CO2 and Acetone + CO2 at Elevated Pressures.* Journal of Chemical and Engineering Data, 1996. **41**(4): p. 839-843.

42. Kordikowski, A.S., A.P.; Van Nielen, R.M.; Peters, C.J., *Volume Expansions and Vapor-Liquid Equilibria of Binary Mixtures of a Variety of Polar Solvents and Certain Near-Critical Solvents.* The Journal of Supercritical Fluids, 1995. **8**: p. 205-216.

43. Daneshvar, M.K., Seecheol; Gulari, Esin, *High-Pressure Phase Equilibria of Poly(ethylene glycol)-Carbon Dioxide Systems.* Journal of Physical Chemistry, 1990. **94**: p. 2124-2128.

44. Weissermel, K.A., H.J., *Benzene Derivatives:Oxidation and Secondary Products of Benzene- Phenol*, in *Industrial Organi Chemistry*, K.A. Weissermel, H.J., Editor. 1997, VCH: New York.

45. Duh, Y.-S.K., C.-S.; Lee, C.; Yu, S. W., *Runaway hazard assessment of cumene hydroperoxide from the cumene oxidation process.* Process Safety and Environmental Protection, 1997. **75**(B2): p. 73-80.

46. Anderson, K.W.I., Takashi; Tundel, Rachel E.; Buchwald, Stephen L., *The Selective Reaction of Aryl Halides with KOH: Synthesis of Phenols, Aromatic Ethers, and Benzofurans.* Journal of American Chemical Society, 2006. **128**: p. 10694-10695.

Chapter V: Siloxylated Phase Transfer Catalysts for Coupling Siloxanes with Biomolecules

5.1 Introduction

In Chapter 2, we discussed the important role solvents play in industrial processes for enabling reactions. This function is especially critical for reactions involving hydrophobic and hydrophilic materials that are not generally miscible with each other or in a common solvent. In previous work, we approached this problem by developing switchable analogs of polar, aprotic solvents that have the capability of dissolving molecules of widely varying properties.[1, 2] However, another option for solving this problem involves the use of phase transfer catalysis (PTC) -- a technique that enables rate enhancement in multiphasic reactions, allowing for mild conditions and simplified processes.[3] These catalysts do require additional processing steps for product separation and catalyst isolation, but they have been successfully adopted in numerous industrial reactions.[4] Hence, these catalysts represent a viable option for improving reaction rates involving biphasic systems. In this work, we use PTC to couple siloxane-containing compounds with biomolecules, such as amino acids. The application of this technique will allow for improved reaction rates between these highly immiscible materials. We also attempt to improve upon conventional systems by developing novel siloxane-based catalysts that can improve interactions with compounds containing siloxane functionality.

5.1.1 PTC Technique

PTC generally involves reactions consisting of two or more reactants in a multiphasic system in which the transfer of one component enables improvement in the reaction rate.[4, 5] Essentially, it overcomes the mass transfer limitations of biphasic reactions by bringing the reactants together to allow for a monophasic reaction. PTCs accomplish this by shuttling the reactant, usually an anion, from a solid or liquid aqueous phase into an organic phase containing the hydrophobic reactant. The concept is illustrated in Figure 5-1. In this typical example, we show the nucleophilic substitution of an alkyl or aryl chloride, with cyanide catalyzed by a quaternary onium salt. The process involves a number of steps. The first requires that the PTC partition into the aqueous phase and then exchange anions with the cyanide salt. The catalyst then shuttles the anion into the organic phase where it can react with the organic molecule. After the reaction takes place, the PTC becomes available to start the cycle anew.

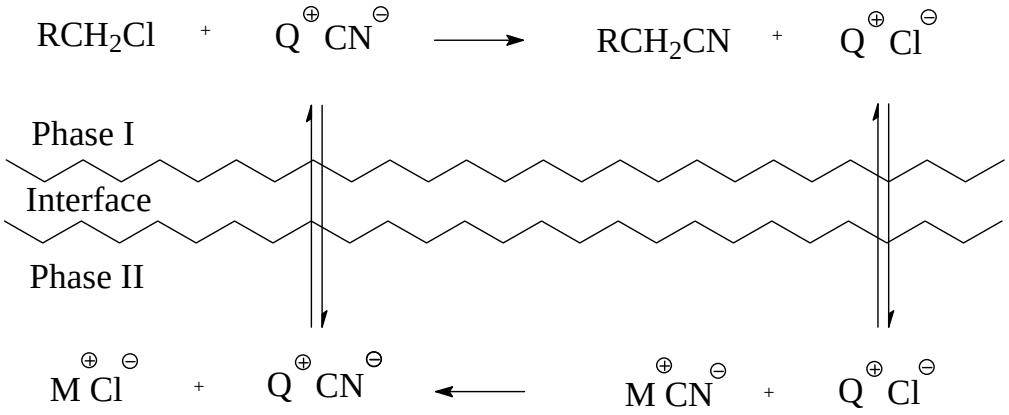

Figure 5-1 General Scheme for Phase Transfer Catalysis

5.1.2 Types of PTC

The example above illustrates traditional liquid-liquid (L-L) PTC, which represents the most commonly used method.[3] However, PTC has been extended to a myriad of multiphasic systems, including solid-liquid (S-L), liquid-liquid-liquid (LLL), liquid-gas-expanded liquid (L-GXL), and solid-supercritical fluid (S-SCF).[3, 6, 7] Liquid-liquid PTC usually involves a biphasic system, consisting of an aqueous and organic phase. Generally, the process proceeds as described above, where the reactant is transferred from the aqueous phase to the organic for reaction. Less frequently, the process can occur in the reverse direction for systems known as inverse PTC. In solid-liquid PTC, the biphasic mixture consists of a solid reagent, usually a salt, and an organic phase containing the hydrophobic reactant. It is also worthwhile to note that the addition of small amounts of water can make a significant impact on the reaction rate, usually causing it to reach a maximum value at low levels of water. This is often attributed to the creation of an omega phase, which is a PTC rich, third phase located at the surface of the salt. This highly reactive phase results from the coating of the solid particles with water and the subsequent partitioning of the PTC into the new phase.[4, 8] In recent work with S-SCF PTC, in which the organic phase is replaced with supercritical fluid carbon dioxide, the data suggested that the reaction of benzyl chloride and potassium cyanide actually took place within the catalyst-rich omega phase.[9] Others have shown similar effects with the more typical L-L systems.[8, 10] In this research, we will focus on only S-L PTC, but the techniques could be easily extended to the more typical L-L systems.

5.1.3 PTC Catalysts

The most common soluble catalysts are based on quaternary onium salts, such as ammonium and phosphonium, crown ethers, cryptands, and polyethylene glycols (PEG).[4, 11] Figure 5-2 illustrates a typical quaternary ammonium salt, tetrabutylammonium chloride (TBACl), and crown ether, 18-crown-6. The transfer mechanism for these compounds is slightly different between the quaternary salts and ethers (crowns and PEGs). The first uses direct anion exchange to transport the reactant, while the second actually complexes with the inorganic cation, bringing the anion along with it to the reaction phase. These are all highly tunable through structural variations, allowing for modification of transfer properties and optimization of rates. The quaternary ammonium salts will be the main type of catalyst utilized within this work.

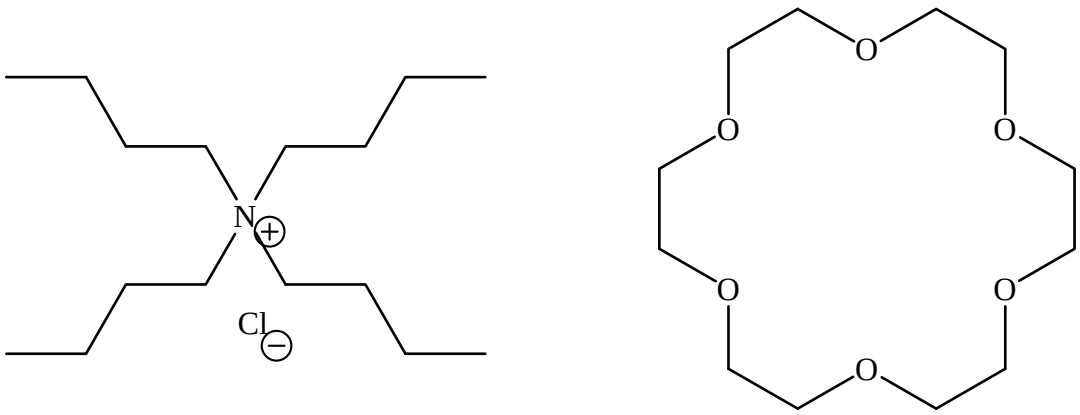

Figure 5-2 Common Phase Transfer Catalysts: Tetrabutylammonium chloride (left) and 18-crown-6 (right)

There are also numerous insoluble PTCs that eliminate the difficulties associated with separating homogenous catalysts. These include resin-bound, inorganic solid-bound, and third-phase PTCs.[4]

5.1.4 PTC Kinetics

In order to characterize the efficiency of the catalysis, we usually do kinetic studies to determine the rate constant for the reaction. The general form of the rate expression for PTC is illustrated below:

$$-\frac{d[R-X]}{dt} = k\ [Q^+Y^-]\ [R-X] \qquad 5\text{-}1$$

where t is the reaction time, k is the rate constant, Q^+ is the quaternary onium cation, Y^- is the reactant anion, and R-X is the hydrophobic reactant.

We can simplify the rate expression to pseudo-first order conditions by using an excess of the ionic nucleophile, which generates a constant concentration of the quaternary onium salt with the reactant anion. It is also important to ensure that the system is intrinsically rate-limited and not restricted by the transfer step in the reaction. In our work, we maintain a stirring speed that allows the transfer rate to exceed significantly the intrinsic rate. Hence, these conditions reduce the rate equation to the following:

$$-\frac{d[R-X]}{dt} = k_1\ [R-X] \qquad 5\text{-}2$$

where k_1 is the pseudo-first-order rate constant.

The expression can then be transformed into the well known first order equation relating the rate constant to the concentration of reactant:

$$k_1 t = \ln\left(\frac{C_{A0}}{C_A}\right) \qquad 5\text{-}3$$

Where C_{A0} is the initial concentration of the limiting reactant, and C_A is the concentration of the reactant at time t.

5.1.5 Novel Siloxane Biomolecules

In this work, we use PTC in order to couple siloxane-containing compounds with biomolecules. These siloxylated biomolecules could be useful in numerous applications, especially in the personal care industry. In related Dow Corning patents, the uses range from health products, such as lotions and make-up, to industrial fluids, such as surfactants and lubricants.[12, 13] Their primary advantage over more typical siloxylated materials relates to enhanced conditioning and moisturizing that can be imparted in hair and skin products.[12] These materials could also be useful in analytical fields for detection of peptides and amino acids, similar to the silylated materials that have enabled rapid GC analysis.[14]

This research is primarily related to the development of synthetic techniques that allow for efficient siloxylation of amino acids. Literature referring to these types of syntheses is scarce. However, there is a great deal of research on the derivatization of amino acids with silyl compounds as well as UV/fluorescence tags. These

functionalizations are primarily used for analysis of biomolecules and enable easy detection of peptides and amino acids.

Amino acids have been modified by numerous reactions, including acylation, alkylation, and silylation.[14] Numerous silylated functionalities, like trimethylsilyl groups, have been incorporated into amino acids, such as leucine and aspartic acid. Generally, these reactions proceed without the aid of PTCs, because the silylating agent can be readily dissolved within mixed solvent media.[15] In some cases, researchers have used polar, aprotic solvents to accomplish the coupling, but this represents less of a problem for analytical processes since large scale product isolation is not necessary.[16] Our application involves the manufacture of these materials for incorporation into chemical products, thereby requiring efficient product isolation and limiting the usage of these high-boiling solvents. There are, however, several processes that use PTC to functionalize biomolecules, due to the increased immiscibility that results with more hydrophobic substrates. In one example, researchers used PTC to tag negatively charged amino acids and peptides with a fluorescent molecule to enable faster analysis.[17]

In this research, we have two primary goals for enabling the coupling of siloxanes with biomolecules. The first objective is to determine if PTC will allow for effective reaction between these highly immiscible materials. We want to use this technique to overcome the mass transfer limitations of this biphasic system. Our goal is to develop a solvent-less system, in which we can react the solid hydrophilic molecule with a siloxylated moiety in the liquid phase. The second objective is to design and develop novel catalysts that can improve the efficiency of the reaction. These materials will

contain siloxane functionality that can improve the interaction of the siloxylated substrate and the catalyst, resulting from “like-like” effects.

In order to assess the efficacy of PTC in this process, we selected a siloxane-tagged benzyl chloride **(1)** as the model compound. For the initial reactions, we focused on the reaction between the siloxylated benzyl chloride and several salts, including potassium cyanide, potassium thiocyanate, and potassium acetate. The model reaction is shown in Figure 5-3. We started with these simple reactions due to the ease of analysis of both the starting material and the substituted siloxane product. The salts are essentially analogs of the small biomolecules, representing the general hydrophilic reactants we will test eventually.

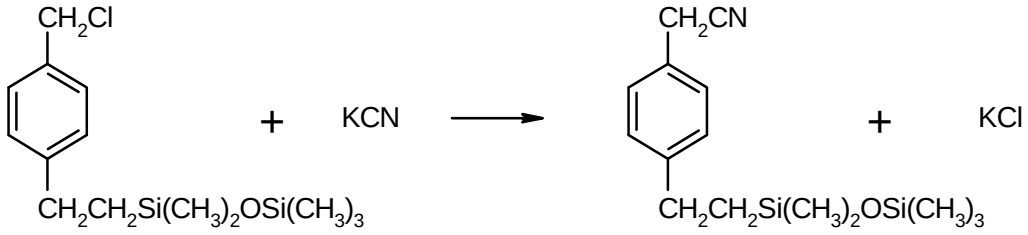

Figure 5-3 Reaction of Potassium Cyanide with Siloxylated Benzyl Chloride (1)

After completion of the initial study, we shifted the focus for the reaction to the target nucleophile, the amino acid L-lysine. This reaction is illustrated in Figure 5-4. We compared the PTC reaction efficiency to previous work involving mixed solvents, containing acetonitrile and methanol. These reactions were extremely poor with only 70% conversion after 22 hours.

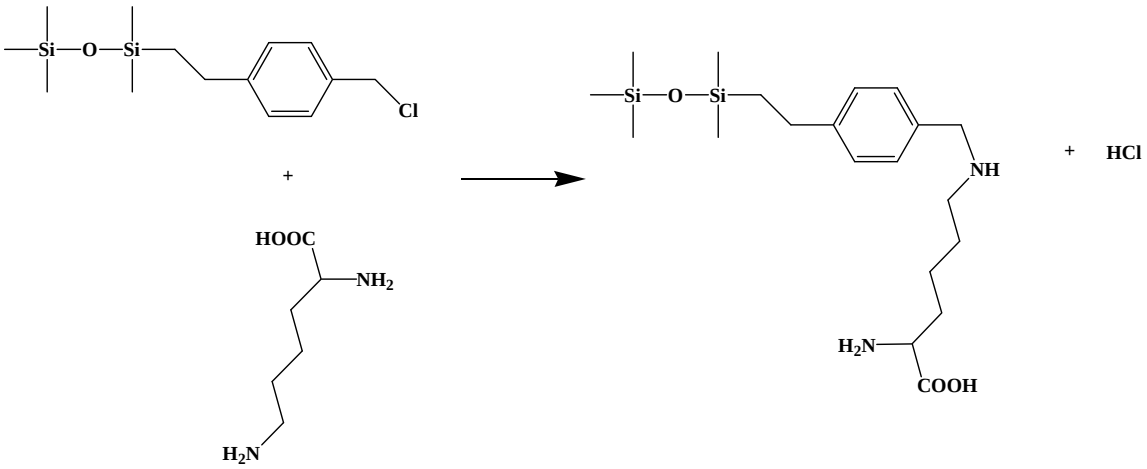

Figure 5-4 Reaction of L-lysine with Siloxylated Benzyl Chloride (1)

For the next objective, we synthesized two novel, siloxylated phase transfer catalysts. We developed these molecules because PTC is highly dependent on catalyst and solvent selection. The choices for these options can influence the transfer and intrinsic rate of the reaction by influencing the catalyst partitioning, anion activation, and accessibility of the catalyst.[4] In most cases, a polar, organic solvent coupled with an organic PTC enables rapid reaction of organic molecules with hydrophilic reagents. However, in our case, we are using a siloxylated material as the reactant. These materials can vary in properties from typical organic reactants and may not interact as readily with common organic PTCs. In order to maximize this interaction, we wanted to utilize a catalyst with siloxane functionality. In the literature, these types of catalysts are rare. However, Sonnek *et al.* developed several siloxane functionalized catalysts, such as 2-siloxanylpropoxy-a,a',w-trihydrofluoroalkanes in order to synthesize fluorocarbon surfactants.[20] These materials contained relatively little siloxane functionality due to the focus on the fluorous aspect of the molecule and the application to fluorocarbon

synthesis. Thus, we designed, synthesized and characterized several siloxylated catalysts that may be able to improve interaction with the siloxane reactant and enhance the reaction rate. The reaction scheme for this research is illustrated in Figure 5-5. It shows the system with two immiscible phases in which the organosilicon-functional phase-transfer catalyst positions itself primarily at the interface of the two phases. The key molecules for this study are shown in Figures 5-6 and 5-7. In order to assess their potential, we compare the kinetics of these novel catalysts with two common organic PTCs, including tetrabutylammonium chloride (TBACl) and Aliquat 336 (trioctylmethylammonium chloride).

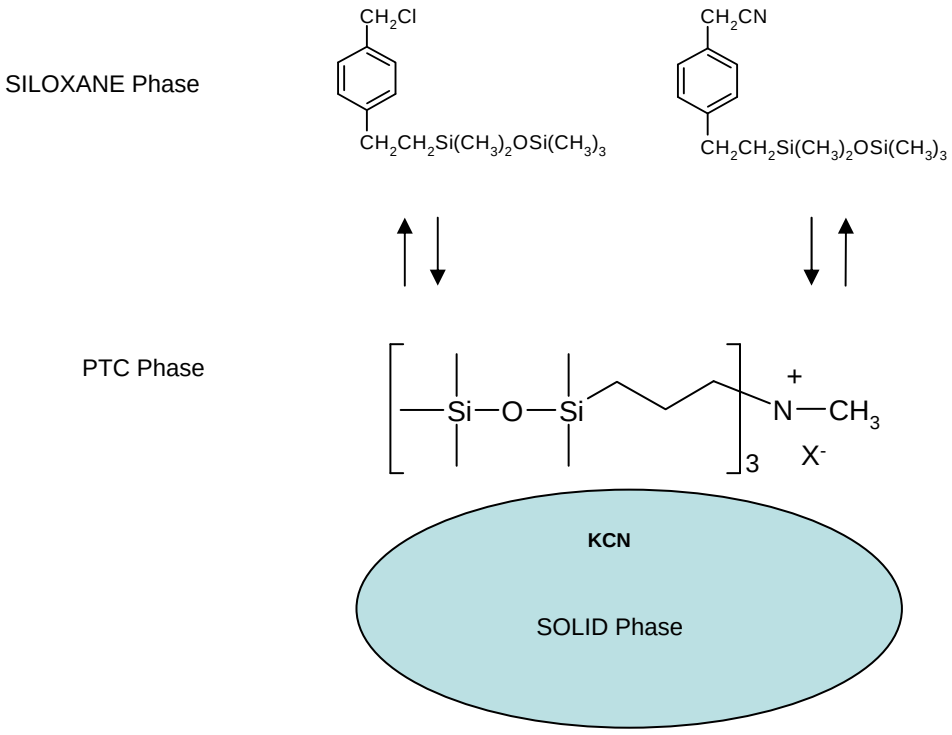

Figure 5-5 Scheme for the Reaction of Siloxylated Benzyl Chloride with Potassium Cyanide Catalyzed by Organosilicon-PTCs

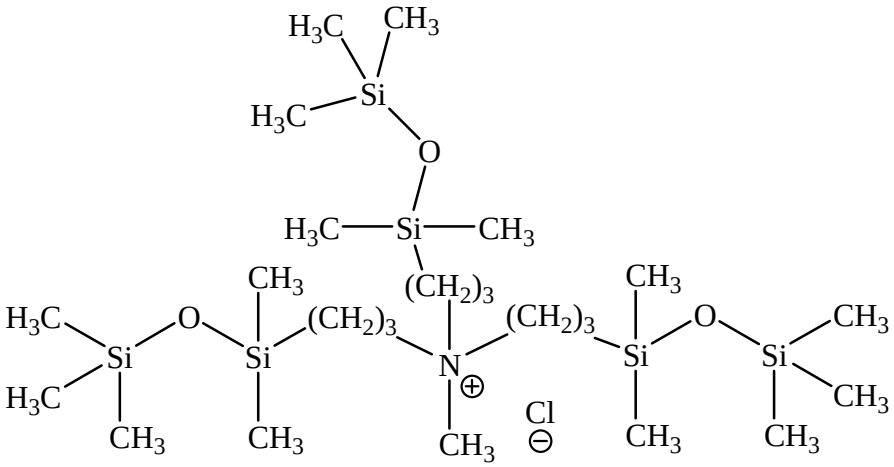

Figure 5-6 Novel Siloxane PTC: Methyl-tris-[3-(1,1,3,3,3-pentamethyl-disiloxanyl)-propyl]-ammonium chloride (2 or SiMePTC)

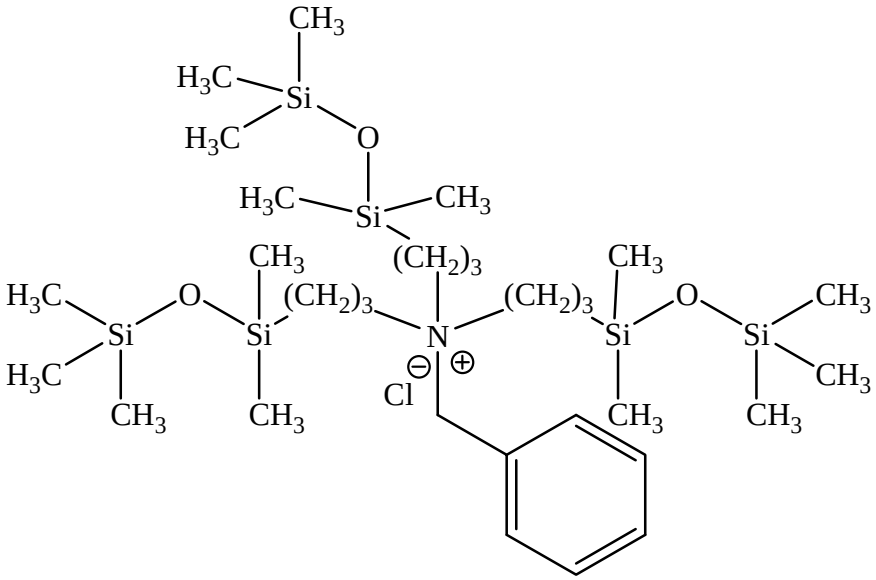

Figure 5-7 Novel Siloxane PTC: Benzyl-tris-[3-(1,1,3,3,3-pentamethyl-disiloxanyl)-propyl]-ammonium chloride (3 or SiBzPTC)

5.2 Experimental Section

5.2.1 Materials

The following materials were used as received: Ethyl acetate, 99.5% reagent grade (Sigma-Aldrich), Tetrabutylammonium chloride hydrate, 98%, Tetrabutylammonium bromide, 98+% (Aldrich), Tetraoctylammonium bromide (Sigma), 1-butyl-3-methylimidizolium chloride (Fluka), Aliquat 336 (Aldrich), Potassium chloride (Fisher Scientific), Potassium cyanide, 97% (Aldrich), Potassium thiocyanate, reagent grade (Fisher Scientific), Potassium acetate, 99+% A.C.S. reagent (Sigma-Aldrich), Decane, 99% (Acros Organic), Toluene, 99.5% reagent grade (Sigma-Aldrich), L-lysine hydrate, 97% (Aldrich).

5.2.2 Synthesis

5.2.2.1 Synthesis of the siloxane electrophile

The 4-vinyl-benzyl chloride (5.0g, 0.0337mol) was added to 20 mL of heptane and put under nitrogen. The mixture was heated to 75ºC. The catalyst platinum(0)-1,3-divinyl-1,1,3,3-tetramethyl disiloxane complex (3 wt% xylene) (DVDS-Pt) (1.7 g, 1%wt) was added to the solution. The pentamethyl disiloxane (5.75g, 0.0388mol, 1.15 equiv) in 5 mL of heptane was added slowly drop wise. The solution changed from a light yellow to a dark brown upon addition and the addition was stopped whenever the reaction temperature increased by more than 2ºC. After the addition was complete, the temperature was reduced to 70ºC and the reaction was heated for 3 hours. After 3 hours, the reaction was allowed to cool to room temperature and was stirred overnight. To work

up the reaction, the heptane was removed under reduced pressure. A column of silica gel in hexane was run and all the fractions combined. The hexane was removed under reduced pressure to give a clear liquid. Yield was 50% with two isomers.

1-[2-(4-chloromethyl-phenyl)-ethyl]-1,1,3,3,3-pentamethyldisiloxane: ^{1}H NMR ($CDCl_3$) ppm: 0.1 (15, m), 0.9 (2, m), 1.3 (2, d), 2.3 (2, q), 2.7 (2, m), 4.6 (2, s), 7.2 (4, m). ^{13}C NMR ($CDCl_3$) ppm: 1.516-2.156, 20.39, 29.2533; 46.49, 129.42-127.44 , 134.50, 145.56. GC-MS analysis was done on a HP GC 6890/ HP MS 5973. MS(m/z): 300 (M^+). EA: calculated, C, 55.87%, H, 8.41%. Found, C, 55.82%, H, 8.41%.

5.2.2.2 Synthesis of organosilicon-functional phase-transfer catalysts (PTCs)

Two organosilicon-functional PTCs were synthesized – Methyl-tris-[3-(1,1,3,3,3-pentamethyl-disiloxanyl)-propyl]-ammonium chloride (**2)** and Benzyl-tris-[3-(1,1,3,3,3-pentamethyl-disiloxanyl)-propyl]-ammonium chloride **(3)**. Organosilicon-functional PTCs **2** and **3** were synthesized according to a slightly modified literature procedure by Arren, Coggio, and Parker.[21] Both were synthesized from tris-[3-(1,1,3,3,3-pentamethyl-disiloxanyl)-propyl]-amine, which was prepared as follows: a 250 mL round-bottom flask under argon was fitted with a magnetic stir bar, a reflux condenser and an addition funnel. The flask was charged with triallyl amine (6.5g, 0.47 mol) and heptane (20 mL). Platinum (0)-1,3-divinyl-1,1,3,3-tetramethyldisiloxane (DVDS-Pt) 3% wt in xylenes complex (2.19g, 1% wt based on amine) was added to this mixture, which was then heated to 85°C. Pentamethyldisiloxane (21.12g, 0.14 mol) in heptane (20 mL) was added slowly dropwise through the addition funnel to the stirred mixture. After the addition was complete, it was observed to be reddish-brown in color. The mixture was

stirred for three hours at 70°C. After three hours, colloidal clay was added. The reaction was allowed to cool to room temperature and stir overnight. The reaction mixture was then filtered and the heptane removed under reduced pressure. A short silica plug with hexane as the eluent was used to purify the product. The product amine was a light yellow (35% yield). *Tris-[3-(1,1,3,3,3-pentamethyl-disiloxanyl)-propyl]-amine:* ^{1}H NMR ($CDCl_3$) ppm: 0.053 (15, m), 0.449 (2, t), 1.444 (2, m), 2.396 (2, t). ^{13}C NMR ($CDCl_3$) ppm: 0.751, 2.428, 16.439, 21.059, 57.980. GC-MS analysis was done on a HP GC 6890/ HP MS 5973. MS(m/z): 406 (M^+-$CH_2CH_2Si(CH_3)_2OSi(CH_3)_3$). EA: calculated C, 48.70%, H, 10.87%, N, 2.30%. Found C, 48.47%, H, 10.66%, N, 2.47%.

To form **2**, Tris-3-(1,1,3,3,3-pentamethyl-disiloxanyl)-propyl-amine (2.4187g, 0.0042 mol) was added to 10 mL of THF. The solution was added to a pressure vessel with methyl chloride at 50 psi and 40ºC (5 g). The reaction was allowed to proceed for three weeks. At the end of three weeks, the pressure vessel was vented to remove the methyl chloride and the THF was removed under reduced pressure and dried in the vacuum oven at 40°C overnight. The resulting thick brown liquid was quantitative in yield. *Methyl-tris-[3-(1,1,3,3,3-pentamethyl-disiloxanyl)-propyl]-ammonium chloride:* ^{1}H NMR ($CDCl_3$) ppm: 0.045 (45, m), 0.528 (6, m), 1.628 (6, m), 3.319 (9, m). ^{13}C NMR ($CDCl_3$) ppm: 2.322, 15.339, 17.031, 48.960, 64.648. MS (m/z): 596.4 (M^+-Cl). EA: calculated C, 47.45%, H, 10.51%, N, 2.21%. Found C, 47.12%, H, 10.26%, N, 2.25%.

To form **3**, Tris-3-(1,1,3,3,3-pentamethyl-disiloxanyl)-propyl-amine (1.1205 g, 0.001717 mol) was put under nitrogen. To the amine, 10 mL of benzyl chloride was added to act as solvent and reactant. The solution was heated gradually to 65^{o}C and allowed to react for five days until ^{1}H NMR showed reaction completion. The resulting product was a brown thick liquid and yield was quantitative. *Benzyl-tris-[3-(1,1,3,3,3-pentamethyl-disiloxanyl)-propyl]-ammonium chloride:* ^{1}H NMR ($CDCl_3$) ppm: 0.046 (45, m), 0.501 (6, m), 1.800 (6, m), 3.200 (6, m), 4.568 (2, s), 7.355 (5, m). ^{13}C NMR ($CDCl_3$) ppm: 2.051, 15.417, 17.086, 46.284, 132.332, 128.539. MS (m/z): 672.4 (M^{+}-Cl). EA: calculated C, 52.53%, H, 9.95%, N, 1.98%. Found C, 52.79%, H, 9.56%, N, 2.35%.

5.2.3 Kinetics

The electrophilic disiloxane, 4-ethyl(1,1,3,3,3-pentamethyl-disiloxane)benzyl chloride (p-SiBzCl, $Me_3SiOSiMe_2(CH_2)_2C_6H_4CH_2Cl$) was reacted with four separate nucleophiles, potassium acetate, potassium cyanide, potassium thiocyanate, and L-lysine hydrate at 30, 50, and 70ºC. The reactions took place in ethyl acetate with four phase transfer catalysts, tetrabutylammonium chloride, Aliquat 336, and **2** and **3**. The reactions were carried out in a 25 mL round bottom flask immersed in an oil bath at the appropriate temperature. The system was stirred at 900 rpm with a Teflon coated magnetic stir rod. A typical reaction consisted of 5 mol% PTC based on the electrophile, 0.1 mL siloxane electrophile, 5 times excess nucleophile, 5 times excess potassium chloride (only salt reactions), 3 mL ethyl acetate, and 0.1 mL decane. The potassium chloride was included to maintain a constant concentration solution for accurate kinetics and the decane was

added as an internal standard. The reaction mixture was sampled at varying intervals by removing 0.05 to 0.075 mL aliquots, which were immediately quenched in ethyl acetate and analyzed by GC-MS. The products of each reaction were isolated after reaction completion with three extractions with ethyl acetate. The solution was evaporated under reduced pressure to remove the solvent and the resulting product was analyzed by NMR. For the salt reactions, the products were confirmed by both GC-MS and ^{1}H and ^{13}C NMR. The L-lysine products were confirmed by ^{1}H and ^{13}C NMR.

5.3 Results & Discussion

5.3.1 Nucleophile Comparison

To test the catalytic capabilities of our new siloxane-containing PTCs, we completed a series of kinetic analyses with four nucleophiles, potassium acetate, potassium thiocyanate, potassium cyanide, and L-lysine. We compared our results for each nucleophile with two commercial organic PTCs, tetrabutylammonium chloride and Aliquat 336, and two siloxane-containing PTCs **2** (SiMePTC) and **3** (SiBzPTC). The pseudo-first order rate plots shown in Figures 5-8 through 5-11 illustrate the rate behavior of reaction of the various nucleophiles with the siloxane electrophile for each of the four PTCs. The pseudo-first order rate constants for both isomers of the siloxane electrophile (**1**) are shown in Tables 5-1 and 5-2.

In general, the traditional organic PTCs outperformed the siloxane-containing PTCs. This is most evident with potassium acetate and L-lysine, which show an order of magnitude difference in rate constants between the two types. However, in the potassium thiocyanate case, the rate constants show far less variability between different PTCs. This is most likely due to increased nucleophile solubility, as illustrated by the fact that the reaction proceeds slowly without any catalyst. On the other hand, with potassium cyanide, there is a pronounced deviation between the tetrabutylammonium chloride case and the remaining PTCs. In fact, we actually show that Aliquat 336 is comparable with the siloxane-containing PTCs, with **3** showing a slightly higher rate constant. This is an important distinction because it is one illustration where our newly developed PTCs show improvement over the current methods.

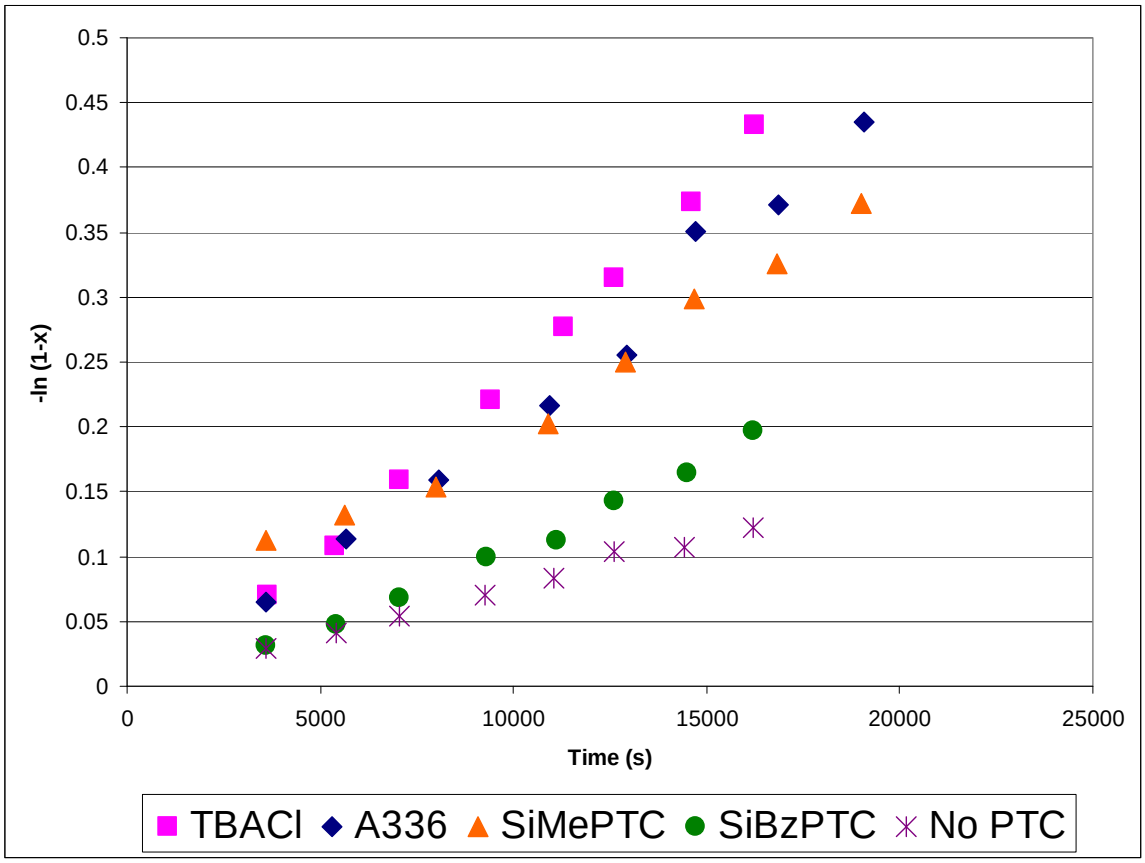

Figure 5-8 Time dependent behavior of potassium thiocyanate with siloxane electrophile and various PTCs at 70 °C and 900 rpm stirring

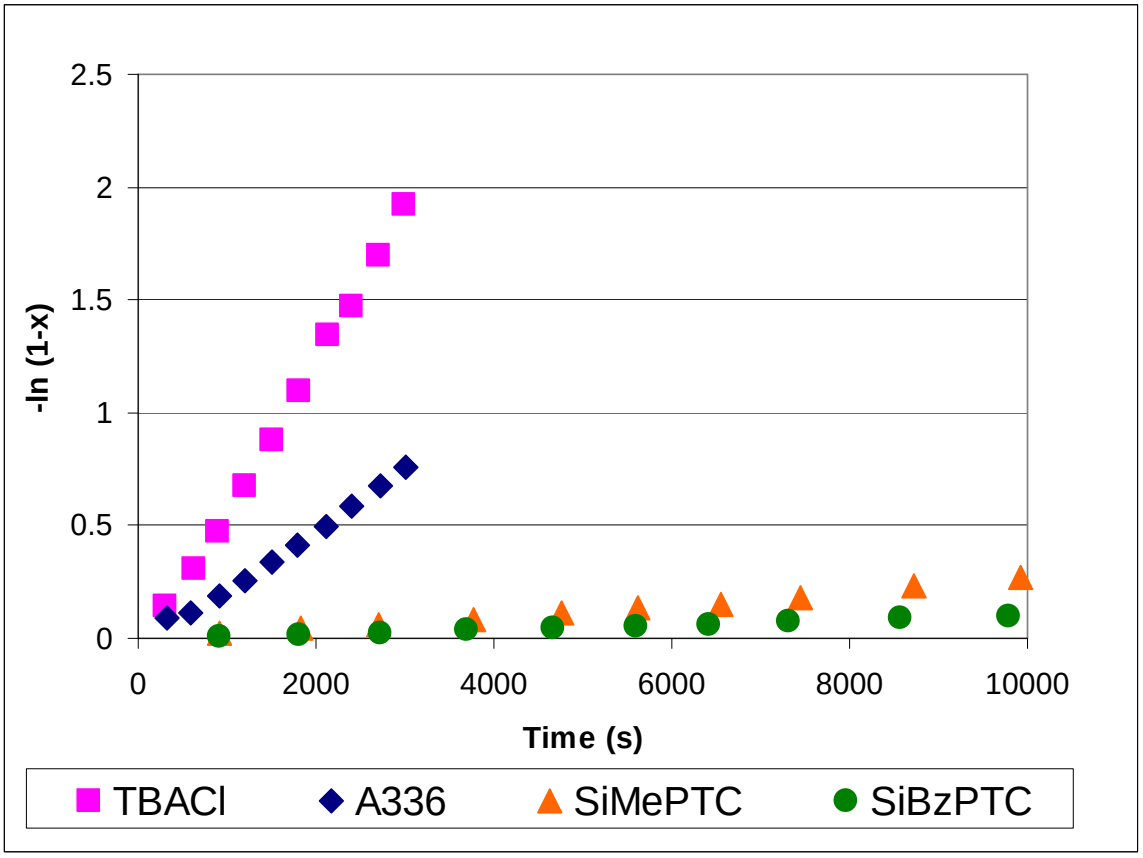

Figure 5-9 Time dependent behavior of potassium acetate with siloxane electrophile and various PTCs at 70 °C and 900 rpm stirring

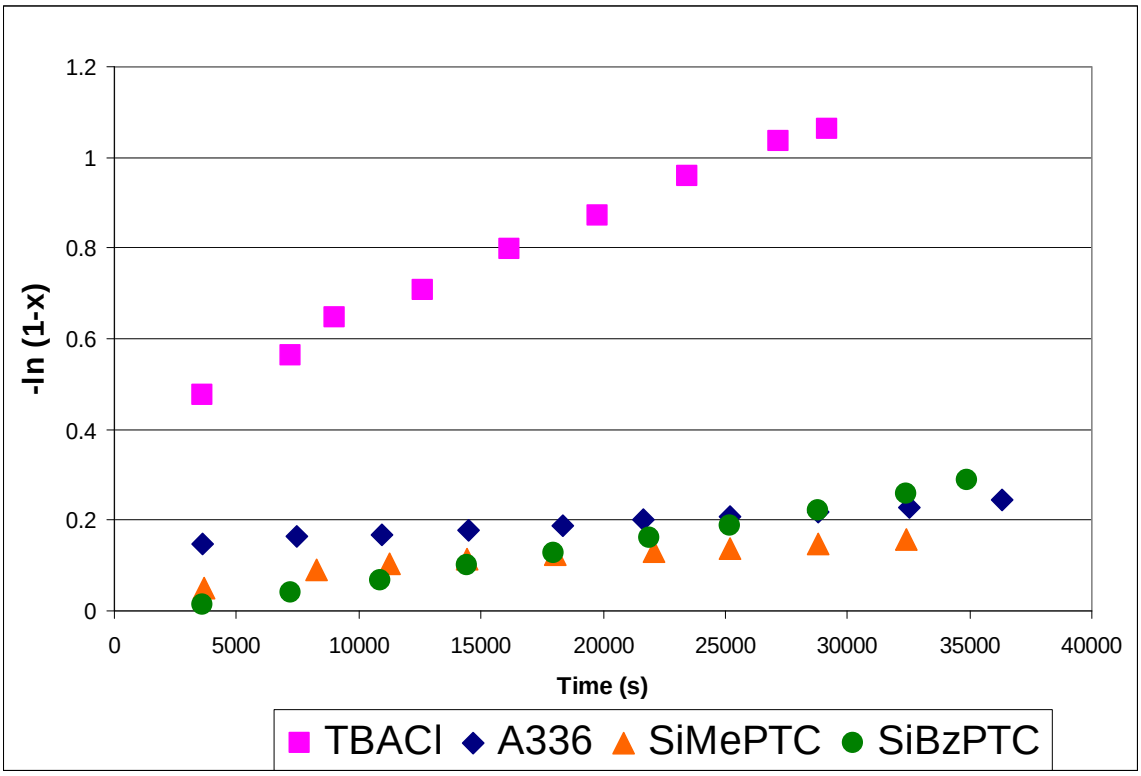

Figure 5-10 Time dependent behavior of potassium cyanide with siloxane electrophile and various PTCs at 70 °C and 900 rpm stirring

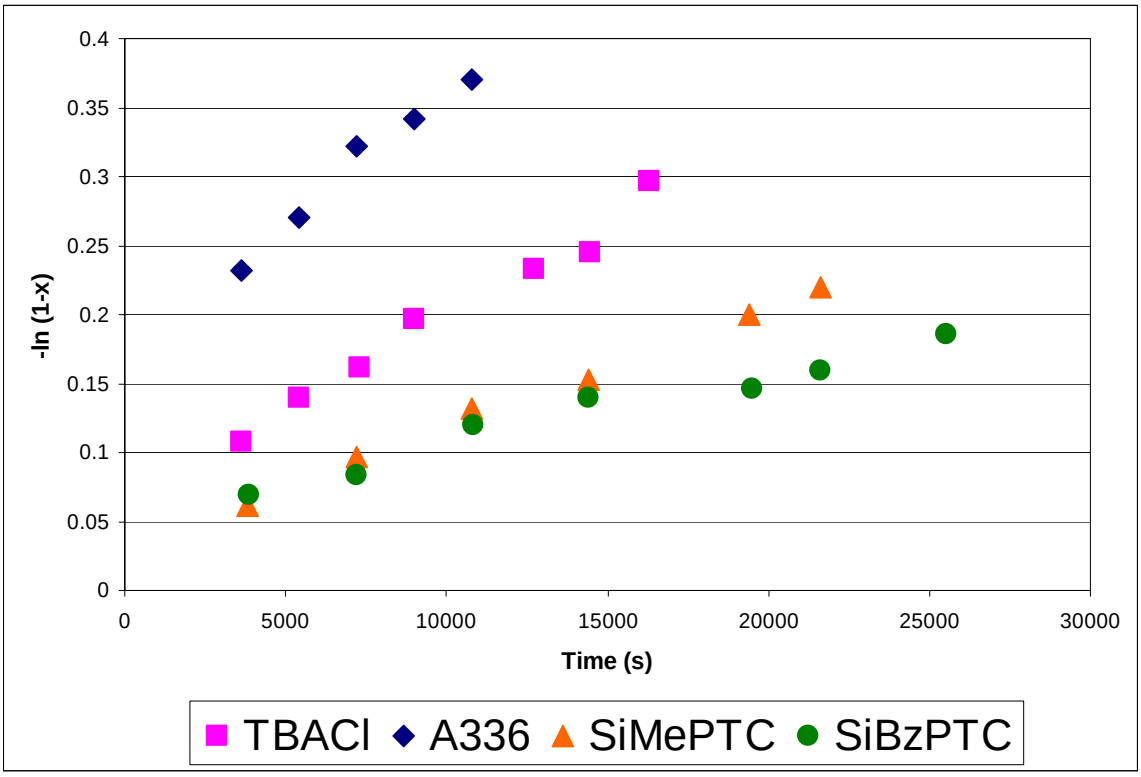

Figure 5-11 Time dependent behavior of L-lysine with siloxane electrophile and various PTCs at 70 °C and 900 rpm stirring

Table 5-1 Pseudo-first order rate constants for the reaction of several nucleophiles with 1-siloxane electrophile and various PTCs at 70 °C and 900 rpm stirring

	Pseudo-First Order Rate Constant * 10^5 (s^{-1})			
PTC (5%)	**KOAc**	**KSCN**	**KCN**	**Lysine**
None	No Rxn	0.800 ± 0.08	No Rxn	No Rxn
TBACl	56.5 ± 3	2.57 ± 0.1	1.76 ± 0.05	1.14 ± 0.09
Aliquat 336	22.2 ± 1	2.62 ± 0.2	0.177 ± 0.03	1.59 ± 0.2
2	2.04 ± 0.2	1.91 ± 0.1	0.118 ± 0.01	0.627 ± 0.08
3	0.802 ± 0.03	1.17 ± 0.02	0.751 ± 0.03	0.428 ± 0.01

Table 5-2 Pseudo-first order rate constants for the reaction of several nucleophiles with 2-siloxane electrophile and various PTCs at 70 °C and 900 rpm stirring.

	Pseudo-First Order Rate Constant * 10^5 (s^{-1})			
PTC (5%)	**KOAc**	**KSCN**	**KCN**	**Lysine**
None	No Rxn	0.773 ± 0.05	No Rxn	No Rxn
TBACl	65.2 ± 4	2.74 ± 0.2	2.54 ± 0.5	1.35 ± 0.01
Aliquat 336	24.9 ± 2	2.64 ± 0.2	0.254 ± 0.04	1.66 ± 0.01
2	2.33 ± 0.04	1.90 ± 0.2	0.251 ± 0.006	0.862 ± 0.01
3	0.986 ± 0.04	1.26 ± 0.03	0.904 ± 0.03	0.566 ± 0.08

Overall, this illustrates that phase transfer catalysis is highly dependent on the nucleophile with both traditional and novel PTCs, making it consistent with numerous systems tested in the literature.[4] Additionally, the data confirm that PTC is an effective method for the coupling of siloxane-containing compounds with biomolecules, with rates comparable to the potassium salts. This result provides important evidence for the implementation of this technique on an industrial scale, because it overcomes the mass transfer limitations associated with the biphasic system.

The comparable rates were a significant finding since the mechanisms may be different for the salt reactions and L-lysine. The salts operate in a similar manner to Figure 5-1, as previously described in the background section. This is the typical mechanism by which phase transfer catalysis functions to facilitate reactions. Essentially, these systems work by exchanging and shuttling anions between phases. However, with the L-lysine nucleophile, we have the possibility of several effects that dictate the mechanism of the reaction, as shown in Figure 5-12. The first is related to the ionic interaction between the positively charged ammonium center on the PTC and the negatively charged carboxylic acid on the amino acid. This interaction is dependent on the pH of the system, which is constantly driven lower by the reaction due to formation of the hydrochloric acid byproduct. We did not control the pH during our kinetic studies. However, we believe that the concentration was too low to be able to see the rate reduction that would arise with the protonation of the carboxylic acid and, thus, elimination of the ionic effect. Hence, we have not proven that this effect is the dominating mechanism for phase transfer catalysis with L-lysine. In higher concentrations or solvent-less conditions, the acid by-product and subsequent loss of the

ionic effect may be more impactful on the system, which could illustrate the slowing of the rate that would accompany this effect. The second mechanism that could drive the reaction could be hydrogen bonding between the chloride anion and the alpha and epsilon amino hydrogen.

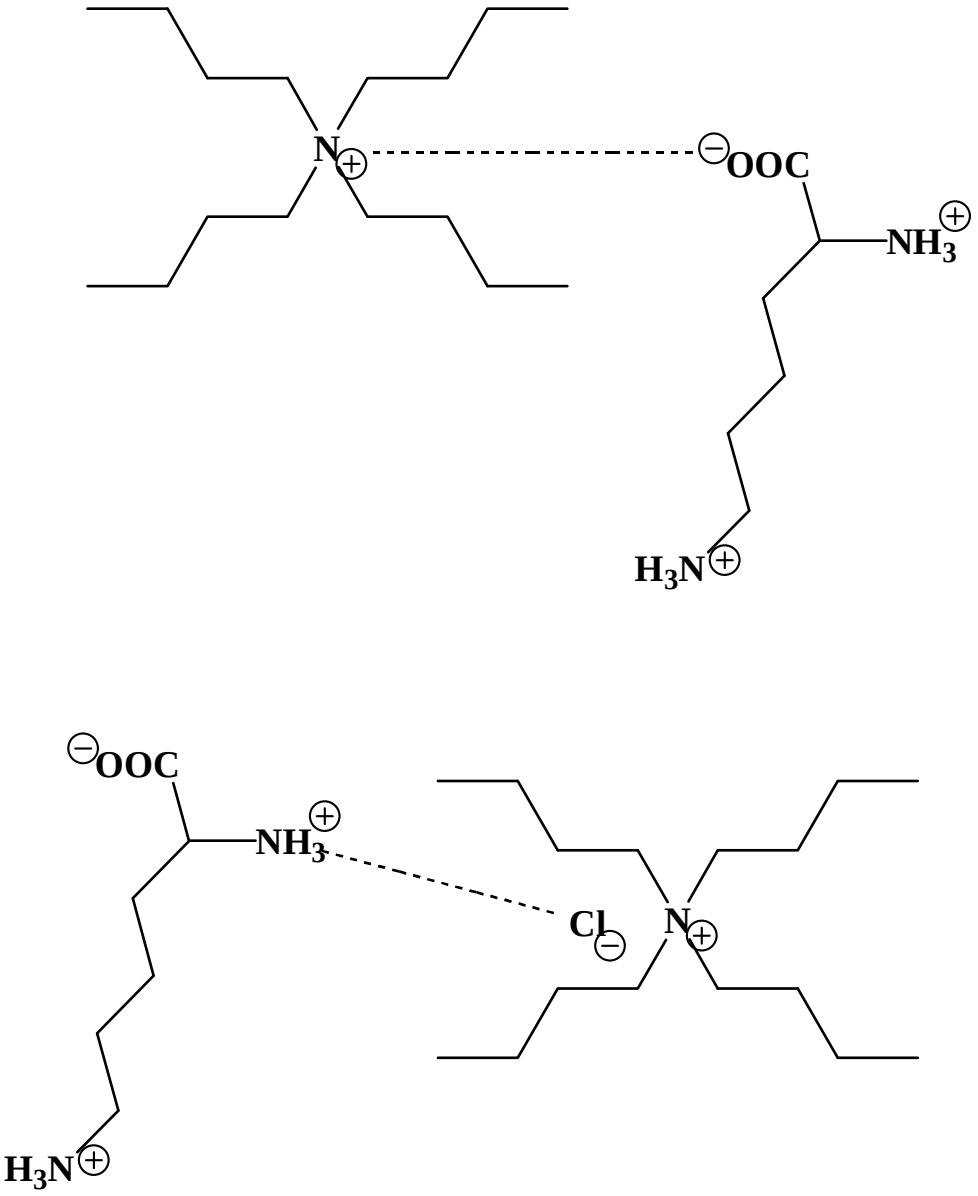

Figure 5-12 Possible mechanisms for L-lysine PTC reaction: Ionic Interaction (Top) and Hydrogen bonding (Bottom)

The mechanism for the L-lysine reaction is important for the further application of this technique on larger molecules, such as poly-L-lysine and Cytochrome c. The ionic interaction is highly limited on the polymeric system, which would greatly slow the reaction if this is the dominating effect. The hydrogen bonding would be far more prevalent.

5.3.2 Solvent Effect

The final point of observation is related to the performance of the siloxane-containing PTCs. Despite lower rates for most of the cases studied, both PTCs showed catalytic functionality for all of the systems tested. The difference could possibly be attributed to the system in which we obtained the kinetic data. In all of the cases, we used ethyl acetate as the solvent for the reaction. In general, solventless conditions would be preferred in order to reduce waste associated with solvent removal. This was possible in our reaction due to the fact that the siloxane electrophile is a liquid. However, we found that the kinetics were very difficult to measure due to the large amount of nucleophile required to create pseudo-first order conditions (five times excess for all of our studies). Hence, we shifted to the solvent system to obtain accurate kinetics, which essentially changed our system to an organic environment. Also, the siloxane electrophile contained a relatively small amount of siloxane functionality, as compared to a molecule like polydimethylsiloxane (PDMS). Hence, we decided to investigate the influence of these parameters by manipulating the solvent system and the extent of siloxane functionality.

We tested the effect by modifying the solvent with various concentrations of PDMS, which provides the solvent with different levels of siloxane character. We looked at three different solvent systems to assess the influence of siloxane functionality on the efficacy of our novel PTCs. The first represents the pure organic case, in which we used only ethyl acetate as the solvent. The next uses 50% organic and 50% PDMS. The last case uses only PDMS as the solvent system, illustrating the most favorable environment for the novel siloxylated PTCs. The pseudo-first order rate constants for tetrabutylammonium chloride, **2**, and **3** are shown for each case in Figure 5-13 and Table 5-3. Due to the vast differences in reaction rate, we normalized the data to one order of magnitude in Figure 5-14. This helps to illustrate the trends for the siloxylated PTCs, which are difficult to decipher in the rate plot due to their low values.

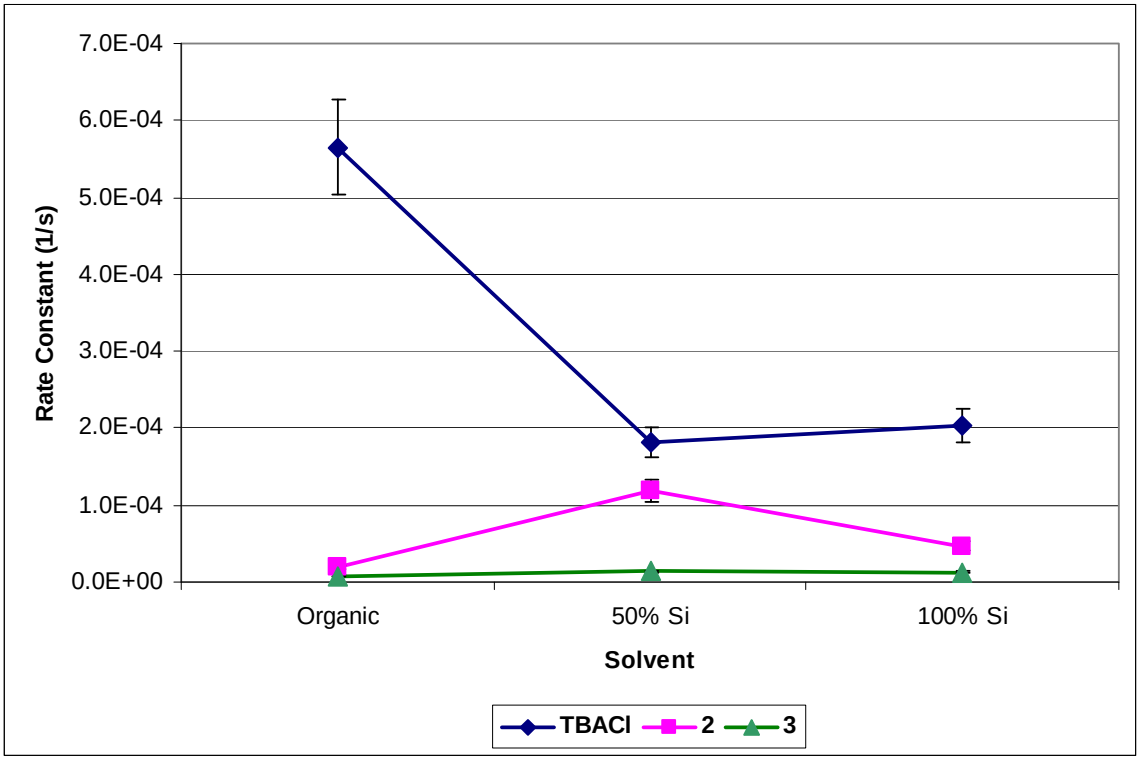

Figure 5-13 Solvent Dependence of SiBzCl and KOAc Reaction at 70°C and 5% PTC

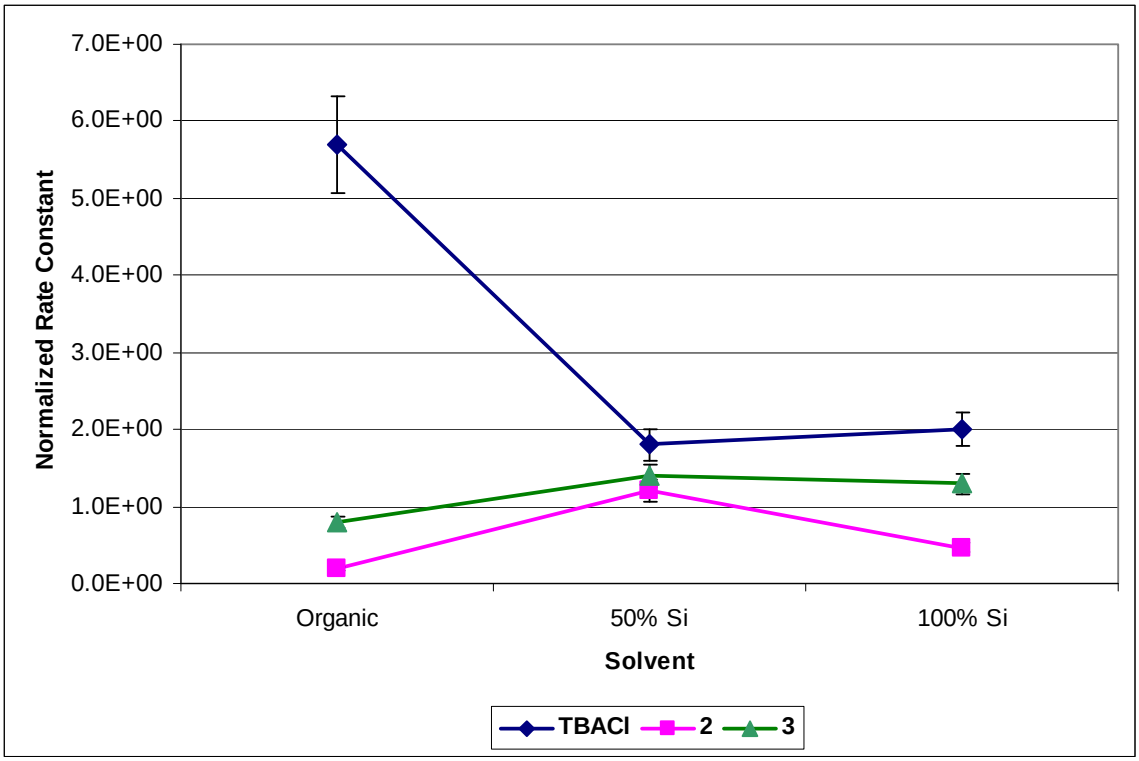

Figure 5-14 Normalized for One Order of Magnitude to Illustrate Variation in Solvent Dependence of SiBzCl (1) and KOAc Reaction at 70ºC and 5% PTC

Table 5-3 Solvent Dependence of SiBzCl (1) and KOAc Reaction at 70ºC and 5% PTC

	Pseudo-First Order Rate Constant * 10^5 (s^{-1})		
PTC (5%)	**Organic**	**50% Si**	**100% Si**
TBACl	56.5 ± 3.0	18.2 ± 3.5	20.3 ± 2.5
2	2.04 ± 0.20	11.8 ± 1.3	4.66 ± 0.60
3	0.80 ± 0.08	1.40 ± 0.20	1.30 ± 0.05

The results for the solvent study illustrate slight, but definitive changes in the rates for all PTCs. In the organic case, TBACl has the highest rate with at least one order of magnitude improvement over **2** and **3**. With 50% PDMS, the traditional PTC, TBACl, shows a distinct drop in reaction rate, lowering by approximately two-thirds of its original value. At the same time, both siloxylated PTCs show increases in rate constant, with both catalysts raising an order of magnitude. The rate constant for the methyl version approximately equals that of the traditional PTC, indicating that the siloxylated nature of the solvent makes a significant impact on the rate. At 100% PDMS, TBACl and **3** rate constants remain approximately equal to the previous case, while the **2** reduces slightly.

This study shows that the novel siloxylated PTCs can, at best, reach equivalent rates to the traditional quaternary ammonium PTCs. The data indicate that the performance of the organic PTC reduces with increased siloxane character within the solvent, while the siloxylated PTCs show modest increases. However, additional siloxane character beyond the 50% PDMS case does not make a significant impact on any of the PTCs. This work illustrates the original concept of siloxylated moieties working more efficiently in siloxylated environments, but the organic PTC still outperforms the novel PTCs under most circumstances. However, the novel PTCs contain only modest siloxane character. Therefore, it may be possible to show improvement over the traditional PTCs with highly siloxylated catalysts.

5.3.3 PTC Concentration Dependence

We also completed a study on the PTC concentration dependence of the reaction. Figure 5-15 and Table 5-4 show the pseudo-first order rate constants versus the percentage of PTC for the potassium acetate nucleophile with tetrabutylammonium chloride. The reaction was selected for simplicity due to its high rate at the initial PTC concentration. The data shows 0%, 1%, 5%, and 10% TBACl. The plot illustrates highly linear behavior of the system over the 0-10% range. This is consistent with typical PTC behavior, as described throughout the literature.[4]

Table 5-4 Reaction of KOAc with siloxane electrophile and various amounts of TBACl PTC at 70°C

% TBACl	% Conversion (30 min)	Pseudo-first order rate constant (s^{-1})
0	0	0
1	13	1.6×10^{-4}
5	65	6.5×10^{-4}
10	83	1.2×10^{-3}

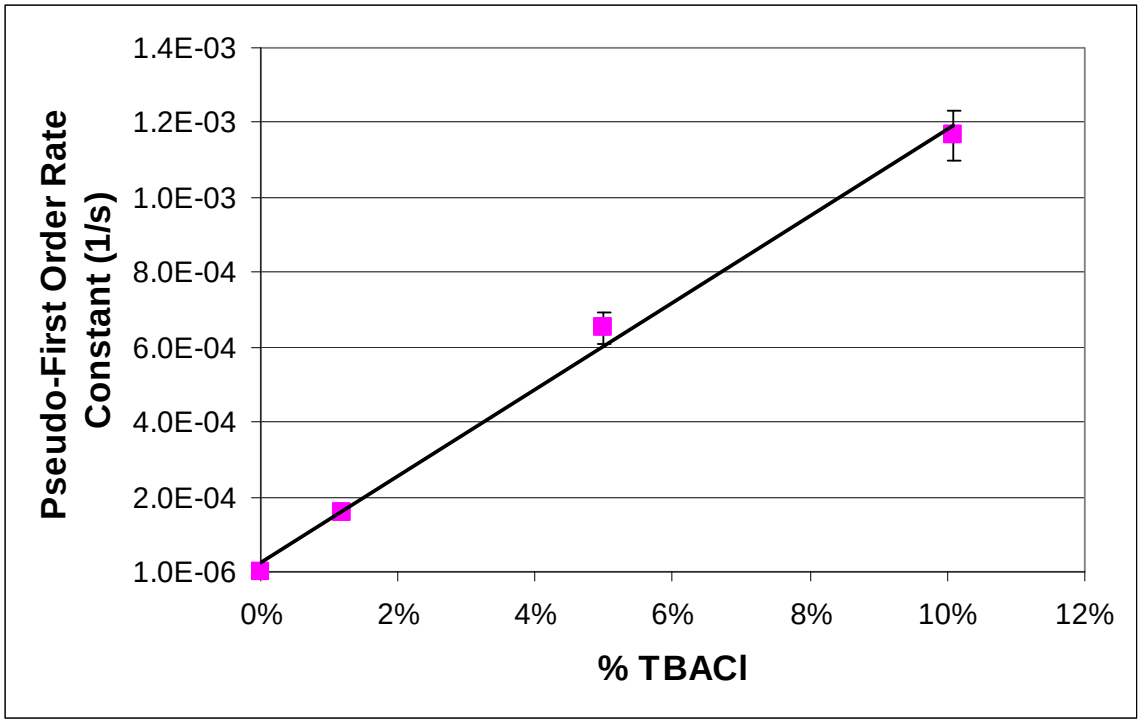

Figure 5-15 Effect of catalyst loading on conversion for reaction of KOAc with siloxane electrophile and various amounts of TBACl PTC at 70°C

5.3.4 Temperature Dependence

Next, we looked at the effect of temperature on the reaction in order to obtain the activation energies. As with the PTC concentration dependence, we chose to focus the study on the reaction of the siloxane electrophile with potassium acetate. However, we studied the effect on both the organic PTCs and the siloxane-containing PTCs. The Arrhenius plots are shown in Figure 5-16 and the rate constants for the different temperatures and PTCs are shown in Table 5-5. Due to low rates for the siloxane-containing PTCs at lower temperatures, the data were taken at 50, 60, and 70ºC. Since the organic PTCs showed reasonable rates at low temperatures, we ran the study at 30,

50, and 70ºC, which should provide slightly more accurate activation energies. The activation energies vary between 95 and 132 kJ/mol, with the organic PTCs on the low end of the range and the siloxane-containing PTCs on the high.

Table 5-5 Reaction of KOAc with (1) and 5% of various PTCs in ethyl acetate at various temperatures. 5x excess KOAc is used in all conditions

	Pseudo-First Order Rate Constant * 10^5 (s^{-1})				**Activation Energy (kJ/mol)**
PTC (5%)	**30°C**	**50°C**	**60°C**	**70°C**	
None	No Rxn	No Rxn	No Rxn	No Rxn	
TBACl	0.692 ± 0.06	6.59 ± 0.06	-	56.5 ± 3	95
Aliquat 336	0.111 ± 0.006	1.42 ± 0.1	-	22.2 ± 1	114
2	-	0.179 ± 0.02	1.46 ± 0.1	2.04 ± 0.2	116
3	-	0.0465 ± 0.005	0.349 ± 0.05	0.802 ± 0.03	132

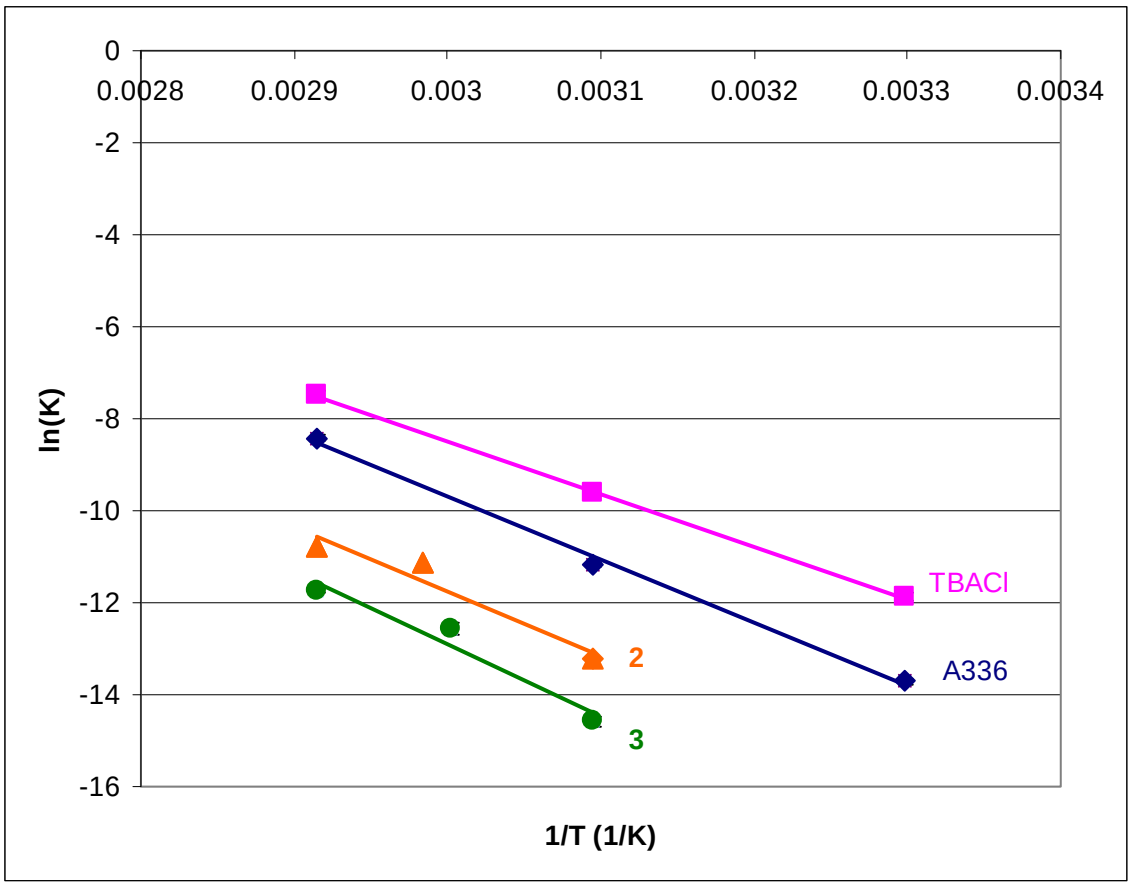

Figure 5-16 Arrhenius plots for reaction of KOAc with (1) and 5% of various PTCs in ethyl acetate at various temperatures

5.4 Conclusions

Phase transfer catalysis is an effective technique for coupling siloxane-containing compounds with small biomolecules. We have illustrated this with a model reaction between a siloxylated compound and several types of nucleophiles, including three salts and the amino acid, L-lysine. The reactions show high reactivity for all nucleophiles and have been studied in both organic and siloxylated media. In general, the common catalysts, tetrabutylammonium chloride and Aliquat 336, show superior activity to the novel siloxylated compounds. Thus, we have successfully applied PTC to this area, but have not seen significant improvement from the development of siloxylated catalysts. The next step for this research involves application of this technique to larger biomolecules, such as poly-L-lysine and Cytochrome c.

5.5 References

1. Vinci, D.D., M.; Hallett, J. P.; John, E. A.; Pollet, P.; Thomas, C. A.; Grilly, J. D.; Jessop, P. G.; Liotta, C. L.; Eckert, C. A., *Piperylene sulfone: a labile and recyclable DMSO substitute.* Chemical Communications, 2007. **14**: p. 1427-1429.

2. Jiang, N.V., Daniele; Liotta, Charles L.; Eckert, Charles A.; Ragauskas, Arthur J., *Piperylene Sulfone: A Recyclable Dimethyl Sulfoxide Substitute for Copper-Catalyzed Aerobic Alcohol Oxidation.* Industrial and Engineering Chemistry Research, 2008. **47**(3): p. 627-631.

3. Yadav, G.D., *Insight into green phase transfer catalysis.* Topics in Catalysis, 2004. **29**(3-4): p. 145-161.

4. Starks, C.M., C.L. Liotta, and M. Halpern, *Phase Transfer Catalysis: Fundamentals, Applications, and Industrial Perspectives*. 1994, New York: Chapman & Hall.

5. Dehmlow, E.V. and S.S. Dehmlow, *Phase Transfer Catalysis*. 3rd ed. 1993, New York: VCH.

6. Xie, X.B., James S.; Joseph, Paul J.; Liotta, Charles L.; Eckert, Charles A., *Phase-transfer catalyst separation by CO2 enhanced aqueous extraction.* Chemical Communications, 2002: p. 1156-1157.

7. Dillow, A.K., Yun, S.L. Jimmy, Suleiman, David; Boatright, David L., Liotta, Charles L., Eckert, Charles A., *Kinetics of Phase-Transfer Catalysis Reaction in Supercritical Fluid Carbon Dioxide.* Industrial and Engineering Chemistry Research, 1996. **35**: p. 1801-1806.

8. Yadav, G.D.J., Yogeeta B., *Role of Omega Phase in the Analysis and Intensification of Solid-Liquid Phase Transfer Catalyzed Reactions.* Langmuir, 2002. **18**: p. 5995-6002.

9. Chandler, K.C., Christy W.; Lamb, David R.; Liotta, Charles L.; Eckert, Charles A., *Phase-Transfer Catalysis in Supercritical Carbon Dioxide: Kinetic and Mechanistic Investigations of Cyanide Displacement on Benzyl Chloride.* Industrial and Engineering Chemistry Research, 1998. **37**(8): p. 3252-3259.

10. Yadav, G.D.D., Neesha M., *Selectivity Engineering of Phase Transfer Catalyzed Alkylation of 2'-Hydroxyacetophenone: Enhancement in Rates and Selectivity by Creation of a Third Liquid Phase.* Organic Process Research & Development, 2005. **9**: p. 749-756.

11. Chen, J.S., Scott K.; Huddleston, Jonathan G., Rogers, Robin D., *Polyethylene glycol and solutions of polyethylene glycol as green reaction media.* Green Chemistry, 2005. **7**: p. 64-82.

12. Drake, R.P., Stephanie, *WO2007141565: Amino-Acid Functional Siloxanes, Methods of Preparation and Applications*. 2007.

13. Lane, T.H.L., Charles L.; Brandstadt, Kurt F.; Hand, James H.; Charney, Reagan; Bommarius, Adreas S.; Eckert, Charles A.; Polizzi, Karen M.; Pollet, Pamela; Hallett, Jason P., *WO2008033908: Organosilicon-Functional Phase Transfer Catalysts*. 2008.

14. Husek, P.M., Karel, *Gas Chromatography of Amino Acids.* Journal of Chromatography, 1975. **113**: p. 139-230.

15. Gehrke, C.W.L., Kenneth, *Trimethylsilylation of Amino Acids: Effects of Solvents on Derivatization Using Bis(Trimethylsilyl)trifluoroacetamide.* Journal of Chromatography, 1970. **53**: p. 201-208.

16. Rodier, C.S., R.; Raulin, F.; Vidal-Madjar, C., *Chemical derivatization of amino acids for in situ analysis of Martian samples by gas chromatography.* Journal of Chromatography A, 2001. **915**: p. 199-207.

17. Zhou, F.X.K., I.S.; Feibush, B., *Solid-phase derivatization of amino acids and peptides in high-performance liquid chromatography.* Journal of Chromatography, 1993. **648**: p. 357-365.

18. Sang-Sup, P.H.-G.J.B.-S.Y.M.-S.L.J.-H.P.M.-K.L.Y.-J.K.M.-J.J., *Highly enantioselective and practical cinchona-derived phase-transfer catalysts for the synthesis of alpha-amino acids.* Angewandte Chemie, 2002. **41**(16): p. 3036-3038.

19. Goetheer, E.L.V.B., M.W.P.L.; van den Broeke, L.J.P.; Meijer, E.W.; Keurentjes, J.T.F., *Functionalized Poly(propylene imine) Dendrimers as Novel Phase Transfer Catalysts in Supercritical Carbon Dioxide.* Industrial and Engineering Chemistry Research, 2000. **39**: p. 4634-4640.

20. Sonnek, G.R., Christiane; Schmaucks, Gerd; Kaden, Reinfried; Lehms, Ingeburg, *Oligosiloxanes with functional groups. XI. Synthesis of sodium .alpha.,.alpha.,.omega.-trihydroperfluoroalkoxypropanesulfonate and .alpha.,.alpha.,.omega.-trihydroperfluoroalkoxypropoxysiloxanes.* Journal of Organometallic Chemistry, 1991. **405**(2): p. 179-182.

21. Arren, D.H.C.C., W.D.; Parker, D.S., *US5654374*. 1997: USA.

Chapter VI: Conclusions and Recommendations

6.1 Piperylene Sulfone: Characterization and Reaction Media

Piperylene sulfone represents an excellent alternative to polar, aprotic solvents, providing a medium for difficult reactions along with easy separation. We have demonstrated that the molecule has similar solvent properties to DMSO, allowing for enhanced dissolution of highly varying materials, such as salts and organics. For separation, piperylene sulfone has a built-in, thermal switch that enables the decomposition of the solvent to volatile components. These can be retrieved to enable the reformation of the solvent for complete recycle. We have applied piperylene sulfone to a number of reactions, finding success in nucleophilic substitutions and asymmetric transfer hydrogenations (ATH). The next step in this research involves continued work on ATH reactions. We are currently working on proving the full recycle process, which will extend the capabilities of the solvent to organometallic-catalyzed reactions.

We have additional research being conducted in another lab related to the use of piperylene sulfone as a carrier for mass spectroscopy. In this work, we only need a one-way switch from the solvent to the decomposition products. Hence, we are now looking at additional retro-cheletropic reactions that are not reversible. These extend beyond the SO_2 based solvents, utilizing CO and CO_2 as the decomposition products. Figure 6-1 illustrates two examples of molecules that can undergo a one-way switch.

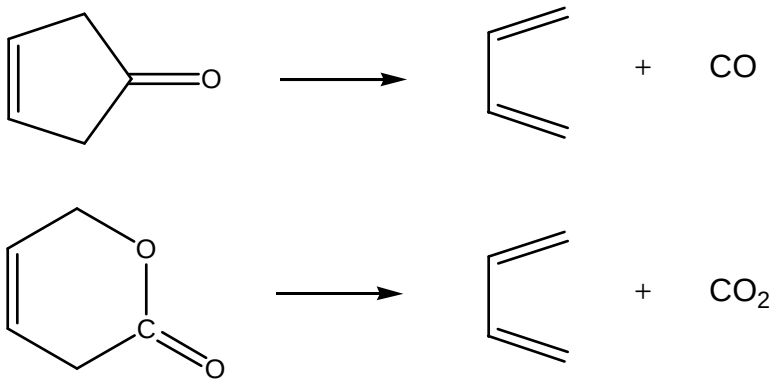

Figure 6-1 Retro-Cheletropic Reaction for the Formation of CO and CO_2 Decomposition Products

The retro-cheletropic reactions for these materials are known, but have not been well studied. However, the first reaction involving the decomposition of cyclopentenone to carbon monoxide and butadiene has been studied briefly. Dolbier *et al.* determined its activation energy at 35.2 kcal/mol[1], which is higher than the previous switchable solvents with piperylene sulfone and butadiene sulfone at 19.5 kcal/mol and 27.3 kcal/mol, respectively[2]. This indicates that the decomposition may require higher temperatures, making the process slightly more difficult than our current materials. However, an initial investigation of both systems will be worthwhile to determine the ease of separation and the effectiveness in the mass spectroscopy application.

6.2 Switchable Solvents for *In-Situ* Acid Catalyzed Reactions

We have shown that the switchable solvents, butadiene sulfone and piperylene sulfone, can act not only as reaction media but also as acid catalysts. Due to the equilibrium reaction for the solvents, we can generate sulfurous acid *in-situ* to catalyze several reactions, including the hydrolysis of β-pinene and the benzopinacol rearrangement. We completed a broad study on the hydrolysis reaction to test an

important industrial application and expand our understanding of the catalysis potential. Based on the study, the switchable solvents show excellent reactivity with slight improvements in selectivity for the desired hydrolysis products.

The next step in this work involves further exploration of the benzopinacol rearrangement, as illustrated in Figure 6-2. The initial study was limited, showing that reaction and product isolation are possible with the switchable solvent. We would like to look into this application further, because it utilizes both the reaction and separation properties designed into the solvent. These include excellent solvent properties, acid catalysis, and product isolation through solvent decomposition. Therefore, a broader study is required to optimize the reaction and to illustrate the full potential of the switchable solvent.

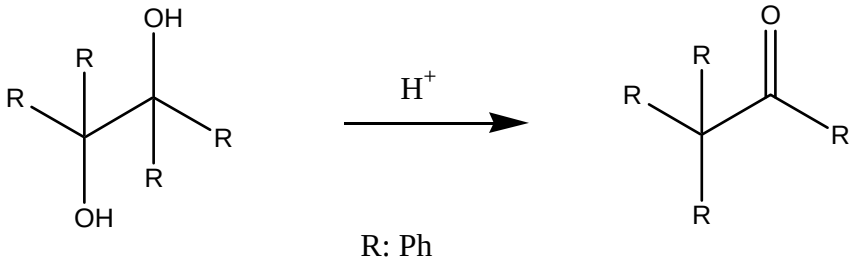

Figure 6-2 Pinacol Rearrangement (R=Ph for Benzopinacol)

Additionally, we are investigating a number of applications related to biomass pretreatment and production of biofuels. Biomass pretreatment is an important area of research due to the need to transition from food-based sources of ethanol to non-edible materials. The food-based sources, such as corn, are easily fermented into ethanol, but they have recently led to the debate between food versus fuel. Hence, researchers have looked to additional sources of biomass that are not used for food production. These

include a number of lignocellulosic materials, such as cornstovers, switchgrass, and wood chips. These sources are more difficult to ferment due to their highly bound structure, so they are often pretreated to open the structure and ease the fermentation process.[3] The effect of the pretreatment process is illustrated in Figure 6-3.

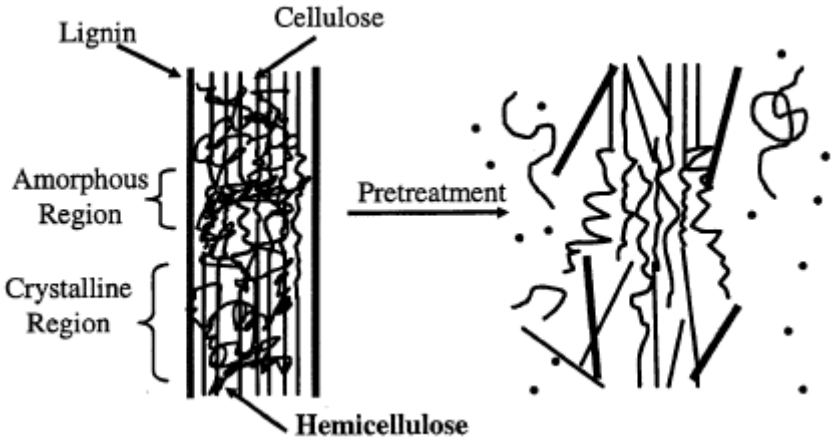

Figure 6-3 Effect of Pretreatment on the Structure of Lignocellulosic Materials[3]

We are attempting to use piperylene sulfone for this pretreatment task, utilizing its excellent solvent properties for the dissolution of lignin and cellulose and its acid catalysis to help with the breakdown of the polymeric sugars.

The next application involves the production of biofuels of a different variety. Instead of ethanol, the desired compound is 5-hydroxymethylfurfural (HMF), which has been recently targeted by researchers for production of bio-derived compounds. It can be produced from biomass polysaccharides through the acid-catalyzed dehydration of hexoses, as illustrated in Figure 6-4.[4]

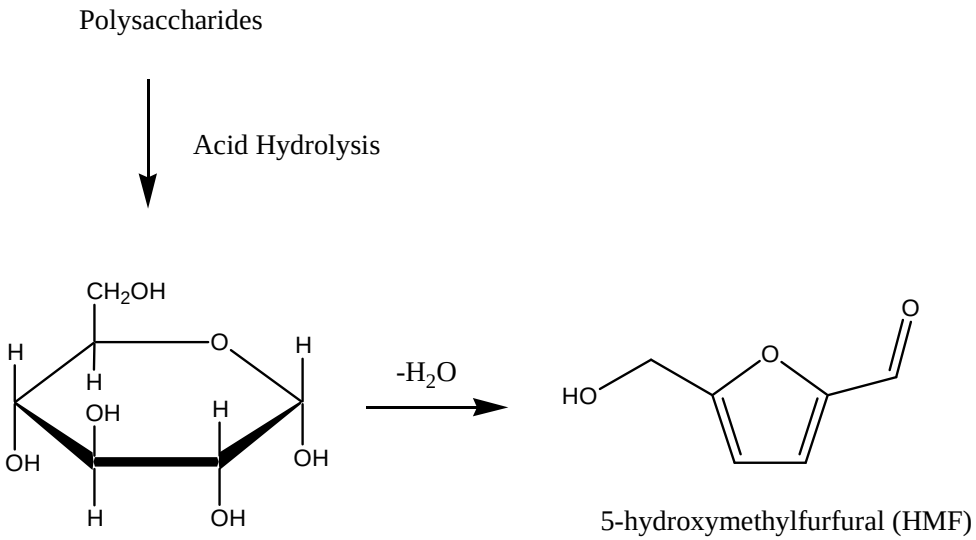

Figure 6-4 Acid-Catalyzed Production of HMF from Polysaccharides

HMF is an important intermediate for the expansion of bio-derived materials, because it can be further processed to produce compounds useful in polymers, fine chemicals, and biofuels.[5] Recently, Dumesic *et al.* illustrated the synthesis of HMF with a biphasic system consisting of an aqueous and organic phase.[4] The organic phase, containing MIBK and 2-propanol, helps to improve the selectivity by extracting the products, limiting negative side reactions. The selectivity is further improved by modification of the aqueous phase with DMSO, which can help stabilize the furanose form of the hexoses. However, the addition of DMSO causes difficulties in the product isolation due to extraction of small amounts of the solvent into the extractant phase. Therefore, we recommend the replacement of DMSO with piperylene sulfone, which can simultaneously overcome the separation difficulties and enhance the reaction rate due to the *in-situ* acid, eliminating the need for an additional catalyst. We have completed initial work on this application and see preliminary indications of HMF production.

However, further analysis and optimization is required to confirm and improve upon these results.

6.3 Phase Behavior of Polyethylene Glycol with CO_2 and Common Organic Solvents

PEG-tunable systems enable the coupling of homogeneous reaction with heterogeneous separation through reversible phase separation with CO_2-expanded liquids. We have illustrated this reaction and separation technique with PEG, conventional organic solvents, and CO_2. These systems show homogeneous behavior at atmospheric conditions, but can phase separate upon addition of CO_2 pressure. In our work, we studied the compositions of the heterogeneous system over a small pressure range. This allows us to ascertain the quality of the separation and thus, the potential for application in homogeneous catalyst recovery. We have studied and modeled the phase behavior of PEG-400 and CO_2 with 1,4-dioxane or acetonitrile. We showed that 1,4-dioxane at 25ºC has the optimal separation, with excellent purity of both phases. Acetonitrile, on the other hand, does not separate as well, indicating that it has less potential for clean product and catalyst recovery.

We applied the dioxane system to the production of phenols. These are usually generated through the hazardous cumene process, but have recently been investigated with homogeneous catalysts. Other group members have worked on the reaction in PEG, while we have focused on the separation potential. Therefore, our initial study focused on the partitioning of the phenol in the heterogeneous system. We found that we can achieve good separation with certain substrates. However, the study was only preliminary, so additional conditions need to be tested to optimize the product recovery.

We also need to assess the catalyst and ligand partitioning to ensure immobilization in the PEG-rich phase. The next step is to complete a full recycle study, in which we run the reaction in the PEG/dioxane mixture and then use CO_2 to induce the phase split. We can then remove the dioxane phase containing the product and recycle the immobilized catalyst in the PEG-rich phase.

We have recently shifted the reaction focus from the production of phenols to ethers, which can be produced from similar reactions. These materials are valuable to the pharmaceutical industry as drug intermediates. By changing the ratio of starting materials, we can produce selectively ethers instead of phenols. We started the study with the original reaction materials, but the goal reaction will involve larger molecules, such as benzothiophene derivatives. The model reaction is shown in Figure 6-5.

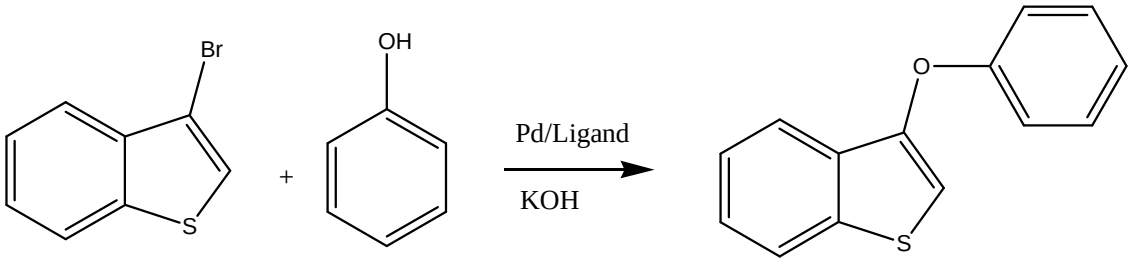

Figure 6-5 Synthesis of Benzothiophene Ether Intermediates for the Production of Pharmaceuticals

This illustrates the formation of ether intermediates that can be further reacted to produce important pharmaceutical products. In this case, the derivatives are useful for the production of estrogen replacement drugs that can reduce the negative side effects associated with hormone replacement therapy[6]. David *et al.* recently developed a reaction scheme toward the synthesis of benzothiophene derivatives.[6] However, they

had to oxidize the starting material to the sulfoxide in order to produce the ether. The modification is necessary to enable efficient reaction, but it complicates the synthesis, requiring not only the oxidation, but also the reduction to remove the sulfoxide functionality in later steps. The process becomes even more difficult through the use of DMF as the solvent, which necessitates a difficult separation of the products. Therefore, this represents an excellent opportunity for application of the PEG-tunable systems.

The first step in this investigation is to optimize the reaction activity and selectivity in PEG, since very little research has been completed with these catalysts for ether synthesis and the reaction has never been studied in this medium. Then, we will study the partitioning to ensure that we can achieve good recovery of the products. However, we believe that the partitioning should actually show improvements over the phenols due to their bulky, organic character and reduced hydrogen bonding ability with PEG. Finally, we will have to show the complete recycle process with good recovery of both products and catalysts.

We also want to look into the development of the phase behavior with other organic solvents. Specifically, we want to investigate the possibilities of using isopropanol, which is considered one of the greener solvents and can be more accommodating to enzymes.[7] This would extend the benign nature of the process by not only using less solvent through utilization of CO_2, but also making all the materials involved green. Also, the utilization of isopropanol and PEG could lead to development of improved enzymatic systems, which can benefit from enhanced enzyme stability over THF and 1,4-dioxane mixtures and reduced acidity.[8] In OATS, the dissolution of CO_2 into water causes the formation of carbonic acid, resulting in the significant decrease in

pH. In past research, we have had to use buffer salts to ensure that the enzymes can survive the separation.[9, 10] It has not yet been proven, but it is conjectured that PEG would not form such an acidic medium in the presence of CO_2.[11] Therefore, the combination of isopropanol and PEG may reduce the toxicity of the medium for enzymes. Our initial work on the phase behavior with isopropanol showed that pressure range between the three-phase heterogeneous system and the two-phase liquid-fluid equilibrium was extremely small, indicating that the pressures are very near the critical point for the mixture. Thus, we were unable to measure the phase behavior of the three-phase region. However, we can operate the system in the liquid-fluid regime by extracting the products into the fluid-like phase. For the application, we recommend looking into reactions that have been completed in similar systems, such as those tested in scCO_2/PEG mixtures. One possible example is the lipase-catalyzed acylation of 2-phenylethanol by vinyl acetate.

6.4 Siloxylated PTCs for Coupling of Siloxanes with Biomolecules

We have shown that phase transfer catalysis (PTC) can enable the coupling of siloxane-containing compounds and biomolecules. We have also synthesized novel, siloxylated PTCs to improve the activity in the siloxane environment, but these proved to be less effective than their conventional counterparts. The biomolecules in this study were limited to amino acids, specifically L-lysine for the primary research. Thus, the future research work involves expanding to larger biomolecules, such as peptides and proteins. We recommend a number of common biomolecules, including poly-L-lysine and Cytochrome c. The reaction with poly-L-lysine is shown in Figure 6-6. This

represents an important extension of the reaction to the polypeptide of L-lysine, which is a key test in the implementation of the technique for larger molecules.

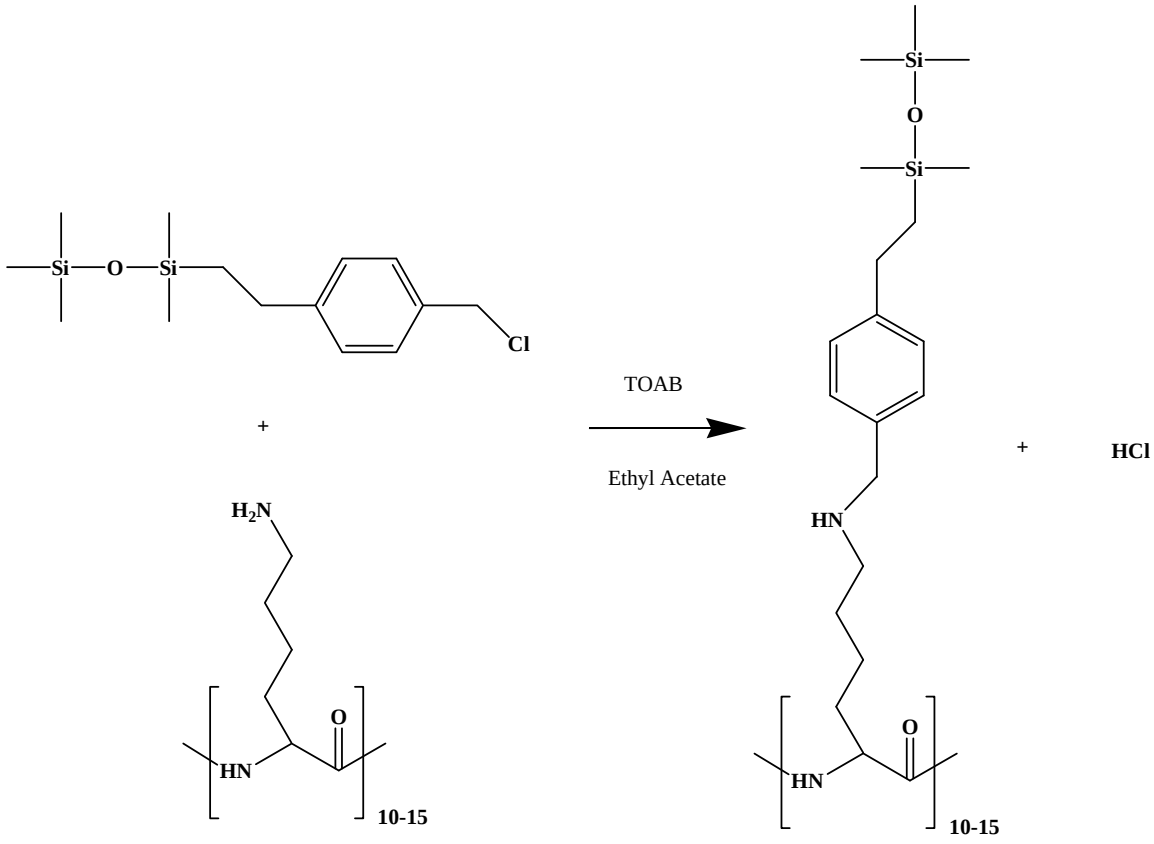

Figure 6-6 Reaction of Poly-L-Lysine with Siloxylated Benzyl Chloride by Tetraoctylammonium Bromide (TOAB) in Ethyl Acetate

The Cytochrome c reaction represents the ultimate goal for this work, illustrating the potential for PTC to enable efficient coupling of siloxanes with highly immiscible, large biomolecules. Cytochrome c is a water-soluble, globular protein that is important for electron transfer in the cells. The structure of this protein is shown in Figure 6-7, which illustrates the heme group as a red bar and lysine residues as spheres.[12, 13] We

plan on using these lysine residues to enable the coupling with the siloxane electrophile. The lighter spheres indicate the more accessible residues for nucleophilic attack.

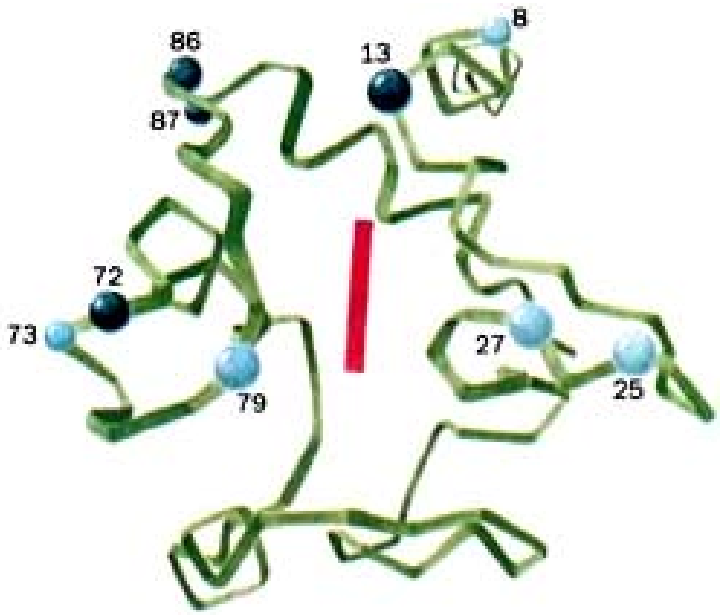

Figure 6-7 Ribbon Structure of Cytochrome c with Lysine Resides (red bar indicates the heme and the light balls are more accessible than dark balls)[12, 13]

Using the PTC technique, we conducted an initial study with poly-L-lysine and Cytochrome c, attempting to couple these with the siloxylated benzyl chloride. However, we were unable to detect any product via MS and NMR. The analyses could not confirm whether or not any reactions took place due to the low concentrations of materials and the large molecular weight of the substrates. Hence, the next step in the work is to improve the analysis of the molecules. We believe that by increasing the concentration of the reactants, we may be able to use NMR to detect the product formation. Also, we may need to work our way up to these large molecules, continuing the work with smaller peptides that may be easier to detect.

In general, there is a great deal of potential for many of the systems addressed in this work, especially for the switchable and tunable solvents. By developing applications for some of the difficult engineering problems that exist today, we can truly make these environmentally benign alternatives viable for a number of important processes.

6.5 References

1. Dolbier, W.R.F., Henry M., *Thermal Decomposition of Cyclopen-3-enone.* Journal of the Chemical Society, Perkin Transactions 2: Physical Organic Chemistry, 1974. **14**: p. 1674-1676.

2. Drake, L.R., S.C. Stowe, and A.M. Partanksy, *Kinetics of the Diene Sulfur Dioxide Reaction.* Journal of the American Chemical Society, 1946. **68**: p. 2521-2524.

3. Mosier, N.W., Charles; Dale, Bruce; Elander, Richard; Lee, Y.Y.; Holtzapple, Mark; Ladisch, Michael, *Features of promising technologies for pretreatment of lignocellulosic biomass.* Bioresource Technology, 2005. **96**: p. 673-686.

4. Chheda, J.N.R.-L., Yuriy; Dumesic, James A., *Production of 5-hydroxymethylfurfural and furfural by dehydration of biomass-derived mono- and poly-saccharides.* Green Chemistry, 2007. **9**: p. 342-350.

5. Ragauskas, A.J.W., Charlotte K.; Davison, Brian H.; Britovsek, George; Cairney, John; Eckert, Charles A.; Frederick, William J.; Hallett, Jason P.; Leak, David J.; Liotta, Charles L.; Mielenz, Jonathan R.; Murphy, Richard; Templer, Richard; Tschaplinski, Timothy, *The Path Forward for Biofuels and Biomaterials.* Science, 2006. **311**: p. 484-489.

6. David, E.P., Julie; Pellet-Rostaing, Stephane; Fournier dit Chabert, Jeremie; Lemaire, Marc, *Efficient Access to 2-Aryl-3-Substituted Benzo[b]thiophenes.* Journal of Organic Chemistry, 2005. **70**: p. 3569-3573.

7. Capello, C.F., Ulrich; Hungerbuehler, Konrad, *What is a green solvent? A comprehensive framework for the environmental assessment of solvents.* Green Chemistry, 2007. **9**(9): p. 927-934.

8. Khmelnitsky, Y.L.M., Vadim V.; Belova, Alla B.; Sergeeva, Maria V.; Martinek, Karel, *Denaturation capacity: a new quantitative criterion for selection of organic solvents as reaction media in biocatalysis.* European Journal of Biochemistry, 1991. **198**: p. 31-41.

9. Broering, J.M.H., Elizabeth M.; Hallett, Jason P.; Liotta, Charles L.; Eckert, Charles A.; Bommarius, Andreas S., *Biocatalytic reaction and recycling by using CO2-induced organic-aqueous tunable solvents.* Angewandte Chemie, 2006. **45**(28): p. 4670-4673.

10. Hill, E.M.B., James M.; Hallett, Jason P.; Bommarius, Andreas S.; Liotta, Charles L.; Eckert, Charles A., *Coupling chiral homogeneous biocatalytic reactions with benign heterogeneous separation.* Green Chemistry, 2007. **9**(8): p. 888-893.

11. Jessop, P.G., *Catalysis using supercritical solvents. SCFs and liquid polymers.* Multiphase Homogeneous Catalysis, 2005. **2**: p. 676-688.

12. Voet, D.V., Judith G., *Chapter 22: Electron Transport and Oxidative Phosphorylation*, in *Biochemistry*, D.F. Harris, Patrick, Editor. 2004, John Wiley and Sons, Inc.: Hoboken, N.J.

13. Mathews, F.S., Progress in Biophysics and Molecular Biology, 1986. **45**: p. 45.

Appendix A: Piperylene Sulfone: Scale-Up

A.1 Introduction

In Chapters 1 and 2, we illustrate a number of successful applications of the switchable solvent, piperylene sulfone. We also have a variety of potential applications recommended in Chapter 6. In order to test these reactions, we need to have a steady supply of piperylene sulfone, which is not commercially available. Therefore, we have developed a scale-up process for the production of larger amounts of solvent. For this work, we designed and built a new 5 L, glass pressure vessel, allowing for five times the original production capacity. We also optimized the reaction and purification steps to improve the recovery process, assessing the need for polymerization inhibitor and the possibility of supercritical CO_2 extraction.

A.2 Experimental

A.2.1 Materials

The following materials were used as received from the suppliers except where noted: sulfur dioxide (Air Gas, 99.98%). 1,3-pentadiene (90 %, mixture of isomers), N-phenyl-2-naphthylamine (Sigma-Aldrich, 97%), dichloromethane (VWR), and distilled water (Unit Operations Laboratory at Georgia Tech). The carbon dioxide was SFC grade (Air Gas, 99.999%) and further purified to remove trace water and other impurities with a Matheson gas purifier and filter cartridge (Model 450B, Type 451 filter). Note: The 1,3-pentadiene is not available as mixture of isomers anymore from Sigma-Aldrich, so we

have switched to 1,3-pentadiene mixture of isomers (45% -trans and 23% -cis) from ChemSampCo.

A.2.2 Set-up for Synthesis

- 5 L 1 Pc Pressure Reactor (Ace Glass)
- 3" RSD RG Stir Magnet (Ace Glass)
- Condenser West with Ace Thred (Ace Glass)
- 5MMID 290MM Shouldered Thermo Well for use with 5 L one piece Pressure Reactor and #15 Bushing. (Ace Glass)
- 7MM Solid PTFE Plug, 7855-707 FETFE O-RING Front Seal (Ace Glass)
- 15MM ACE-THRED Nylon Bushing, -110 FETFE O-RING (Ace Glass)
- 15MM Solid cx PTFE PLUG, FETFE O-RING Front Seal (Ace Glass)
- 25MM 1/4" Adapter without O-RING (Ace Glass)
- 3-50 PSI ADJ 1/4" Valve Pressure Relief (Ace Glass)
- 65 PSI 1.25" Rupture Disc Graphite (Ace Glass)
- #7 ACE-THRED To 1/4"ID ACE-SAFE Tubing Connector (Ace Glass)
- 15MM 1/4" Teflon Adapter (Ace Glass)
- Stainless Steal-Case Gauge +/- 2% Accuracy
- Thermo Electron Corporation, Neslab RTE7 Refrigerated Bath

A.2.3 Set-up for work-Up:

- VWR Pump, Variable Flow, Med.-Hi Flow, 4.0 to 600 mL/min (VWR)
- NSF Certified HI-Density Polyethylene Pail 5-1/2 Gallon
- 1/8” plastic HPLC tubing

- Mechanical overhead stirred with dual bladed stirrer

A.2.4 Synthesis of Piperylene Sulfone: Scale-Up

The reaction vessel is a 5 L glass pressure vessel with a maximum working pressure of 45 psig and is equipped with a condenser, pressure gauge, and inlet valve for inputting the sulfur dioxide, as shown in Figure A-1. The safety components include a pressure relief valve that unseats at 45 psig and a coated graphite rupture disk that bursts at 65 psig. The vessel sits directly in an ethylene glycol bath connected to a chiller via a cooling coil. To start the synthesis, the temperature bath is cooled to -10 ºC in order to reduce the temperature to the vapor pressure of sulfur dioxide. Then, 5 mol % N-phenyl-2-naphthylamine (inhibitor) and approximately 1 L of sulfur dioxide are mixed with a large magnetic stir bar in the reaction vessel. The system is allowed to vent sulfur dioxide for a short period of time to ensure that the system is at atmospheric pressure. Degassed 1,3-pentadiene is then slowly pumped under nitrogen directly into the liquid sulfur dioxide through a septa using an HPLC pump. After the diene addition is complete, at least 2.5 L of additional sulfur dioxide is added to the vessel and the mixture is allowed to react for two days at 20 °C.

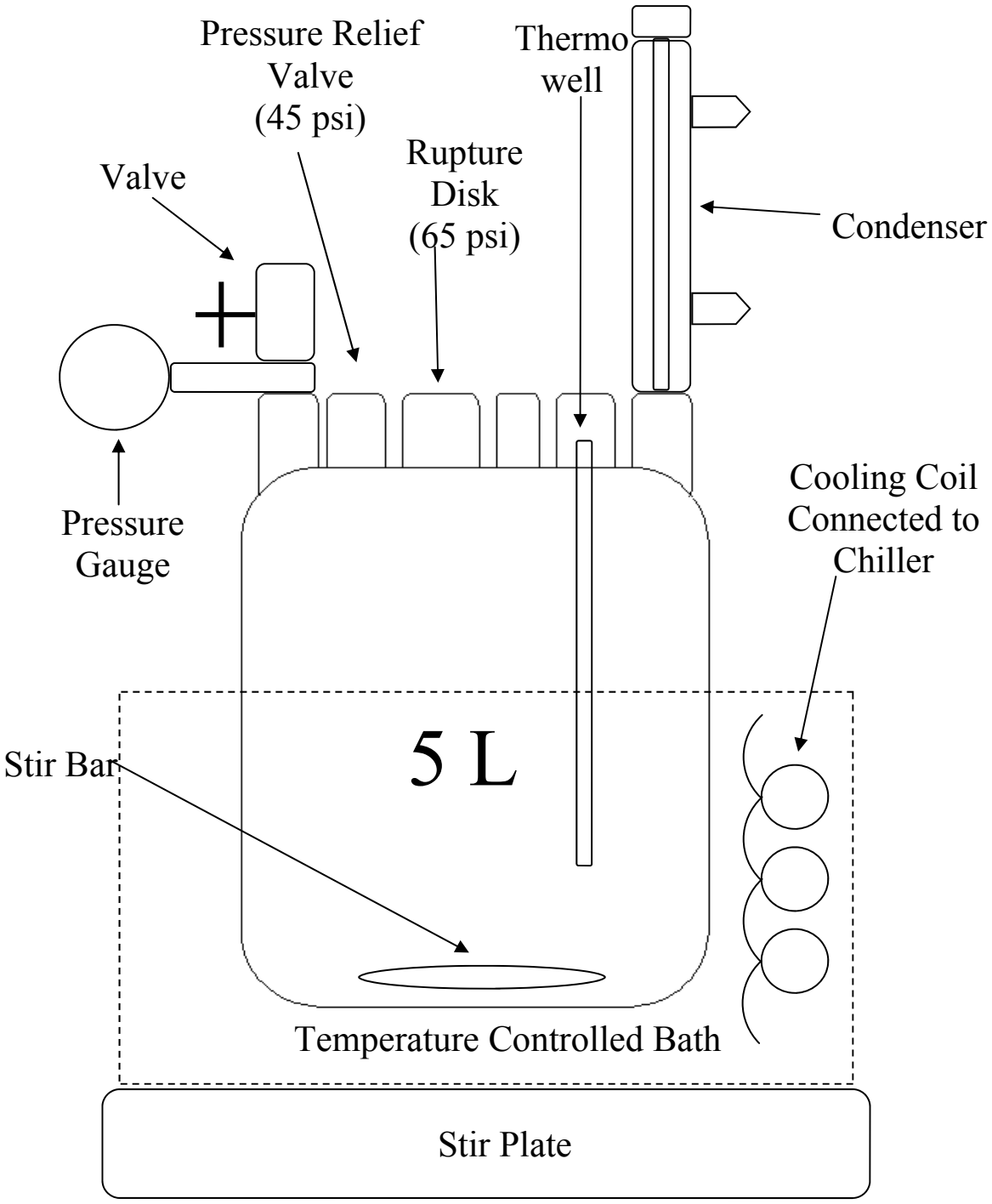

Figure A-1 Scale-Up Vessel Set-Up for Piperylene Sulfone Synthesis

Before proceeding to the work-up, the vessel was vented slowly to remove the excess sulfur dioxide. The crude material was poured into a polyethylene bucket and mixed with 3 L of water. The slurry was stirred via an electric overhead stirrer for at least one hour. The aqueous layer was pumped into a separate bucket and extracted with 1 L of CH_2Cl_2. This mixture was stirred via the electric overhead stirrer for at least 30 minutes. The dichloromethane layer was then pumped into large round bottom flasks that were set aside for purification. The organic extraction was repeated at least once to ensure that all the piperylene sulfone was removed from the water.

Dichloromethane was removed under vacuum and filtered over a short path of activated carbon and SiO_2. The solvent was removed in vacuo to yield piperylene sulfone, which was then dried over $MgSO_4$ to remove water. The material was analyzed by ^1H and ^{13}C NMR (^1H NMR (ppm): δ = 1.36 (d, 3H), 3.69 (m, 3H), 5.96 (m, 2H), ^{13}C NMR (ppm): δ = 12.9, 54.8, 59.4, 122.5, 131.4)

A.2.5 Optimization of Inhibitor Concentration

We optimized the synthesis of piperylene sulfone in the presence of N-phenyl-2-naphthylamine (inhibitor) by testing the reactions under varying concentrations of inhibitor. We ran the reactions for three hours at 20ºC in a 15 mL glass pressure vessel. The system included a pressure gauge, pressure relief valve (set for 60 psi), inlet valve, and ethylene glycol bath connected to a chiller via a cooling coil. The procedure for the synthesis was similar to the scale-up process. The inlet was equipped with tubing leading directly to the bottom of the pressure tube, so we were able to use an air-tight syringe to inject 1 mL of the degassed-piperylene directly into the liquid SO_2.

A.2.6 Solubility Measurements for Mixed Components in CO_2

The solubility of piperylene sulfone and N-phenyl-2-naphthylamine (inhibitor) was investigated by direct high pressure sampling. The system was a high pressure, Jerguson cell equipped with a sample loop, similar to the apparatus shown in Figure 4-5 in Chapter 4. For a typical set-up, the cell was cleaned, vacuumed, and then loaded with a known quantity of piperylene sulfone and inhibitor. Then, the cell was pressurized with carbon dioxide from a syringe pump (ISCO, model 500D) at a known temperature and pressure. By noting the volume difference on the pump and the density from the Span-Wagner equation of state, the mass amount of CO_2 added to the system could be determined. We used the sample loop to obtain the vapor phase sample, and then analyzed it by GC-MS and UV-vis to determine the composition of piperylene sulfone and inhibitor, respectively. The exact concentrations were determined by calibration curves for each component. We used this technique to study the solubility for pure piperylene sulfone and mixed systems, containing the solvent and inhibitor.

A.2.7 Solubility Measurements for Pure Components in CO_2

The pure component solubility of N-phenyl-2-naphthylamine was studied at varying conditions by high pressure, UV-vis spectroscopy. Ngo *et. al.* detailed the procedure, in which we entirely dissolve a known amount of inhibitor in the $scCO_2$.[1] For extremely small sample sizes, we created a solution of known concentration and then added a small fraction of it to the cell. Then, the cell was vacuumed to remove the solvent, leaving the solute behind. After the solvent was completely removed, we placed a Teflon-coated magnetic stir bar in the vessel and sealed it shut with a Teflon o-ring.

We then vacuumed it to remove the air and added CO_2 to pressurize it up to the appropriate level. The vessel was connected to an ethylene glycol chiller to control the temperature. In order to determine the solubility, we monitored the absorbance at increasing levels of CO_2 until the absorbance reached a maximum value. We allowed the system to equilibrate at each pressure point for 12 hours to ensure equilibrium. The actual solubility can be calculated by looking at a plot of absorbance versus CO_2 density, which should show a plateau at the point where the entire solute has been dissolved in the supercritical phase.

A.3 Results

A.3.1 Scale-Up Process

The experimental procedure for the piperylene sulfone synthesis is the optimized method that we are currently using. The primary differences from the initial procedure include degassing the piperylene and pumping it into the reactor slowly and directly in the liquid sulfur dioxide. We found that these steps were key in reducing polymerization and maximizing the production.

A.3.2 Optimization of the Inhibitor

The polymerization inhibitor, N-phenyl-2-naphthylamine, is the main contaminant present in piperylene sulfone. The molecule is illustrated in Figure A-2. The presence of inhibitor can be reduced by distillation of piperylene sulfone under vacuum. However, this purification process leads to substantial losses of solvent due to decomposition.

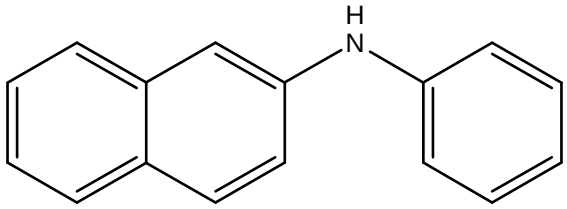

Figure A-2 Structure of N-phenyl-2-naphthylamine

In order to solve the problem, we studied the synthesis of piperylene sulfone in the absence of inhibitor under small scale conditions. During initial testing, we used a crude methodology to get preliminary results for the synthesis without inhibitor. Unfortunately, after 3 hours, the main product observed was polymer, indicating that the presence of inhibitor in the synthesis of piperylene sulfone was crucial to avoid polymerization of piperylene.

As a consequence, we decided to study the synthesis of piperylene sulfone in the presence of 5.0, 2.5, and 1.0 % N-phenyl-2-naphthylamine (inhibitor). The reactions were each run for three hours at 20ºC and the results are illustrated in Table A-1.

Table A-1 Piperylene Sulfone Yield with N-Phenyl-2-Naphthylamine

INHIBITOR (mol %)	YIELD (%)*
5	28
2.5	30
1	30
0	38

*Yield based on reaction of *trans*-piperylene for 3 hours at 20ºC

The yields were approximately 30% for each of the cases studied, with no variation between the three different inhibitor concentrations. Since the 1.5% inhibitor worked as well as the higher concentrations, we decided to reevaluate the reaction without inhibitor in our new set-up. As shown in the table, we found that the yield actually increased to 40% for the 0% inhibitor case. This result clearly contradicts our initial tests. However, we believe the differences can be attributed to the methodology of the two experiments, illustrating the importance of careful, slow addition of degassed-piperylene directly into the liquid SO_2. In the initial screening, this procedure was not followed, allowing for the polymerization to escalate.

A.3.3 Solubility of Piperylene Sulfone and Inhibitor

As previously noted, the original purification could not remove all of the N-phenyl-2-naphthylamine (inhibitor), which can create issues in certain processes that require high purity. Therefore, we attempted to extract the piperylene sulfone into supercritical CO_2, which we thought would allow for clean separation from the inhibitor. To assess this hypothesis, we tested both the individual solubilities of piperylene sulfone and the inhibitor, along with the mixed system. The data is illustrated in Table A-2.

Table A-2 Solubility of Piperylene Sulfone and N-phenyl-2-naphthylamine in Supercritical CO_2 at 55ºC and 12.4 MPa

System	Wt% PS	Wt% INH
piperylene sulfone (PS)	2.7	-
N-phenyl-2-naphthylamine (INH)*	-	6.0E-5
PS + INH	2.7	0.7

* Pure inhibitor data was taken at 45ºC and 10 MPa

The solubility data show good partitioning of piperylene sulfone into the $scCO_2$ at approximately 3 wt% for both the pure and the mixed systems. However, the mixture had high solubility of the inhibitor at almost 1 wt%, indicating poor separation of the piperylene sulfone away from the inhibitor. The high solubility of inhibitor in the $scCO_2$ phase was a result of cosolvent effects from the presence of piperylene sulfone, which is illustrated by the fact that the pure inhibitor solubility is miniscule in comparison to the mixed data.

In order to reduce the inhibitor solubility, we made a slight modification to the structure, using a magnesium salt version of the molecule, as illustrated in Figure A-3. Salts generally have extremely low $scCO_2$ solubility, so we believe that this will reduce the partitioning during the piperylene sulfone extraction. However, we have only completed an initial analysis with the material, testing its inhibiting capabilities for the synthesis. We observed little polymer formation, but have not quantified the yields for these reactions. The next step will be to quantify the reaction data and test the CO_2 solubility with piperylene sulfone.

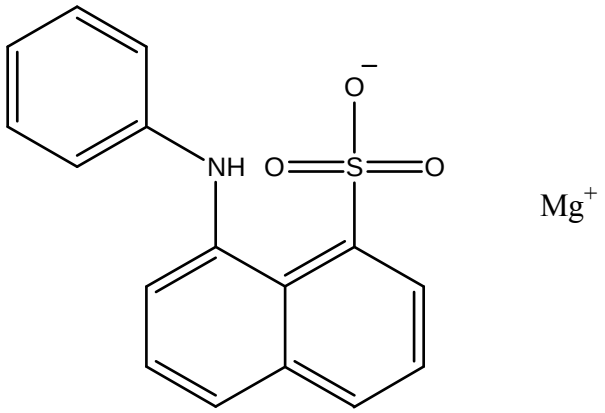

Figure A-3 Structure of Magnesium Salt Version of Polymerization Inhibitor

A.4 Conclusions

The scale-up process has worked effectively for the production of piperylene sulfone. There could be improvements through development of a continuous process, but this is beyond the scope of the work addressed here. In the purification process, we showed that we do not need as much polymerization inhibitor as previously believed, but we need to attempt the modified process on the full scale to see if the results translate to the larger system. For the CO_2 extraction, we found poor separation of the inhibitor and the piperylene sulfone, indicating that we will need to change the inhibitor to make the process feasible. We are currently in the process of testing the salt version of the inhibitor, which should improve the separation.

A.5 References

1. Ngo, T.T.B., David; Ecker, Charles A., *Spectroscopic Measurement of Solid Solubility in Supercritical Fluids.* AIChE Journal, 2001. **47**(11): p. 2566-2572.

Appendix B: Reversible Ionic Liquids under Pressure

B.1 Introduction

In Chapter 2, we described some of the reversible ionic liquids based on amidines or guanidines in combination with alcohols.[1] These materials form ionic liquids when CO_2 is bubbled through the liquid, requiring only atmospheric pressure to enable the reaction. They can reverse back to the molecular liquid by bubbling nitrogen through the ionic liquid or heating it. We have been able to use these systems for reactions and separations by exploiting the change in polarity between the molecular and ionic forms. This is due to the fact that the molecular forms are miscible with alkanes, while the ionic are not, allowing for extraction of the products into the alkane phase. In these solvents, we have used a variety of primary alcohols, but we found that the reaction was much more difficult for secondary or tertiary alcohols. Hence, we wanted to test the possibility of enhancing the reaction by using CO_2 under pressure. This could also allow for a new separation mechanism in which heat or nitrogen may not be required to switch the solvent. The ionic liquid could possibly reverse by simply removing the pressure.

In this brief study, we explored the reaction of 1,8-diazabicyclo-[5.4.0]-undec-7-ene (DBU) with CO_2 and either tert-butyl alcohol, 2-pentanol, or isopropanol, as shown in Figure B-1.[2] We studied the conductivity under pressure to assess the formation of the ionic liquid.

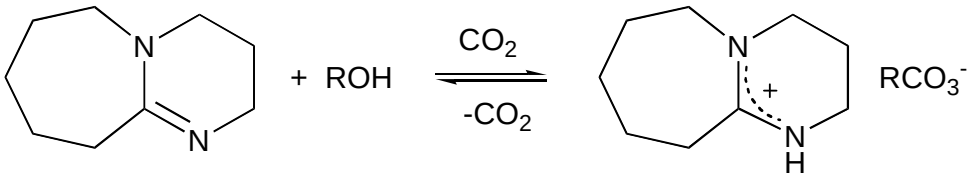

Figure B-4 Amidine Reversible Ionic Liquid with DBU

B.2 Experimental

B.2.1 Materials

The following materials were used as received from the supplier: Water (HPLC grade), 1,8-diazabicyclo-[5.4.0]-undec-7-ene (DBU, Sigma-Aldrich, 98%), tert-butyl alcohol (Sigma, minimum 99%), isopropanol, 2-pentanol, and potassium chloride (Fisher Scientific). The carbon dioxide was SFC grade (Air Gas, 99.999%) and further purified to remove trace water and other impurities with a Matheson gas purifier and filter cartridge (Model 450B, Type 451 filter).

B.2.2 Experimental

We used a custom concentric probe that has recently been used for dielectric measurements. The two cylinders are made out of stainless steel, with the inner diameter at 1.750", the outer at 2.000", and the height of both at 0.900". They are screwed together with Teflon screws and attached to solid probe wires with stainless steel screws. The wires and the probe are suspended in a 300 mL Parr pressure reactor, where they are insulated with Teflon tubing and attached via PEEK fittings. The probes are connected via alligator clips to a HP LCR model 4285A. The Parr was cleaned and vacuumed to remove any traces of air and the solvent was added through gas tight syringes. The entire

probe was covered by the solvent. The vessel was then heated with a heating mantle attached to a temperature controller to the appropriate temperature for the reaction. The resistance, the inverse of the conductivity, was calculated from the recorded data. The system was calibrated with potassium chloride by measuring the conductivity over a range of temperatures.

B.3 Results

The calibration of the system with potassium chloride was not consistent due to slight movements of the probe in the reaction vessel. Hence, we decided to assess the reaction from only a qualitative perspective, observing the changes in the conductivity instead of the quantitative values. We tested the DBU, 2-pentanol, and CO_2 reaction from atmospheric pressure to 7 MPa. We observed a significant increase in the conductivity at just 0.7 MPa with only slight increases with elevated pressures. However, we found that the conductivity stayed at approximately the same level after release of the CO_2 pressure. We originally believed that release of the pressure would cause the reaction to reverse back to the molecular liquid. On the contrary, it appears to stay in the ionic form for a significant length of time. This could be due to the high viscosity of the ionic liquid, which could slow the release of CO_2. We observed similar behavior for isopropanol, but saw the formation of a solid with tert-butyl alcohol, indicating that the ionic material is not a room temperature ionic liquid. In general, the qualitative data indicates the formation of the ionic material under pressure, but we are unable to determine whether or not the reaction goes to completion.

B.4 Conclusions

The work has shown, from a qualitative perspective, that we can extend the reversible ionic liquids to secondary and tertiary alcohols under pressure. However, we have not been able to quantitatively assess the extent of reaction to the ionic liquid. We completed this part of the research due to the limitations of the apparatus. We do believe that the quantitative data could be obtained by other means, such as high pressure NMR and IR, which we have worked with in the past.

B.5 References

1. Phan, L., et al., *Switchable Solvents Consisting of Amidine/Alcohol or Guanidine/Alcohol Mixtures.* Industrial and Engineering Chemistry Research, 2007.

2. Jessop, P.G., et al., *Reversible non-polar-to-polar solvent.* Nature, 2005. **436**: p. 1102.

Appendix C: OATS Phase Behavior

C.1 Introduction

In order to apply the organic-aqueous tunable solvents (OATS) to enzymatic systems, we needed to complete additional phase behavior at 25ºC. Most of the OATS phase behavior has been completed at 40ºC, but the 1,4-dioxane and acetonitrile systems were not determined at the lower temperatures.[1, 2] This is necessary for the enzymatic reactions, because many are run at room temperature to maintain enzyme activity. Therefore, we determined liquid-liquid equilibria of water, CO_2, and either 1,4-dioxane or acetonitrile at 25ºC.

C.2 Experimental

C.2.1 Materials

The following materials were used as received from the supplier: Water (HPLC grade), 1,4-dioxane (Sigma-Aldrich, anhydrous, 99.8%), and acetonitrile (Sigma-Aldrich, anhydrous, 99.8%). The carbon dioxide was SFC grade (Air Gas, 99.999%) and further purified to remove trace water and other impurities with a Matheson gas purifier and filter cartridge (Model 450B, Type 451 filter).

C.2.2 Experimental

The experiments were conducted in the sapphire cell set-up explained in Chapter 4. The procedure is exactly the same as previously described, except that we use water in the place of PEG-400.

C.3 Results

The liquid-liquid equilibria for water and CO_2 with 1,4-dioxane or acetonitrile at 25ºC are shown in Figures C-1 and C-2 with the data enumerated in Tables C-1 and C-2. The phase behavior for the dioxane system shows good separation with high purity of both the aqueous and organic phases. The organic contains a substantial amount of CO_2 at almost 90 mol%, which is significantly higher than the 40ºC behavior that was previously published. However, there is less than 5 mol% water in the organic, indicating high potential for homogeneous catalyst recovery with this system. In the acetonitrile equilibria, the aqueous phase shows excellent purity with 95 mol% water, but the organic does not have quite as clean a separation with over 10 mol% water in the phase. Compared to the 40ºC data, there is a significant increase in CO_2 content up 20% from the higher temperature behavior to 71 mol%. In this case, it may be better to operate at 40ºC to ensure good partitioning of catalysts and products.

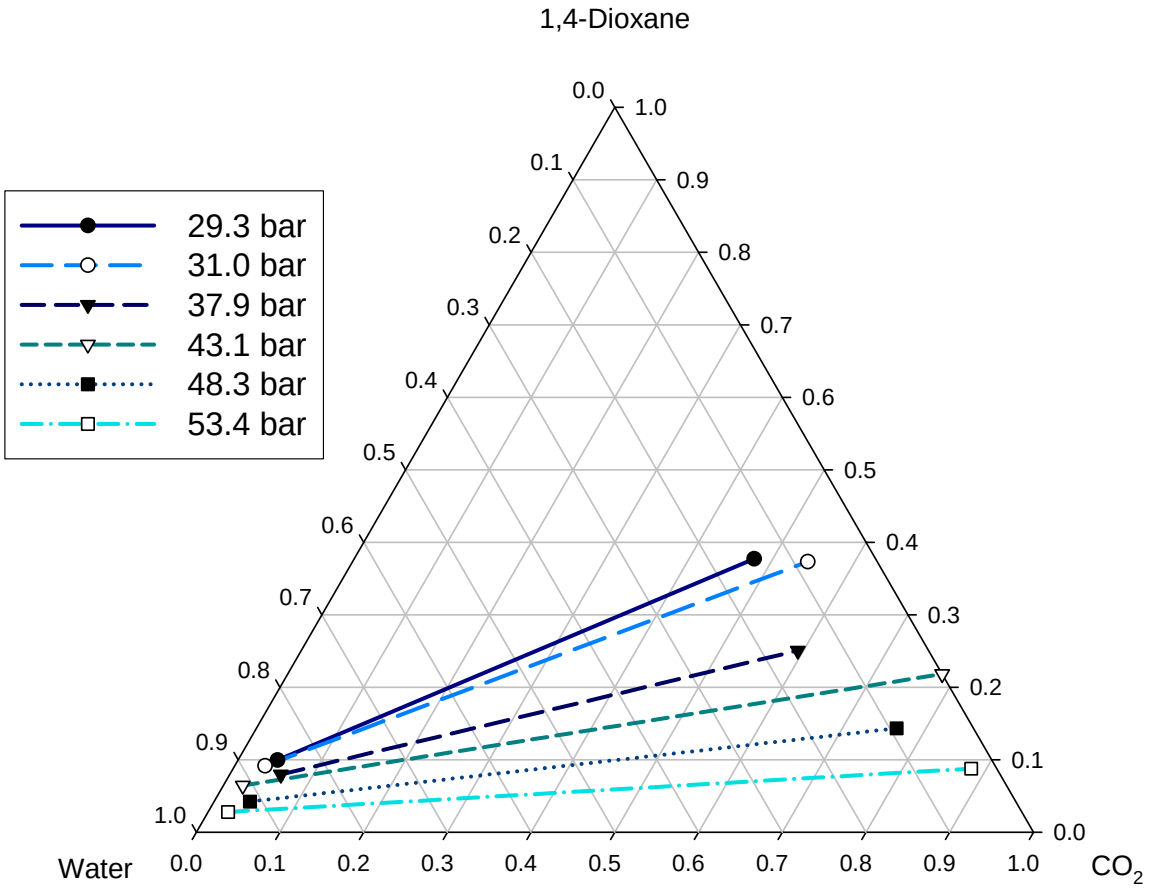

Figure C-5 Liquid-Liquid Equilibria for 1,4-Dioxane/CO_2/Water at 25ºC

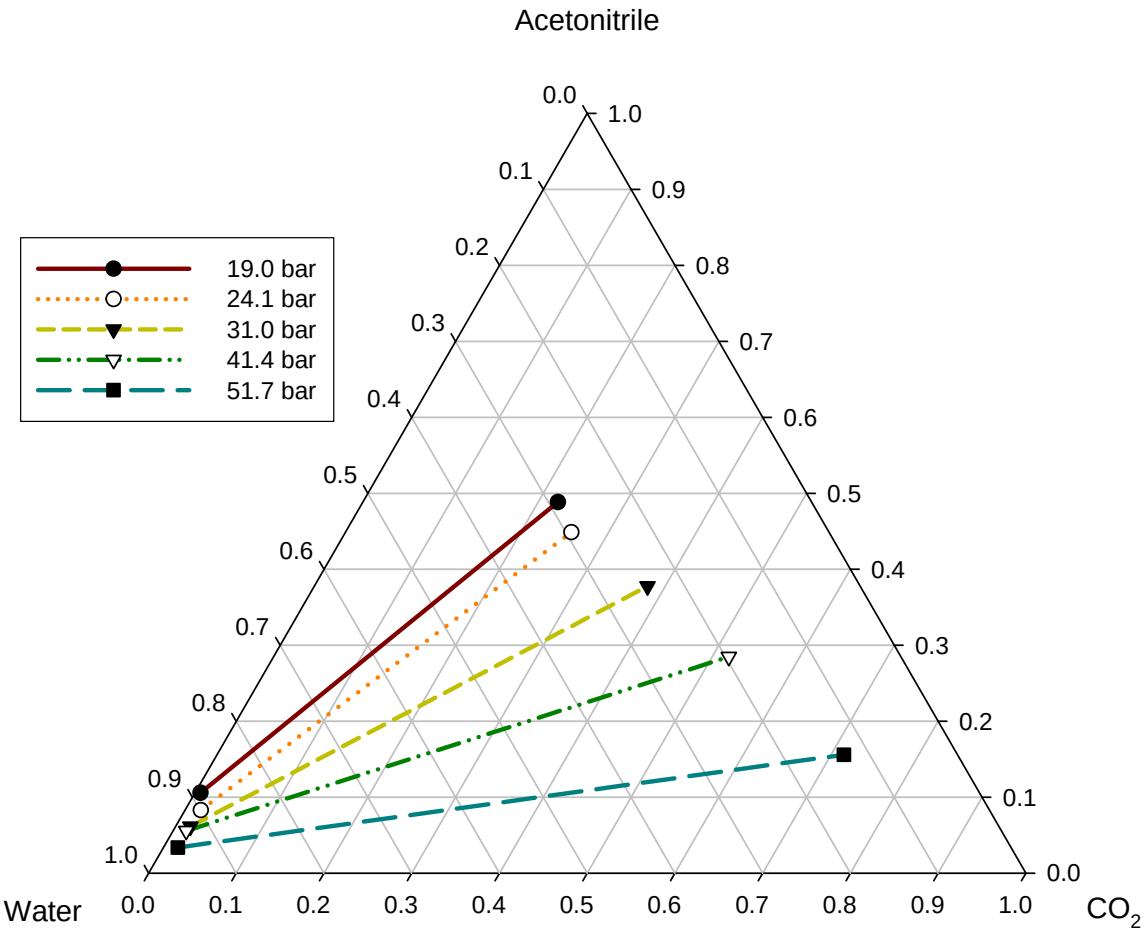

Figure C-6 Liquid-Liquid Equilibria for Acetonitrile/CO_2/Water at 25°C

Table C-3 Liquid-Liquid Equilibria for 1,4-Dioxane/CO_2/Water at 25ºC

T (K)	P (bar)	Liquid Phase 1 (L1)					Liquid Phase 2 (L2)					Vapor Phase (V)
		x_{CO2}	x_{DIOX}	x_{H20}	v_{L1} (cm^3/mol)		x_{CO2}	x_{DIOX}	x_{H20}	v_{L2} (cm^3/mol)		v_V (cm^3/mol)
298	29.3	0.047	0.099	0.853	19.7		0.478	0.377	0.145	55.8		706.2
298	31.0	0.036	0.092	0.872	19.9		0.544	0.373	0.083	57.0		657.9
298	37.9	0.061	0.080	0.859	18.5		0.593	0.251	0.156	51.1		506.9
298	43.1	0.023	0.064	0.912	18.3		0.782	0.218	0.000	55.5		423.1
298	48.3	0.043	0.042	0.915	18.1		0.765	0.143	0.092	47.5		355.0
298	53.4	0.024	0.028	0.948	18.0		0.882	0.088	0.031	48.5		297.0

Table C-4 Liquid-Liquid Equilibria for Acetonitrile/CO_2/Water at 25ºC

T (K)	P (bar)	Liquid Phase 1 (L1)					Liquid Phase 2 (L2)					Vapor Phase (V)
		x_{CO2}	x_{ACNT}	x_{H20}	v_L (cm^3/mol)		x_{CO2}	x_{ACNT}	x_{H20}	v_L (cm^3/mol)		v_V (cm^3/mol)
298	19.0	0.006	0.106	0.888	20.1		0.222	0.488	0.289	37.4		1175.1
298	24.1	0.018	0.083	0.899	19.0		0.257	0.449	0.294	37.0		891.7
298	31.0	0.017	0.061	0.922	18.6		0.380	0.377	0.243	35.5		658.5
298	41.4	0.015	0.055	0.929	18.6		0.519	0.285	0.196	36.4		449.5
298	51.7	0.016	0.034	0.950	18.1		0.715	0.156	0.130	39.8		316.1

C.4 Conclusions

The phase behavior, in general, shows similar trends to the previous measurements that were completed at 40ºC, indicating that the systems should enable effective separations at 25ºC. These measurements were used to develop the biocatalysis separation for OATS.[3, 4] However, the addition of buffer salts to the mixture significantly impacted the phase behavior, requiring additional equilibria measurements.

C.5 References

1. Lazzaroni, M.J.B., D; Jones, Rebecca; Hallet, Jason P.; Liotta, Charles L.; Eckert, Charles A., *High-pressure phase equilibria of some carbon dioxide-organic-water systems.* Fluid Phase Equilibria, 2004. **224**: p. 143-154.

2. Lazzaroni, M.J.B., David; Brown, James S.; Eckert, Charles A.. *High-pressure vapor-liquid equilibria of some carbon dioxide + organic binary systems.* Journal of Chemical and Engineering Data, 2005. **50**(1): p. 60-65.

3. Broering, J.M.H., Elizabeth M.; Hallett, Jason P.; Liotta, Charles L.; Eckert, Charles A.; Bommarius, Andreas S., *Biocatalytic reaction and recycling by using CO2-induced organic-aqueous tunable solvents.* Angewandte Chemie, 2006. **45**(28): p. 4670-4673.

4. Hill, E.M.B., James M.; Hallett, Jason P.; Bommarius, Andreas S.; Liotta, Charles L.; Eckert, Charles A., *Coupling chiral homogeneous biocatalytic reactions with benign heterogeneous separation.* Green Chemistry, 2007. **9**(8): p. 888-893.

Appendix D – Visual Basic Code for Sanchez-Lacombe EOS

Chemical Potential Calculation

```
Const rg As Double = 83.1451 'cc*bar/K mol
Const v0 As Double = 9.75 'cc/mol
Const Z As Double = 10#
Const tol As Double = 0.001


Function u_m_lfinm(phi_l As Variant, P As Double, T As Double, bin As Variant,
        rho_guess As Double, NC As Integer) As Variant
Dim i As Integer, j As Integer
ReDim M(NC) As Double, R(NC) As Double, estar(NC) As Double, vstar(NC) As
        Double, u_m_l(NC) As Double


For i = 1 To NC
M(i) = Cells(i + 1, 3).Value

R(i) = Cells(i + 1, 9).Value

estar(i) = Cells(i + 1, 7).Value

vstar(i) = Cells(i + 1, 8).Value

Next i


'Calculates rmix

Dim calc_rmix_phi_l As Double
Dim rmix_l As Double

rmix_l = 0#
For i = 1 To NC
   rmix_l = rmix_l + phi_l(i) / R(i)
Next i

calc_rmix_phi_l = 1# / rmix_l
```

```
'calcs the average mw from phi matrix

Dim tmp_l As Double, MW_l As Double
ReDim y_l(NC) As Double

For i = 1 To NC
   y_l(i) = phi_l(i) * calc_rmix_phi_l / R(i)
Next i

tmp_l = 0#

For i = 1 To NC
   tmp_l = tmp_l + M(i) * y_l(i)
   Next i

   MW_l = tmp_l



'Calculates vstarmix


Dim calc_vstarmix_phi_l As Double
ReDim binarray(NC, NC) As Double
Dim vstarmix_l As Double

For j = 1 To NC
   For i = 1 To NC
      binarray(i, j) = ((vstar(i) ^ (1# / 3#) + vstar(j) ^ (1# / 3#)) / 2) ^ 3#
   Next i
Next j

vstarmix_l = 0#
For j = 1 To NC
   For i = 1 To NC
      vstarmix_l = vstarmix_l + phi_l(i) * phi_l(j) * binarray(i, j)
   Next i
Next j

calc_vstarmix_phi_l = vstarmix_l



'Calculates estarmix
'etaij is the binary interaction perameter
```

```
Dim estarmix_l As Double, calc_estarmix_l As Double
Dim etaij As Double
ReDim estarij(NC, NC) As Double
ReDim chiij(NC, NC) As Double
Dim temp1 As Double, temp2 As Double

For j = 1 To NC
   For i = 1 To NC
      estarij(i, j) = (estar(i) * estar(j)) ^ 0.5 * bin(i, j)
   Next i
Next j

For j = 1 To NC
   For i = 1 To NC
      chiij(i, j) = (estar(i) + estar(j) - 2# * estarij(i, j)) / (rg * T / 10000#)
   Next i
Next j

estarmix_l = 0#
For j = 1 To NC
   For i = 1 To NC
      estarmix_l = estarmix_l + phi_l(i) * phi_l(j) * estarij(i, j)
   Next i
Next j

calc_estarmix_l = estarmix_l

Dim rhostarmix_l
'returns g/cc

rhostarmix_l = MW_l / (calc_rmix_phi_l * vstarmix_l)


Const tol As Double = 0.000000001
Dim rho_m_l As Double
Dim Tstarmix_l As Double, Pstarmix_l As Double
Dim Tred_l As Double, Pred_l As Double, rhored_l As Double, vred_l As Double
Dim f_rho_l As Double, df_rho_l As Double, rhored_old_l As Double, err_l As Double
Dim rhoact As Double, vact As Double

'calc estar, vstar, Tred, Pred

Tstarmix_l = (estarmix_l * 1000#) / (8.314) 'K
Tred_l = T / Tstarmix_l
```

```
Pstarmix_l = (estarmix_l * 10000#) / vstarmix_l 'bar
Pred_l = P / Pstarmix_l

rhored_l = rho_guess

10 f_rho_l = rhored_l ^ 2# + Pred_l + _
      Tred_l * (Log(1 - rhored_l) + (1# - (1# / calc_rmix_phi_l)) * rhored_l)
   df_rho_l = 2# * rhored_l + Tred_l * (1# - (1# / calc_rmix_phi_l) - 1# / (1# - rhored_l))
   rhored_old_l = rhored_l
   rhored_l = rhored_old_l - f_rho_l / df_rho_l
   err_l = (rhored_l - rhored_old_l) ^ 2# / ((rhored_l + rhored_old_l) / 2#)
   If err_l > 1E-18 Then GoTo 10
   rho_m_l = rhored_l

   vred_l = 1 / (rho_m_l)

'now calc all of the terms for the chemical potental calc
'all terms from Condo 1996 pg 1117 eq# 27

Dim sum2_l As Double
Dim K As Integer
ReDim Ti_red_l(NC) As Double, Pi_red_l(NC) As Double, Pstar_i_l(NC) As Double,
          sum1_l(NC) As Double

For i = 1 To NC

Ti_red_l(i) = T / (estar(i) * 1000# / (8.314))
Pstar_i_l(i) = estar(i) * 10000# / vstar(i)
Pi_red_l(i) = P / Pstar_i_l(i)

Next i

For i = 1 To NC

sum1_l(i) = 0#

   For j = 1 To NC
   sum1_l(i) = sum1_l(i) + phi_l(j) * chiij(i, j)
   Next j

sum1_l(i) = sum1_l(i)

Next i

sum2_l = 0#
For K = 1 To NC
```

```
    For j = 1 To NC
        If j > K Then
            sum2_l = sum2_l + phi_l(j) * phi_l(K) * chiij(j, K)
        End If
    Next j
Next K

Dim term_l(7) As Double 'these are from Sandler 1994 page 202

For i = 1 To NC
    term_l(1) = Log(phi_l(i)) + 1# - (R(i) / calc_rmix_phi_l)
    term_l(2) = R(i) * rho_m_l * (sum1_l(i) - sum2_l)
    term_l(3) = -R(i) * rho_m_l / Ti_red_l(i)
    term_l(4) = R(i) * Pi_red_l(i) * vred_l / Tred_l
    term_l(5) = R(i) * ((vred_l - 1#) * Log(1# - rho_m_l))
    term_l(6) = Log(rho_m_l)

        u_m_l(i) = term_l(1) + term_l(2) + term_l(3) + term_l(4) + term_l(5) + term_l(6)

Next i


    u_m_lfinm = u_m_l

End Function
```

Calculation of r

```
Function RRmix(phi_l As Variant, P As Double, T As Double, bin As Variant, NC As
        Integer) As Variant

Dim i As Integer, j As Integer
ReDim M(NC) As Double, R(NC) As Double, estar(NC) As Double, vstar(NC) As
        Double, u_m_l(NC) As Double, bin(NC, NC) As Variant


For i = 1 To NC
M(i) = Cells(i + 1, 3).Value

R(i) = Cells(i + 1, 9).Value

estar(i) = Cells(i + 1, 7).Value

vstar(i) = Cells(i + 1, 8).Value
```

```
Next i

Dim rho_guess As Double
rho_guess = Cells(15, 3).Value

Dim calc_rmix_phi_l As Double
Dim rmix_l As Double

rmix_l = 0#
For i = 1 To NC
   rmix_l = rmix_l + phi_l(i) / R(i)
Next i

calc_rmix_phi_l = 1# / rmix_l

RRmix = calc_rmix_phi_l

End Function

Function u_pure(P As Double, T As Double, rho_guess As Double, vstar As Double,
        estar As Double, R As Double) As Double
Dim M As Double, u_p As Double


M = Cells(3, 3).Value

R = Cells(3, 9).Value


Const tol As Double = 0.000000001
Dim rho_m_l As Double
Dim Tstarmix_l As Double, Pstarmix_l As Double
Dim Tred_l As Double, Pred_l As Double, rhored_l As Double, vred_l As Double
Dim f_rho_l As Double, df_rho_l As Double, rhored_old_l As Double, err_l As Double
Dim rhoact As Double, vact As Double

'calc estar, vstar, Tred, Pred

Tstarmix_l = (estar * 1000#) / (8.314) 'K
Tred_l = T / Tstarmix_l
Pstarmix_l = (estar * 10000#) / vstar 'bar
Pred_l = P / Pstarmix_l

rhored_l = rho_guess
```

```
200 f_rho_l = rhored_l ^ 2# + Pred_l + _
      Tred_l * (Log(1 - rhored_l) + (1# - (1# / R)) * rhored_l)
   df_rho_l = 2# * rhored_l + Tred_l * (1# - (1# / R) - 1# / (1# - rhored_l))
   rhored_old_l = rhored_l
   rhored_l = rhored_old_l - f_rho_l / df_rho_l
   err_l = (rhored_l - rhored_old_l) ^ 2# / ((rhored_l + rhored_old_l) / 2#)
   If err_l > 1E-18 Then GoTo 200
   rho_m_l = rhored_l

   vred_l = 1 / (rho_m_l)


   u_p = R * (vred_l - 1#) * Log(1 - rho_m_l) + Log(rho_m_l) - R * rho_m_l / Tred_l +
         R * Pred_l * vred_l / Tred_l

   u_pure = u_p

End Function

Function rho_pure(P As Double, T As Double, rho_guess As Double, vstar As Double,
        estar As Double, R As Double) As Double
Dim M As Double, u_p As Double, rhostar As Double


M = Cells(3, 3).Value

R = Cells(3, 9).Value


Const tol As Double = 0.000000001
Dim rho_m_l As Double
Dim Tstarmix_l As Double, Pstarmix_l As Double
Dim Tred_l As Double, Pred_l As Double, rhored_l As Double, vred_l As Double
Dim f_rho_l As Double, df_rho_l As Double, rhored_old_l As Double, err_l As Double
Dim rhoact As Double, vact As Double

'calc estar, vstar, Tred, Pred

Tstarmix_l = (estar * 1000#) / (8.314) 'K
Tred_l = T / Tstarmix_l
Pstarmix_l = (estar * 10000#) / vstar 'bar
Pred_l = P / Pstarmix_l

rhored_l = rho_guess

200 f_rho_l = rhored_l ^ 2# + Pred_l + _
```

```
      Tred_l * (Log(1 - rhored_l) + (1# - (1# / R)) * rhored_l)
   df_rho_l = 2# * rhored_l + Tred_l * (1# - (1# / R) - 1# / (1# - rhored_l))
   rhored_old_l = rhored_l
   rhored_l = rhored_old_l - f_rho_l / df_rho_l
   err_l = (rhored_l - rhored_old_l) ^ 2# / ((rhored_l + rhored_old_l) / 2#)
   If err_l > 1E-18 Then GoTo 200
   rho_m_l = rhored_l

   rhostar = Cells(3, 6).Value

   rho_pure = rho_m_l * rhostar

End Function
```

Calculation of Pure Component Parameters

```
Function P_pure(P As Double, T As Double, rho_guess As Double, vstar As Double,
        estar As Double, R As Double) As Double
Dim M As Double, P_p As Double


M = Cells(3, 3).Value

R = Cells(3, 9).Value


Const tol As Double = 0.000000001
Dim rho_m_l As Double
Dim Tstarmix_l As Double, Pstarmix_l As Double
Dim Tred_l As Double, Pred_l As Double, rhored_l As Double, vred_l As Double
Dim f_rho_l As Double, df_rho_l As Double, rhored_old_l As Double, err_l As Double
Dim rhoact As Double, vact As Double

'calc estar, vstar, Tred, Pred

Tstarmix_l = (estar * 1000#) / (8.314) 'K
Tred_l = T / Tstarmix_l
Pstarmix_l = (estar * 10000#) / vstar 'bar
Pred_l = P / Pstarmix_l

rhored_l = rho_guess

200 f_rho_l = rhored_l ^ 2# + Pred_l + _
      Tred_l * (Log(1 - rhored_l) + (1# - (1# / R)) * rhored_l)
   df_rho_l = 2# * rhored_l + Tred_l * (1# - (1# / R) - 1# / (1# - rhored_l))
```

```
    rhored_old_l = rhored_l
    rhored_l = rhored_old_l - f_rho_l / df_rho_l
    err_l = (rhored_l - rhored_old_l) ^ 2# / ((rhored_l + rhored_old_l) / 2#)
    If err_l > 1E-18 Then GoTo 200
    rho_m_l = rhored_l

    vred_l = 1 / (rho_m_l)


    P_p = R * (vred_l - 1#) * Log(1 - rho_m_l) + Log(rho_m_l) - R * rho_m_l / Tred_l +
          R * Pred_l * vred_l / Tred_l

    P_pure = P_p

End Function
```

Appendix E – Binary Modeling of the Sanchez-Lacombe EOS for Determination of Binary Interaction Parameters

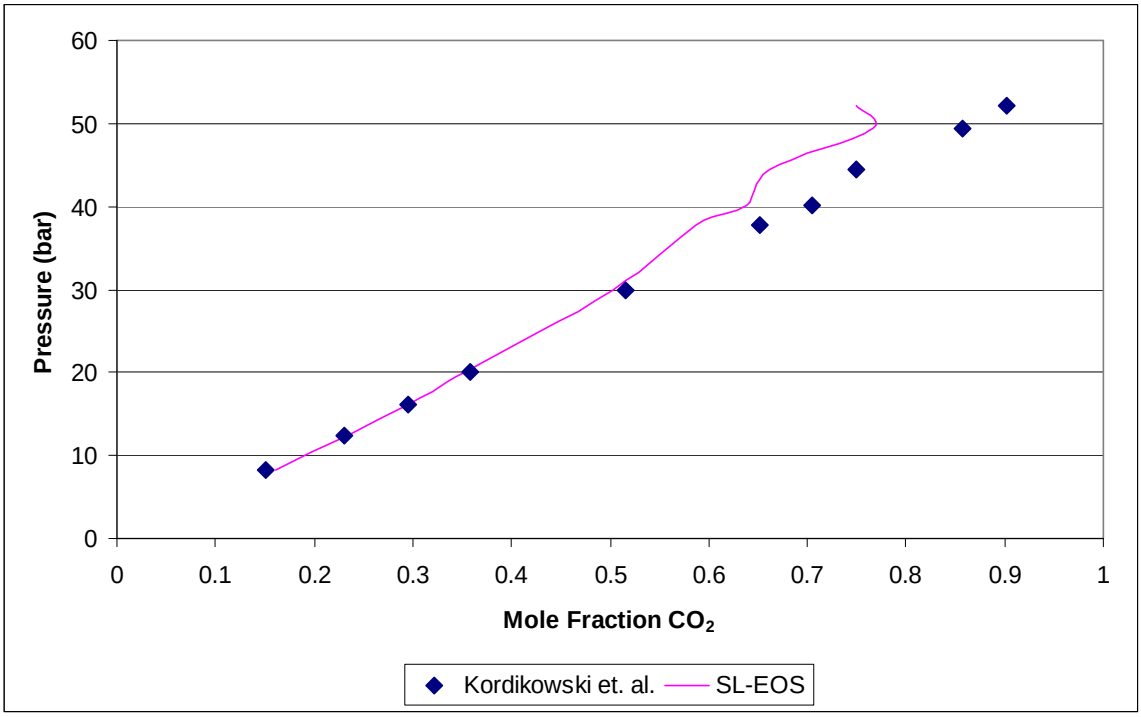

Figure E-7 Application of Sanchez-Lacombe EOS to 1,4-Dioxane/CO_2 Binary Data at 25°C, ζ=1.044 [1]

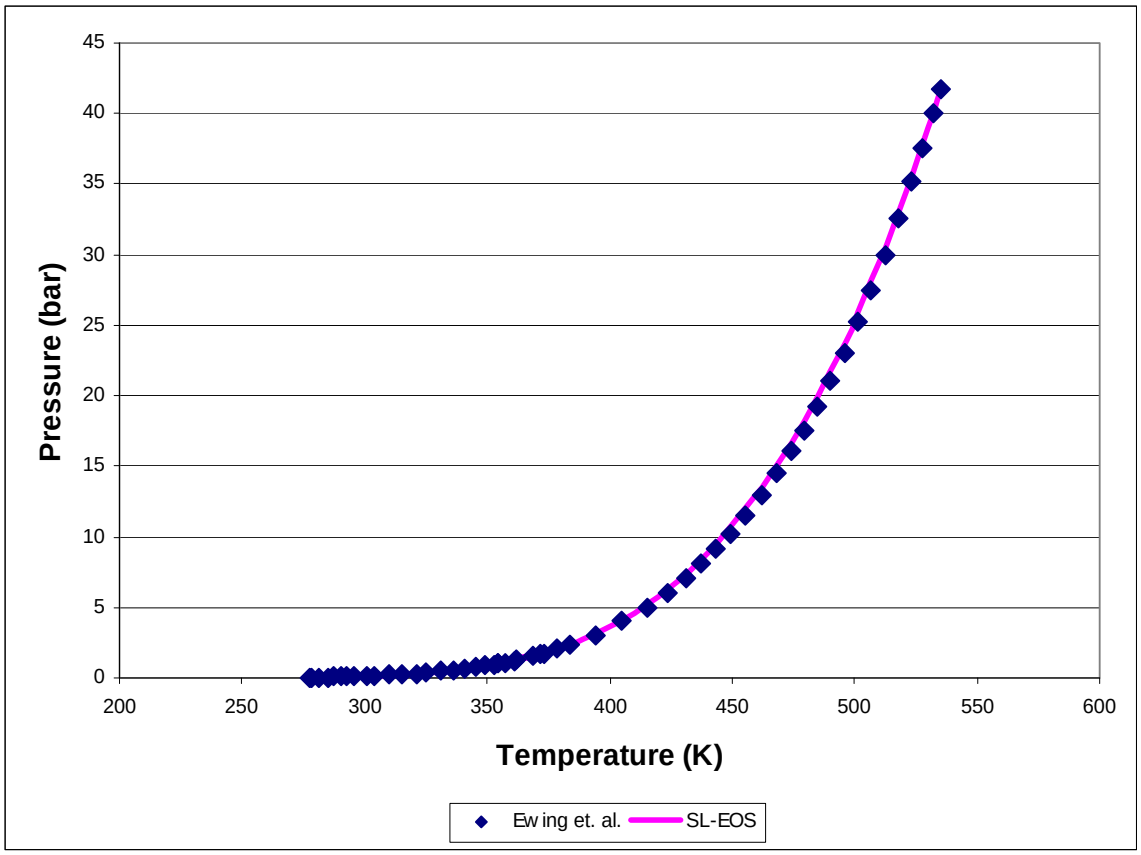

Figure E-8 Vapor Pressure Curve for Acetonitrile for Sanchez-Lacombe Parameters [2]

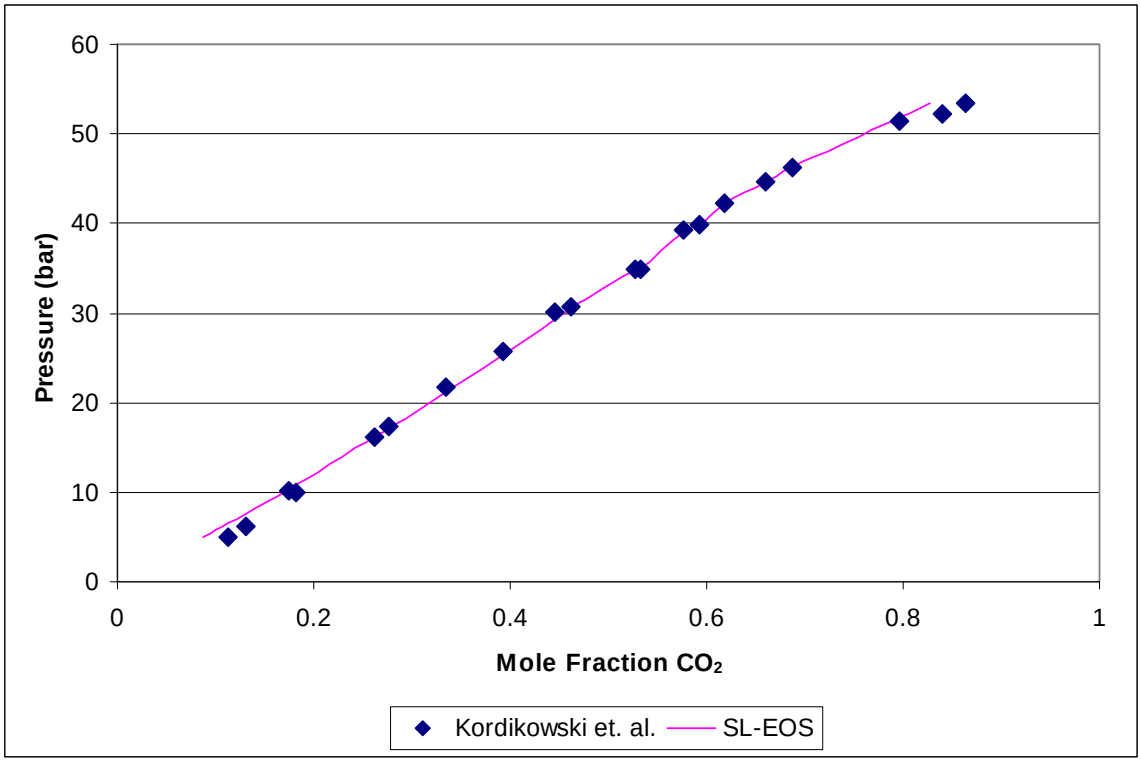

Figure E-9 Application of Sanchez-Lacombe EOS to Acetonitrile/CO_2 Binary Data at 25°C, ζ=1.054 [1]

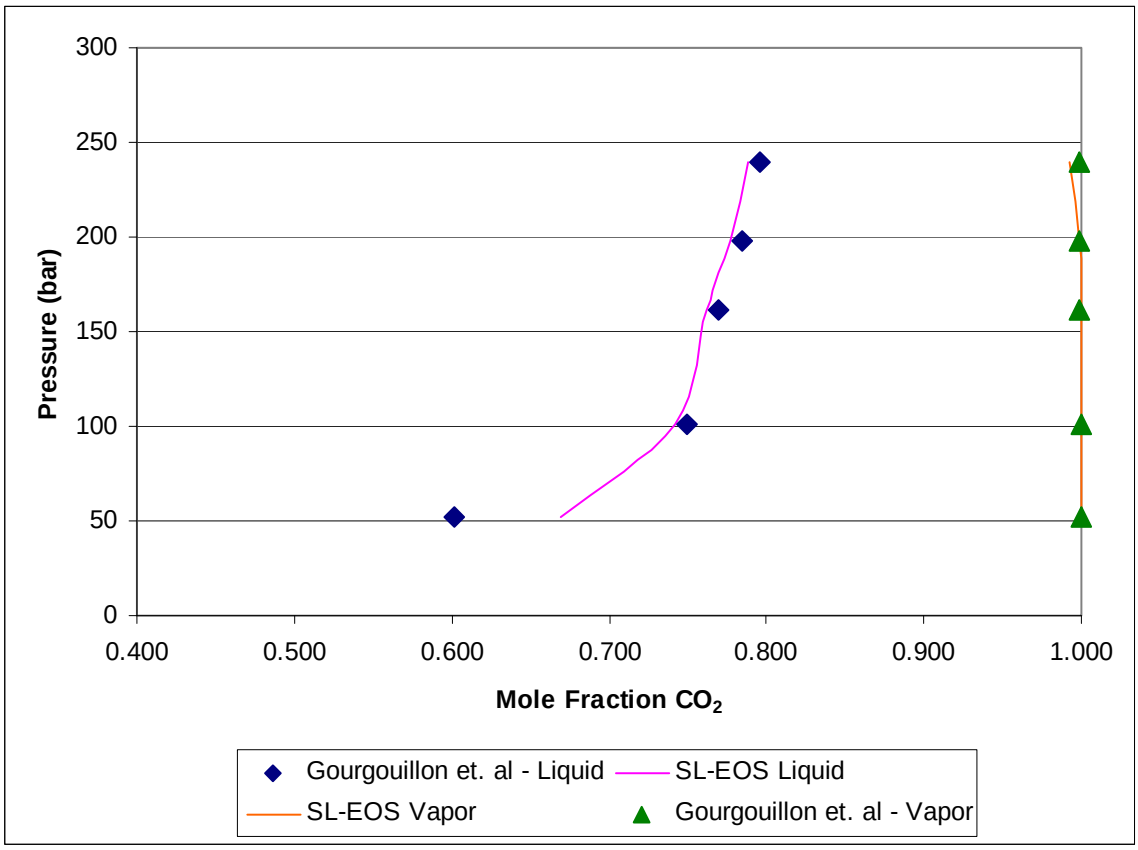

Figure E-10 Application of Sanchez-Lacombe EOS to PEG 400/CO_2 Binary Data at 25°C, ζ=1.134 [3]

E.1 References

1. Kordikowski, A.S., A.P.; Van Nielen, R.M.; Peters, C.J., *Volume Expansions and Vapor-Liquid Equilibria of Binary Mixtures of a Variety of Polar Solvents and Certain Near-Critical Solvents.* The Journal of Supercritical Fluids, 1995. **8**: p. 205-216.

2. Ewing, M.B.O., J.C. Sanchez. *Vapour Pressure of Acetonitrile Determined by Comparative Ebulliometry*. in *Fifteenth Symposium of Thermophysical Properties*. 2003. Boulder, Colorado, USA.

3. Gourgouillon, D.N.d.P., Manuel, *High pressure phase equilibria for poly(ethylene glycol)s + CO2: experimental results and modelling.* Physical Chemistry Chemical Physics, 1999. **1**: p. 5369-5375.

Vita

Megan Elizabeth Donaldson was born in Southfield, Michigan on March 27, 1982 to Bill and Lisa Donaldson. She was raised with her two sisters in northern Michigan and graduated from Roscommon High School in 2000. While there, she met her boyfriend Jesse Bookless. She went on to attend Michigan Technological University in Houghton and graduated Summa Cum Laude with a Bachelors of Science in Chemical Engineering. Then, she attended Georgia Institute of Technology for a Doctorate in Chemical and Biomolecular Engineering. She was advised by Dr. Charles Eckert and Dr. Charles Liotta and will receive her degree in summer of 2008. Her future plans involve a retreat to the great outdoors in which she will hike the Appalachian Trail for a month. She will then move back to Michigan where she has accepted a research position at Dow Chemical in Midland. Selected publications and presentations follow.

Selected Publications

Donaldson, Megan E., Llopis-Mestre, Veronica, Vinci, Daniele, Liotta, Charles L., Eckert, Charles A. Switchable Solvents for In-Situ Acid Catalyzed Hydrolysis of β-Pinene. Manuscript in progress for Industrial & Engineering Chemistry Research.

Donaldson, Megan E., Draucker, Laura C., Blasucci, Vittoria, Liotta, Charles L., Eckert, Charles A. Liquid-Liquid Equilibria of Polyethylene Glycol (PEG) 400 and CO_2 with Common Organic Solvents. Manuscript in progress for Fluid Phase Equilibria.

Vinci, D., Donaldson, Megan E., Hallett, J. P., John E. A., Pollet P.,Thomas C. A., Grilly J. D., Jessop P. G., Liotta C. L., Eckert C. A. Piperylene Sulfone: a Labile and Recyclable DMSO Substitute, *Chemical Communications*, 2007, 1427-1529.

Selected Presentations

Donaldson, Megan E. (Speaker), Vinci, D., John, E., Hallett, J., Pollet, P., Eckert, C., Liotta, C. β-Pinene hydrolysis by in situ acid catalysis in reversible smart solvents, AIChE National Meeting, Oral Presentation, Nov. 2007.

Donaldson, Megan E. (Speaker), Draucker, L.., Eckert, C., Liotta, C. Ternary Phase Behavior Of Liquid Polyethylene Glycol With CO_2 And Organic Solvents, AIChE National Meeting, Oral Presentation, Nov. 2007.

Donaldson, Megan E. (Speaker), Vinci, D., John, E., Hallett, J., Pollet, P., Eckert, C., Liotta, C. β-Pinene hydrolysis by in situ acid catalysis in reversible smart solvents, ACS National Meeting, Oral Presentation, August 2007.

Donaldson, Megan E. (Speaker), Charney, R., Hallett, J., Polizzi, K., Eckert, C., Liotta, C. Development of Organosilicon-Phase Transfer Catalysts, Georgia Tech Chemical & Biomolecular Engineering Graduate Research Symposium, Oral & Poster, March 2007.